REVIEW ARTICLE

# Review on Low-Temperature Electrolytes for Lithium-Ion and Lithium Metal Batteries

Sha Tan[1] · Zulipiya Shadike[1,6] · Xinyin Cai[6] · Ruoqian Lin[1] · Atsu Kludze[2] · Oleg Borodin[3,7] · Brett L. Lucht[4] · Chunsheng Wang[5] · Enyuan Hu[1] · Kang Xu[3,7] · Xiao-Qing Yang[1]

## Abstract

Among various rechargeable batteries, the lithium-ion battery (LIB) stands out due to its high energy density, long cycling life, in addition to other outstanding properties. However, the capacity of LIB drops dramatically at low temperatures (LTs) below 0 °C, thus restricting its applications as a reliable power source for electric vehicles in cold climates and equipment used in the aerospace. The electrolyte engineering has proved to be one of the most effective approaches to mitigate LIB performance degradation at LTs. In this review, we summarize the important factors contributing to the deterioration in $Li^+$ transport and capacity utilization at LTs while systematically categorize the solvents, salts and additives reported in the literature. Strategies to improve the $Li^+$ transport kinetics, in the bulk electrolyte and across the interphases, are discussed. In particular, the formation mechanism of solid electrolyte interphase and its functionality for LT electrolytes are analyzed. Perspectives on the future evolution of this area are also provided.

**Keywords** Electrolyte · Lithium battery · Low temperature · Solid electrolyte interphase · Ionic conductivity

## Abbreviations

| | |
|---|---|
| 1,3-PS | 1,3-Propanesultone |
| AGG | Aggregates |
| AI-ISC | Anion-induced ion–solvent-coordinated |
| AN | Acetonitrile |
| BETI | Bis[(pentafluoroethyl)sulfonyl]imide |
| BN | Butyronitrile |
| BTFE | Bis(2,2,2-trifluoroethyl) ether |
| CE | Coulombic efficiency |
| CEI | Cathode electrolyte interphase |
| CIP | Contact ion pairs |
| CMDO | 4-Chloromethyl-1,3,2-dioxathiolane 2-oxide |
| $CO_2$ | Carbon dioxide |
| Cryo-EM | Cryogenic electron microscopy |
| D2 | 1,1,2,2-Tetrafuoro-1-(2,2,2-trifuoroethoxy) ethane |
| DEE | Diethyl ether |
| DFEC | Difluoro ethylene carbonate |
| DMC | Dimethyl carbonate |
| DME | 1,2-Dimethoxyethane |

S. Tan and Z. Shadike contributed equally.

✉ Zulipiya Shadike
zshadike@sjtu.edu.cn

✉ Enyuan Hu
enhu@bnl.gov

✉ Kang Xu
kang.xu@ses.ai

✉ Xiao-Qing Yang
xyang@bnl.gov

1 Chemistry Division, Brookhaven National Laboratory, Upton, NY 11973, USA

2 Robert Frederick Smith School of Chemical and Biomolecular Engineering, Cornell University, Ithaca, NY 14850, USA

3 Battery Science Branch, Energy Science Division, Army Research Directorate, US Army Research Laboratory, Adelphi, MD 20783, USA

4 Department of Chemistry, University of Rhode Island, Kingston, RI 02881, USA

5 Department of Chemical and Biomolecular Engineering, University of Maryland, College Park, MD 20740, USA

6 Institute of Fuel Cells, School of Mechanical Engineering, Shanghai Jiao Tong University, Shanghai 200240, China

7 Present Address: SolidEnergy Systems, (SES), 35 Cabot Rd., Woburn, MA 01801, USA

| | |
|---|---|
| DMS | Dimethyl sulfite |
| DMSO | Dimethyl sulfoxide |
| DEC | Diethyl carbonate |
| DIB | Dual-ion battery |
| DOL | 1,3-Dioxolane |
| DTD | 1,3,2-Dioxathiolane-2,2-dioxide |
| DX | 1,4-Dioxane |
| EA | Ethyl acetate |
| EB | Ethyl butyrate |
| EBC | Erythritol bis(carbonate) |
| EC | Ethylene carbonate |
| EG | Ethylene glycol |
| EIS | Electrochemical impedance spectroscopy |
| EMC | Ethyl methyl carbonate |
| EP | Ethyl propionate |
| ES | Ethylene sulfite |
| EMI-BF$_4$ | 1-Ethyl-3-methylimidazole tetrafluoroborate |
| ETFEC | Ethyl-2,2,2-trifluoroethyl carbonate |
| ETFA | Ethyl trifluoroacetate |
| FB | Fluobenzene |
| FEC | Fluorine ethylene carbonate |
| F-EPE | 1,1,2,2-Tetrafluoroethyl-2,2,3,3-tetrafluoro-propyl ether |
| FI | Fluorosulfonyl isocyanate |
| FM | Fluoromethane |
| FS | 4,4′-Sulfonyldiphenol |
| G1-CN | 3-(2-Methoxyethoxy)propanenitrile |
| G2E | Diethylene glycol diethylether |
| GBL | γ-Butyrolactone |
| HCE | High concentration electrolyte |
| HF | Hydrofluoroether |
| HOMO | Highest occupied molecular orbital |
| iBA | Isobutyl acetate |
| IL | Ionic liquid |
| LCE | Low concentration electrolyte |
| LGE | Liquified gas electrolyte |
| LHCE | Localized high concentration electrolyte |
| LIB | Lithium-ion battery |
| LiBOB | Lithium bis(oxalato)borate |
| LiDFBOP | Lithium difluorobis(oxalato) phosphate |
| LiDFOB | Lithium difluoro(oxalato)borate |
| LEDC | Lithium ethylene di-carbonate |
| LEMC | Lithium ethylene mono-carbonate |
| LiFSI | Lithium bis(fluorosulfonyl)imide |
| LiPO$_2$F$_2$ | Lithium difluorophosphate |
| LiTFSI | Lithium bis(trifluoromethanesulfonyl)imide |
| LNMO | LiNi$_{0.5}$Mn$_{1.5}$O$_4$ |
| LFP | LiFePO$_4$ |
| LMA | Lithium metal anode |
| LMB | Lithium metal battery |
| LSV | Linear sweeping voltammetry |
| LT | Low temperature |
| LUMO | Lowest unoccupied molecular orbital |
| LWiSE | Localized water-in-salt electrolyte |
| MA | Methyl acetate |
| MB | Methyl butyrate |
| MCMB | Meso-carbon microbeads |
| Me$_2$O | Dimethyl ether |
| MF | Methyl formate |
| MFE | Methyl-nonafluorobutyl ether |
| MMDS | Methylene methanedisulfonate |
| MMSE | Multilayer solvation structure electrolyte |
| MP | Methyl propionate |
| MPC | Methyl propyl carbonate |
| MTFP | 3,3,3-Trifluoropropionate |
| NCA | LiNiCoAlO$_2$ |
| NMC | LiNi$_x$Mn$_y$Co$_{1-x-y}$O$_2$ |
| NMP | $N$-Methyl-2-pyrrolidone |
| NMR | Nuclear magnetic resonance |
| PB | Propyl butyrate |
| PBF | $n$-Butylsulfonyl fluoride |
| PC | Propylene carbonate |
| PCS | Propanediolcyclic sulfate |
| PDF | Pair distribution function |
| PEG250 | Poly(ethylene glycol) dimethyl ether |
| PFPMS | 2,3,4,5,6-Pentafluorophenyl methanesulfonate |
| PhMs | Phenyl methanesulfonate |
| PMMA | Poly(methyl methacrylate) |
| PN | Propionitrile |
| PTFEC | Propyl-2,2,2-trifluoroethyl carbonate |
| PVDF | Polyvinylidene difluoride |
| $R_b$ | Bulk resistance |
| $R_{ct}$ | Charge transfer resistance |
| $R_{sl}$ | Surface film resistance |
| RSO$_3$Li | Lithium alkylsulfonate |
| SEI | Solid electrolyte interphase |
| SEM | Scanning electron microscopy |
| SL | Sulfolane |
| SOC | State of charge |
| SPAN | Sulfurized polyacrylonitrile |
| SSIP | Solvent-separated ion pair |
| TEM | Transmission electron microscopy |
| TFEB | 2,2,2-Trifluoroethyl butyrate |
| TFENH | 2,2,2-Trifluoroethyl N-caproate |
| TFME | 1,1,2,2-Tetrafluoroethyl methyl ether |
| THF | Tetrahydrofuran |
| THT1oxide | Tetrahydrothiophene 1-oxide |
| TMSP | Tris(trimethylsilyl)phosphite |
| TTE | 1,1,2,2-Tetrafluoroethyl-2,2,3,3-tetrafluoro-propyl ether |
| VC | Vinyl carbonate |
| WiSE | Water-in-salt electrolyte |
| XPS | X-ray photoelectron spectroscopy |
| XRD | X-ray diffraction |

# 1 Introduction

Since the commercialization of lithium-ion batteries (LIBs) by Sony in 1990s, the high energy and long cycle life of LIBs have made them the choice of power systems for mobile electronics, electric vehicles and large-scale grid storage [1, 2]. The importance of LIB was highlighted by the 2019 Nobel Prize of Chemistry, which was awarded to Whittingham, Goodenough and Yoshino for its invention. However, we are still facing great challenges in improving LIB performance at subzero temperatures, which is very important for the applications in cold climates as well as outer space. At subzero temperatures, LIBs experience severe energy and capacity loss, as well as charging related safety hazards. These challenges primarily come from the anode side. As reported in early 2000, most graphite anode materials can only deliver 12% of room-temperature (RT) capacity when both lithiation and delithiation were carried out at $-20$ °C [3]. Moreover, the energy density and power density of LIBs at $-40$ °C can only retain a very small percentage of their values at RT, respectively [4]. In a paper published in 2015, a LIB was reported to have a significant capacity drop down to about one fifth of its RT capacity at $-30$ °C [5]. The lithium metal ($Li^0$) plating and dendrite formation on the graphite anode surface, both caused by the increased anode polarization at low temperatures (LTs), can cause severe capacity loss and internal short circuit. Such drastically deteriorated performance of LIBs is often simply attributed to the sluggish ion transport at LTs in bulk electrolyte only. However, the ion transport across electrode/electrolyte interphases plays comparable or even more important roles [5].

$Li^+$ transport through the electrolyte is an important step in the whole process of balancing charge and mass transfer between the anode and cathode to sustain the cell reaction. The combination of salts and solvents can influence the transport kinetics of the electrolyte [6]. Generally, the more polar the solvent molecules are, the less likely the counterions would tend to recombine, and similarly, the more delocalized the charges on the anions are, the less likely they would reassociate with the cations after the salt dissolution. The delocalization of charges on anions usually comes from the resonance in a conjugated structure over a large size, as typically exemplified by the most commonly used anions in LIBs by industry and research institutions, such as hexafluorophosphate ($PF_6^-$), bis(fluorosulfonyl)imide ($FSI^-$) or bis(trifluoromethane)sulfonyl imide ($TFSI^-$). However, excessively large size could compromise the mobility of anions and the overall transport property of the electrolyte. Therefore, size and properties of anions need to be balanced. To keep anions and cations effectively apart, as well as to facilitate the $Li^+$ transport at LT applications, solvents need to have high dielectric constants and donor numbers, low viscosity, and low melting points. Since it is difficult to achieve all of these attributes in one solvent alone, mixtures of various solvents are typically used to obtain the desired properties. Beside overall ion conductivity, one important parameter related to transport property that has been often underestimated is the lithium-ion transference number ($t_{Li^+}$), which is defined as the fraction of the current carried by $Li^+$ of the total current. Because it is the $Li^+$ rather than the anion that is usually strongly solvated, the resulting $Li^+$ solvation shell is much bulkier and moves more slowly than the loosely solvated anions, resulting in a low $t_{Li^+}$ (~ 0.4) in most non-aqueous electrolytes at typical salt concentrations around 1 M (molarity, 1 M = 1 mol $L^{-1}$). This means at high charge rates the speed of $Li^+$ transport in the electrolyte cannot catch up with the $Li^+$ entering the electrode, resulting in a steep $Li^+$ concentration profile at the interphase limiting the LIB performance [7, 8]. The effect of low $t_{Li^+}$ would become especially pronounced at high charge/discharge rates [9]. In addition to bulk transport properties, $Li^+$ transport through solid electrolyte interphase (SEI) is often a limiting factor at LTs. The electrolyte type dictates the interphase chemistry on electrodes that operate beyond the electrochemical stability limits. By convention, the SEI is considered as a passivation layer formed on anode surface, consisting of electrolyte decomposition products (i.e., LiF, $Li_2CO_3$, semicarbonates, etc.), which stabilizes the electrolyte at extremely low potentials (< 0.5 V), while the cathode electrolyte interphase (CEI) is a passivation layer of similar function on cathode surface at high potentials (> 4.0 V). A well-developed stable SEI on graphitic anode, e.g., formed by ethylene carbonate (EC) reduction, can facilitate $Li^+$ transportation, insulate electron transfer and prevent further electrolyte reductions at the electrolyte/electrode interface at the low potentials. Therefore, EC has become a widely used solvent in state-of-the-art commercial LIBs. However, the high viscosity and high freezing point (36.4 °C) of EC negatively affect the ionic conductivity, especially at room or low temperatures. Thus, linear carbonates with low melting points and low viscosity are always introduced as cosolvents to address these issues. The EC/linear carbonate mixture electrolyte simultaneously provides sufficient anode protection and rapid ion transportation inside bulk electrolyte at RT.

As mentioned above, severely reduced $Li^+$ transport kinetics at subzero environments deteriorated the electrochemical performance of LIBs. Therefore, it is of great importance to understand how the $Li^+$ transport process is affected by temperature changes. Figure 1 illustrates the journey of $Li^+$ ions in a LIB during the charging process. After being deintercalated from the cathode, $Li^+$ ions are

**Fig. 1** The journey of a Li$^+$ within a Li-ion battery during the charging process. It must travel across the bulk electrolyte (ion conduction), desolvate at the electrolyte/interphase surface (desolvation) and then migrate across the interphase (interphasial diffusion). The most rate-determining step occurs at the interphase. Reprinted with permission from Ref. [10]. Copyright © 2010, American Chemical Society
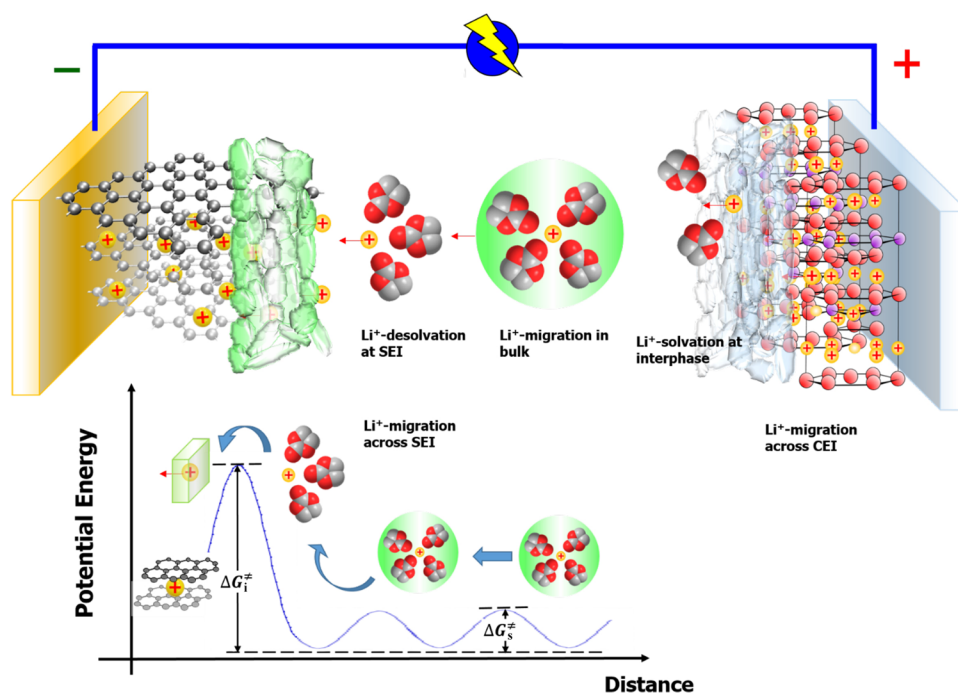
**Fig. 2** Typical impedance spectrum of Li-ion batteries, and Arrhenius plot of electrolyte conductivity and the reciprocal of bulk resistance ($R_b$), surface layer resistance ($R_{sl}$), and charge transfer resistance ($R_{ct}$) measured at 3.87 V (~70% state of charge). Reprinted with permission from Ref. [12]. Copyright © 2020, John Wiley and Sons
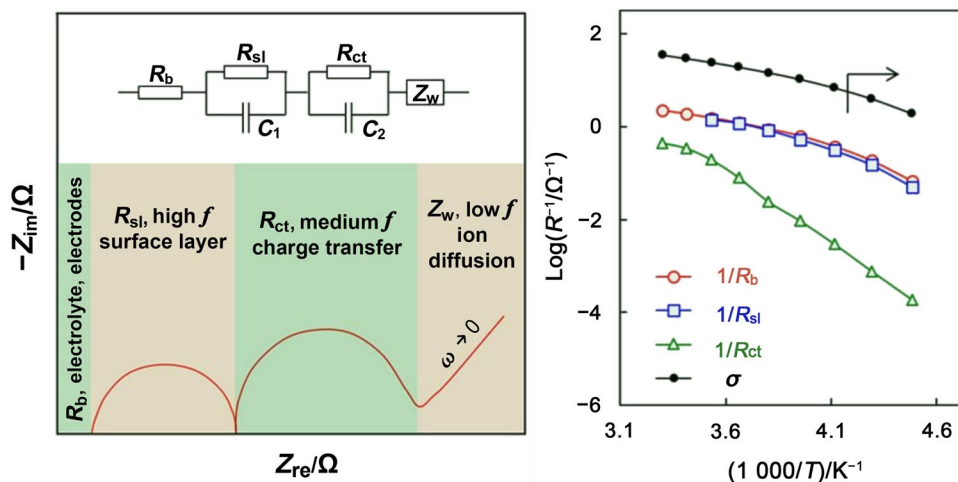
solvated by solvent molecules and migrate from the cathode side to the anode side through the electrolyte. At the anode/electrolyte interface, Li$^+$ ions must be desolvated first, followed by Li$^+$ migration through the SEI interphase. Afterward, Li$^+$ ions intercalate into graphite layers and complete the charging. During the whole charge transfer process, desolvation is identified to be the most sluggish step with the highest energy barrier to be overcome in many systems. This kinetically limited process with an energy barrier of 50–70 kJ mol$^{-1}$ [10] greatly limits fast charging and LT electrochemical performance. There are also discussions in the literature [11] about the nature of SEIs, and the Li$^+$ migration through this layer can have a dominant role upon the charge transfer kinetics. The journey of Li$^+$ ions traveling

within the Li-ion battery during the charging process is illustrated in Fig. 1.

This kinetic barrier becomes even higher at low operating temperatures. When a LIB operates at subzero environments, the decreased temperature severely slows down both the ion transport in the bulk electrolyte and in particular the charge transfer across the interphase. Figure 2 depicts the resistance of each process measured by electrochemical impedance spectroscopy (EIS) at different temperatures [12]. As expected, the electrolyte ionic conductivity drops at LTs because of the increased viscosity, rendering sluggish Li$^+$ migration in the bulk electrolyte. However, the severer impact comes from the resistance of the charge transfer process, as shown in Arrhenius curve in Fig. 2, which has a larger slope indicating the

higher activation energy and increases much more rapidly and becomes the rate-determining step at LTs. Therefore, it is the interphasial process, rather than the bulk process, that has the dominant influence on the overall LT electrochemical performance. For the charge transfer process, however, whether the desolvation at the interphase or the migration inside the interphase is more dominant still remains unclear and could vary case by case. It is well established that desolvation is dominant when the SEI is less pronounced (i.e., on $Li_4Ti_5O_{12}$) or the interphase is highly conductive [11, 13]. Otherwise, $Li^+$ transport inside the SEI still plays a significant role in $Li^+$ charge transfer kinetics. The LT effects on charging and discharging are asymmetric: the charge transfer resistance at LTs in the discharged state is substantially higher, making it much more challenging when charging a discharged LIB at LTs [14, 15].

Therefore, in order to effectively improve the LT performance of a LIB, one must simultaneously improve both charge transfer kinetics and bulk electrolyte ionic conductivity. Various strategies have been reported. One example is through engineering solution of leveraging the joule heat with a specially designed extra Ni-foil integrated in the LIB as self-heating element for electrolyte [16]. Another example is through electrode designs consisting of low electroactive material loadings and small particle sizes. These examples are able to effectively improve electrochemical performance at LTs, but at the expense of increased weight and complexity that result in reduced energy density. In addition, an important effort is through electrolyte engineering by altering electrolyte composition including types and ratios of solvents, salts, and additives, considering the LT constraint is largely caused by EC. This is an effective approach due to its low cost, high flexibility, and convenience, but such approach may introduce unexpected changes in the interphasial chemistry which is not always desirable.

Improving the LT electrochemical performance of LIBs and extending their operating temperature range are ongoing efforts. Such efforts started since 1990s and great progress has been made. However, the systematic review on the related mechanism is still quite limited. This review intends to fill such gap by focusing on the mechanisms and correlating progress in the LT electrolyte performance with changing components such as solvents, salts, and additives, as well as the underlying interphasial chemistry. We hope this systematic analysis can provide valuable information for the future development of LT electrolytes.

## 2 Solvents

The electrolyte solvents are key components in determining the bulk electrolyte ionic conductivity and are major contributors to interphasial chemistry. Solvents with low melting points and low viscosity for achieving rapid ion
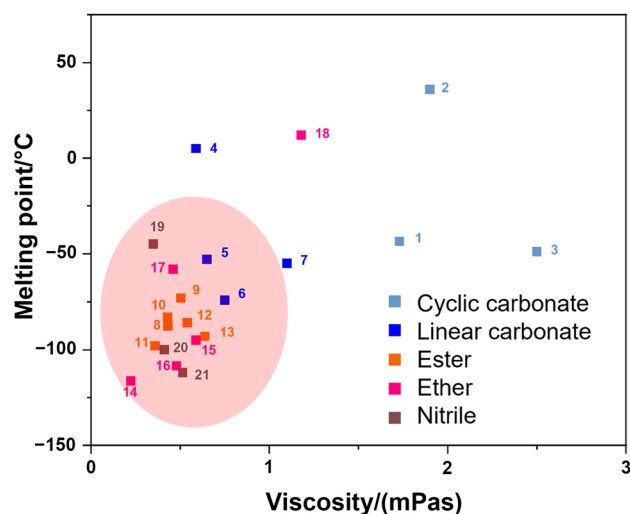


**Fig. 3** Melting points and viscosity of commonly used electrolyte solvents [1, γ-butyrolactone (GBL); 2, ethylene carbonate; 3, propylene carbonate (PC); 4, dimethyl carbonate (DMC); 5, ethyl methyl carbonate (EMC); 6, diethyl carbonate (DEC); 7, methyl propyl carbonate (MPC); 8, methyl propionate (MP); 9, ethyl propionate (EP); 10, ethyl acetate (EA); 11, methyl acetate (MA); 12, methyl butyrate (MB); 13, ethyl butyrate (EB); 14, diethyl ether (DEE); 15, 1,3-dioxolane (DOL); 16, tetrahydrofuran (THF); 17, 1,2-dimethoxyethane (DME); 18, 1,4-dioxane (DX); 19, acetonitrile (AN); 20, propionitrile (PN); 21, butyronitrile (BN)]

transport in bulk are desirable for LT applications. At the same time, solvents with high dielectric constants are still needed. Unfortunately, the most widely used electrolyte solvent, EC, has a high melting point (36.4 °C), which is responsible for the significantly increased electrolyte viscosity at LTs. The widely used EC is based on its high dielectric constant and excellent SEI formation capability. For LT electrolyte designs, there has always been a strong motivation to minimize EC content or to completely replace it with other solvents that have lower melting points and viscosity (the red region in Fig. 3). However, such EC reduction and substitutions should not be done at the expense of stable SEI formation at the graphitic anode. In addition to the protection effectiveness, the desired SEI should also have good ionic transport property as well, which can result in the overall low impedance [17]. In this section, various solvents used for LT electrolytes are categorized according to their functional groups and their performance at LTs. The characteristics and related references of these electrolytes are summarized in Table 1 and Table 2.

### 2.1 Carbonates and Carboxylic Esters

Linear carbonates and carboxylic esters are always desirable for LT electrolytes, owing to their low viscosity and low melting points (Fig. 3). We would like to point out that Fig. 3 only uses two parameters, i.e., the viscosity and the

**Table 1** LT electrolytes with linear carbonates and carboxylic esters as cosolvents

| Electrolyte | [Ionic conductivity/(mS cm$^{-1}$)]/(temperature/°C) | Cell system | [Capacity/(mAh g$^{-1}$) or capacity retention]/(current density or C rate)/(temperature/°C) | References |
|---|---|---|---|---|
| 1 M LiPF$_6$ in EC:DEC:DMC (1:1:1) | ~10/RT, ~2/−20 | Graphite‖LiCoO$_2$ | ~85 %/25 mA/−20 | [20] |
| 1 M LiPF$_6$ in EC:DMC:EMC (1:1:3) | ~10/RT | Graphite‖LiCoO$_2$ | ~95 %/0.1 C/−30, ~80 %/0.1 C/−40, ~98 %/0.1 C/−20 | [26] |
| 1 M LiPF$_6$ in PC:EC:EMC (1:1:3) | ~1.6/−20 | Graphite‖lithium nickel-based mixed oxide | ~83%/0.5 mA cm$^{-2}$/−20 | [48] |
| 1 M LiPF$_6$ in THT1oxide:PC (15:85) | ~6.5/RT | Graphite‖NMC111 | ~70 mAh g$^{-1}$/1 C/0 | [49] |
| 1 M LiPF$_6$ in EC:DEC:DMC:EA (1:1:1:2, volume ratio) | 11.27/25, ~9.7/−20 | Graphite‖NMC111 | 1.49 Ah/NA/−30, 1.24 Ah/NA/−40 | [50] |
| 1 M LiPF$_6$ in EC:EMC:EP (30:30:40) | NA | Graphite‖LiCoO$_2$ | 87%–89%/0.2 C/−20 | [51] |
| 0.75 M LiPF$_6$ in EC:DEC:DMC:EA (1:1:1:1) | 5–8/−20 | Li‖graphite MCMB‖LiCoO$_2$ | Li‖graphite: 37 mAh g$^{-1}$/25 mA/−20 MCMB‖LiCoO$_2$: ~94%/25 mA (~C/20)/−20 | [40] |
| 1 M LiPF$_6$ in EC:EMC:MP (20:60:20) | NA | MCMB‖LiNi$_{0.8}$Co$_{0.2}$O$_2$ | 86.76% /25 mA (~C/16)/−20 74.43% /25 mA (~C/16)/−40 | [41] |
| 1 M LiPF$_6$ in EC:EMC (3:7)+2% VC | NA | Graphite‖NMC111 | ~610 mWh/0.025 C/−14, ~0 mWh/3 C/−14 | [42] |
| 1 M LiPF$_6$ in 95% MP+5% VC | NA | Graphite‖NMC111 | ~650 mWh/0.025 C/−14 ~250 mWh/3 C/−14 | [42] |
| 2 M LiPF$_6$ in MP+10% FEC | 1.50/−60 | Graphite‖LiCoO$_2$ | 72.4%/1 C/−40, 63.2%/1 C/−60 | [43] |

Solvents: tetrahydrothiophene 1-oxide (THT1oxide)

melting point. However, other properties, such as good electrochemical and chemical stability, miscibility with other cosolvents, and a wide liquidus range should also be considered for LT electrolyte solvents. In addition, some solvents listed in Fig. 3 are not suitable for Li-ion batteries, such as diethyl ether (DEE), 1,3-dioxolane (DOL), tetrahydrofuran (THF), 1,2-dimethoxyethane (DME), and 1,4-dioxane (DX). They can be used for low voltage systems, but not in LIBs with high operating voltage.

### 2.1.1 Carbonates

Linear carbonates are generally much less viscous compared with their cyclic counterparts. They are widely used in conventional LIB electrolytes as diluents to keep the overall viscosity low in EC-based systems. For good ion transport properties, linear carbonates with shorter alkyl chains are generally favored as they have lower viscosity than those with longer alkyl chains. When it comes to LT application, not only low viscosity but also low melting point is desired. The phase diagrams of binary and ternary carbonate mixed solvents have been studied by Ding et al. [18]. They suggested that the melting point of the mixed solvent is related to the composition, the melting point of each component, and the relative content. Therefore, the freezing point of different electrolytes can be tuned by adjusting the composition and the content of the solvent.

In addition to the tunable freezing point, the multi-solvent system owns a higher conductivity than the single-solvent system at LTs due to the disordered effect of Li$^+$ coordination in various mixed solvents [19]. According to the phase diagrams constructed for the binary systems of these cyclic and linear carbonates, the liquidus lines, which serve as a demarcation between stable liquid electrolyte and onset for solid precipitation, depend not only on the low melting temperature of the individual components, but also on how much these melting temperatures "match" each other. Under such context, the LT limit of electrolyte may not be provided by the lowest melting linear carbonate. Such example can be found between the binary electrolyte mixtures EC/diethyl carbonate (DEC) and EC/dimethyl carbonate (DMC) [20, 21]. Considering these, Smart et al. [20] suggested using higher order of mixtures like ternary solvent systems for LT application. In addition to EC, two linear carbonates are used as solvents to take the advantage of each, with one having lower viscosity and the other having a lower melting point. Compared to the two binary electrolytes of 1 M LiPF$_6$ in EC:DMC (30:70) and 1 M LiPF$_6$ in EC:DEC (30:70), the ternary electrolyte of 1 M LiPF$_6$ in EC:DMC:DEC (1:1:1) showed the highest ionic conductivity at −20 °C due to synergistic effect as shown in Fig. 4a. This resulted in the largest discharge capacity in a graphite‖LiCoO$_2$ cell using the ternary electrolyte (Fig. 4b). Smart et al. [22] at Jet Propulsion Laboratory

**Table 2** Other LT electrolytes

| Electrolyte | [Ionic conductivity/(mS cm$^{-1}$)]/(temperature/°C) | Cell system | [Capacity/(mAh g$^{-1}$) or capacity retention]/(current density or C rate)/(temperature/°C) | References |
|---|---|---|---|---|
| 1 M LiPF$_6$ in EC:DMC:AN (1:1:1) | 20.5/RT, 8.41/−20 | Graphite‖LiNiCoO$_2$ | Discharge: 67%/0.2 C/−20<br>Charge: 70%/1 C/−20 | [52] |
| 1 M LiPF$_6$ in EC:DMC:PN (1:1:1) | 16.73/RT, 6.39/−20 | Graphite‖LiNiCoO$_2$ | Discharge: 74%/0.2 C/−20<br>Charge: 68%/1 C/−20 | [52] |
| 0.75 M LiPF$_6$ in EC:DEC:DMC:ETFEC (1:1:1:1) | NA | Li‖MCMB | Charged at RT, then discharged at LT: ~0.58 Ah/0.08 C/−20<br>Charged at LT, then discharged at LT: ~0.285 Ah/0.08 C/−20 | [64] |
| 0.75 M LiPF$_6$ in EC:DEC:DMC:PTFEC (1:1:1:1) | NA | Li‖MCMB | Charged at RT, then discharged at LT: ~0.55 Ah/0.08 C/−20 | [64] |
| 1.0 M LiPF$_6$ in EC:EMC:TFEB (20:60:20) | NA | MCMB‖LiNiCoO$_2$ | ~88%/25 mA (C/16)/−20 | [88] |
| 1.0 M LiPF$_6$ in EC:EMC:ETFA (20:60:20) | NA | MCMB‖LiNiCoO$_2$ | ~90%/25 mA (C/16)/−20 | [88] |
| 0.75 M in 1,3-dioxane | NA | Li$_4$Ti$_5$O$_{12}$‖LiCoO$_2$ | ~123 mAh g$^{-1}$/0.1 C/−20<br>~80 mAh g$^{-1}$/0.1 C/−50 | [89] |
| 0.8 M LiTFSI in G2E:MFE:FEC (50:45:5) | 3.8/RT | Graphite‖LiFePO$_4$ | 46.3% (62 mAh g$^{-1}$)/0.1 C/−20 | [90] |
| 1 M LiPF$_6$ in PC:F-EPE:FEC (60:30:30) | 5.04/RT | Graphite‖NMC111 | 70.4% (112.9 mAh g$^{-1}$)/0.1 C/−30 | [91] |
| 1 M LiPF$_6$ in G1-CN:F-EPE:FEC (10:30:60) | 5.42/RT | Graphite‖LiMn$_2$O$_4$ | 57.1% (52.9 mAh g$^{-1}$)/0.1 C/−20 | [92] |
| 1 M LiBOB in GBL:F-EPE (70:30) | 5.53/RT | Graphite‖NMC111 | 14.9 mAh g$^{-1}$/0.1 C/−30 | [93] |
| 1.28 M LiFSI in FEC:FEMC:D2 | >0.01/−80 | Li‖NCA | 160 mAh g$^{-1}$/0.067 C/−42<br>96 mAh g$^{-1}$/0.067 C/−85 | [62] |
| 1 M LiFSI in DEE | 0.368/−60 | Li‖SPAN | 84%/0.1 C/−40<br>76%/0.1 C/−60 | [57] |
| 1 M LiPF$_6$ in EC:EMC:EB (1:1:8) (polymer electrolyte) | NA | Graphite‖LiMn$_2$O$_4$ | 94.61%/0.2 C/−20<br>38.74%/0.2 C/−60 | [72] |
| 1 M LiPF$_6$ in EC:EMC:MB (1:1:8) (polymer electrolyte) | NA | Graphite‖LiMn$_2$O$_4$ | 91.72%/0.2 C/−20<br>53.93%/0.2 C/−60 | [72] |
| 1 M LiAsF$_6$ in EC/EMC/MA/toluene (1:1:1:1) (polymer electrolyte) | 6.87/RT | MCMB‖LiCoO$_2$ | ~92%/0.2 C/−20 | [94] |
| 1 M LiPF$_6$ in EC:DMC:MA (1:1:1) (polymer electrolyte) | 15.808/RT | MCMB‖LiCoO$_2$ | ~83%/0.2 C/−20 | [94] |
| 0.2 M LiTFSI in FM:CO$_2$ (19:1) (liquified gas electrolyte) | 13–14/−20 | Li‖LiCoO$_2$ | 98.3%/0.1 C/−10<br>60.6%/0.1 C/−10 | [74] |

Solvents: diethylene glycol diethylether (G2E); methyl-nonafluorobutyl ether (MFE); 1,1,2,2-tetrafluoroethyl-2,2,3,3-tetrafluoropropyl ether (F-EPE); 3-(2-methoxyethoxy)propanenitrile (G1-CN); propyl-2,2,2-trifluoroethyl carbonate (PTFEC); 2,2,2-trifluoroethyl butyrate (TFEB); 1,1,2,2-tetrafluoro-1-(2,2,2-trifluoroethoxy)ethane (D2); lithium bis(oxalato)borate (LiBOB)

developed a ternary LT electrolyte consisting of 1.0 M LiPF$_6$ in EC:ethyl methyl carbonate (EMC):methyl propionate (MP) (20:60:20 in volume ratio), which has enabled several NASA missions when incorporated into mesocarbon microbead (MCMB)-graphite-LiNiCoAlO$_2$ (NCA) cells where good performance was required for charging and discharging from −30 to 35 °C.

In addition to ion transport properties, SEI properties vary with the type of linear carbonates introduced. It was reported by Ein-Eli et al. [23] that in asymmetric alkyl carbonates a methyl group is required for stable graphite electrode cycling. They showed that EMC can form much stabler SEI on graphite than DMC. The electrolytes using EMC as the single solvent can even work on graphite anodes without EC when LiAsF$_6$ salt was used [24]. Plichta et al. [25] reported an LT electrolyte using ternary carbonate-based solvents of 1.0 M LiPF$_6$ in EC:DMC:EMC (1:1:1 in volume ratio). Xiao et al. [26] systematically compared the different content ratios of EC:DMC:EMC systems and achieved 90% capacity at −40 °C with the optimized solvent ratio (EC:DMC:EMC, 8.3:25:66.7 in weight ratio). The improved LT performance using quaternary solvents
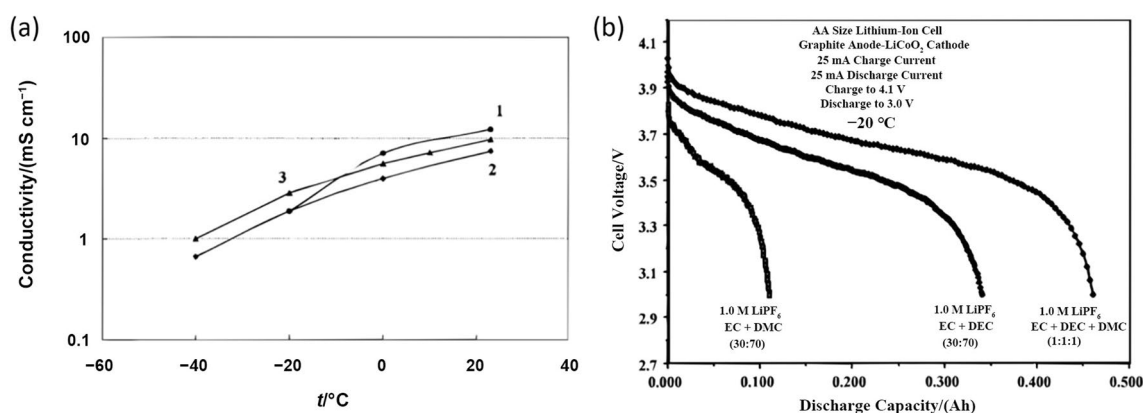
**Fig. 4 a** Conductivity of Li-ion battery electrolyte solutions containing 1 M LiPF$_6$ dissolved in (1) EC+DMC (30:70), (2) EC+DEC (30:70), and (3) EC+DMC+DEC (1:1:1) solvent mixtures. **b** Comparison of the discharge curves of graphite-based AA size (400–500 mAh) Li-ion cells at −20 °C using two binary and one ternary electrolytes. Reprinted with permission from Ref. [20]. Copyright © 1999, IOP publishing

(1.0 M LiPF$_6$ in EC:DEC:DMC:EMC) was reported by Smart et al. [27], demonstrating stable cycling performance at −20 and −40 °C by using a volume ratio of 1:1:1:3 for EC:DEC:DMC:EMC. It was shown by Ein-Eli et al. [28] that the electrolyte using methyl propyl carbonate (MPC) has even more superior SEI formation capability than EMC as a single solvent with both LiPF$_6$ and LiAsF$_6$ salts, but no LT performance improvement was reported. MPC electrolyte could enable reversible lithium intercalation into the graphite anode. These low melting point and low viscosity linear carbonates with stable SEI formation abilities are good candidates as cosolvents and even main solvents for LT applications. For LT operation of LIBs, high Li$^+$ conductivity, stable anode and cathode electrode interphase and lower charge transfer resistance are important factors, among which the reduced charge transfer resistance dominates LT performance which is hard to realize. Wang and coworkers [29] designed a low-polarity-solvent electrolyte consisting of 2.0 M LiFSI in EMC:1,1,2,2-tetrafluoro-1-(2,2,2-trifluoro-ethoxy)ethane (TTE). EMC has a wide liquid temperature range from −53 to 110 °C with a very small dipole moment, which enhances the kinetics and reduces the charge transfer resistance for the desolvation process. Moreover, the electrolyte enables the formation of inorganic-rich SEI and CEI from the anion decomposition induced by the high ratios of the contact ion pairs (CIPs) and the aggregates (AGGs) with the help of TTE. As a result, the graphite-NMC811 pouch cell showed enhanced cyclic stability operating across a wide-temperature range from −40 to 50 °C. In addition to the linear carbonates, propylene carbonate (PC) has been considered as a promising solvent since the early development of lithium metal batteries. PC solvent possesses a wide liquid temperature range (from −49 to 240 °C), high-voltage stability, and good solvation behavior. However, it could not

be used in graphite anode contained battery systems as the major/single solvent due to the solvent co-intercalation and exfoliation of the graphite anodes [30, 31]. Gao et al. [32] demonstrated a possible utilization of PC-based electrolytes with fluoroethylene carbonate (FEC) and LiNO$_3$ additives for LT lithium metal batteries (LMBs). By coupling with the electrochemically activated SEI on a lithium metal anode (LMA), a Li/LiCoO$_2$ cell displayed high-rate charge capability and superior long-term cyclability at −15 °C. Considering the advantage of PC as low melting point solvent to extend the operation temperature range of electrolyte, several strategies have been attempted to stabilize graphite anodes toward PC. 4-Chloromethyl-1,3,2-dioxathiolane 2-oxide (CMDO), a sulfur-containing compound with a similar structure to sulfite, has been used as a coadditive with EC and FEC in PC-based electrolytes [33]. The binary additive systems showed better performance than single FEC or EC additive only by forming thinner and conductive SEI layers, especially under an LT of −10 °C. In addition, adding the linear carbonate can also increase the stability of PC and the stability also increases with the content of the linear carbonate, which is attributed to the lower content of free PC solvent [34]. To systematically analyze the relationship between the stability of PC-based electrolytes and the content of the linear carbonate as cosolvent, Cao's group introduced weakly coordinating DEC as cosolvent with different volume ratios [35]. Moreover, a PC-DEC binary solvent was selected as a model system to investigate the effect of different solvation structures on the electrochemical performance of graphite anode by tuning the salt concentration. An anion-induced ion–solvent-coordinated (AI-ISC) structure has been formed with a salt-solvent molar ratio of 1:5, which can lead to an increase of the lowest unoccupied molecular orbital energy level (LUMO) of the electrolyte,
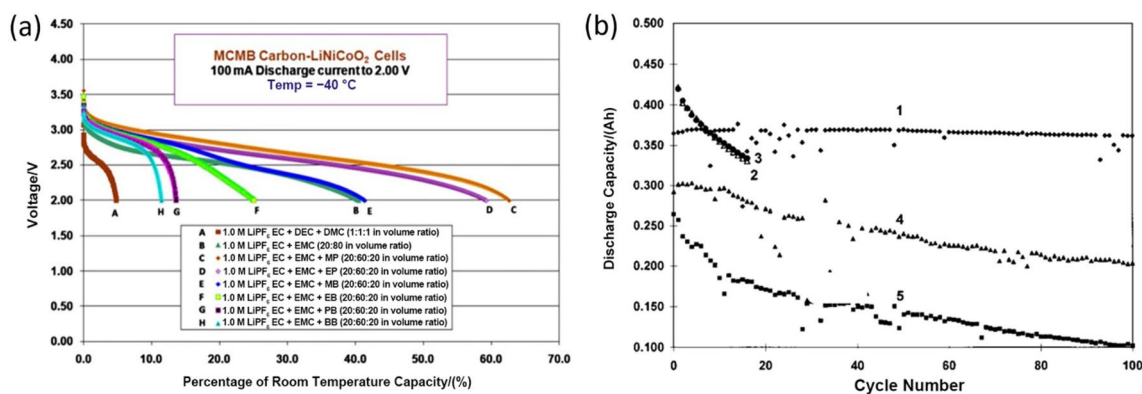
**Fig. 5 a** Discharge capacity of cells at −40 °C containing different electrolytes at a C/4 rate. Reprinted with permission from Ref. [41]. Copyright © 2010, IOP publishing. **b** The effect of electrolyte type upon the cycle life of AA-size lithium-ion prototype cells (400–500 mAh) at −20 °C (50 mA charge to 4.1 V and 50 mA discharge to 3.0 V) using the following electrolytes: (1) 1.0 M LiPF$_6$ in EC:DEC:DMC (1:1:1); (2) 0.75 M LiPF$_6$ in EC:DEC:DMC:MA (1:1:1:1); (3) 0.75 M LiPF$_6$ in EC:DEC:DMC:EA (1:1:1:1); (4) 0.75 M LiPF$_6$ in EC:DMC:MA (1:1:1); and (5) 1.0 M LiPF$_6$ in EC:DEC (30:70). Reprinted with permission from Ref. [40]. Copyright © 2002, IOP publishing

therefore considerably improving the reduction tolerance of the PC solvent. Coupling with film-forming additive FEC, the PC-based electrolyte enables reversible Li intercalation/extraction to/from the graphite anode without destroying its structure and the graphite/NMC532 full cell also exhibited excellent wide-temperature performance. Xie's group [36] developed PC-based wide-temperature electrolytes by tuning the strength and topology of the Li$^+$-PC interactions via non-solvating interactions without altering the solvation structure. By using fluobenzene (FB) as non-solvating cosolvent, the affinity between PC and Li$^+$ was lowered efficiently and the desolvation of electrolyte at graphite surface was also facilitated. As a result, the graphite electrode retains 80% of its initial capacity after 500 cycles and the graphite/NMC811 full cell demonstrated improved electrochemical performance in a wide-temperature range from −40 to 60 °C. These results suggested that co-intercalation of PC-based electrolyte is not only caused by instable SEI but also greatly associated with strong electrostatic interactions of PC-Li$^+$.

### 2.1.2 Carboxylic Esters

Carboxylic esters generally have the advantages of low viscosity and low melting point, favoring lithium-ion transport in the electrolyte. When used as cosolvent in LT electrolytes, they are helpful for the kinetics. However, they generally cannot form stable SEIs by themselves and therefore the use of SEI "enablers" like EC, FEC, and vinylene carbonate (VC) is needed.

Ein-Eli et al. [37] proposed to use methyl formate (MF) as a cosolvent with EC for graphite anodes at LTs. Their results suggested that MF has the advantages of low viscosity, low melting point (−99 °C) and relatively high oxidation

stability. Unfortunately, its reduction product is partially soluble in the electrolyte, hence failing to provide a stable SEI and the improvement of LT performance was not realized [37, 38]. The possibilities of using other carboxylic esters like methyl acetate (MA), ethyl acetate (EA), methyl propionate (MP), ethyl propionate (EP), methyl butyrate (MB), ethyl butyrate (EB), and propyl butyrate (PB) were systematically explored by Smart et al. [39–41]. It was concluded that esters with shorter alkyl chains have the advantage in getting better ionic conductivity for the bulk electrolyte, but the disadvantage in forming more resistive and less protective SEIs as compared to longer chain counterparts. Among various carboxylate esters, MP is particularly promising for LT operation due to its high boiling point of 79.8 °C, extremely low freezing point of −87.5 °C and relatively low viscosity compared to the conventional carbonate solvents. Therefore, LIBs with MP-based electrolytes have been widely investigated within wide operation temperatures. As shown in Fig. 5a, the MP-based electrolyte showed the best performance and delivered the highest capacity at LT (−40 °C). Although using esters as solvent can greatly improve the discharge capacity at LTs due to their desirable melting points and viscosity, a poor SEI formed in such electrolytes was not able to sustain stable long-term cycling under cold conditions. Figure 5b shows the rapid capacity decay at −20 °C when using electrolytes with MA and EA esters (2 and 3), although higher initial capacity was delivered. Therefore, the ester amount in electrolytes was controlled in this study to be below 30% to avoid the poor interphase stability.

Quite interestingly, works from Dahn's group [42] and recently from Chen's group [43] suggested that LT electrolytes containing as much as 90% EA or MP can be used to cycle graphite‖LiNi$_{1-x-y}$Mn$_x$Co$_y$O$_2$ (NMC) and
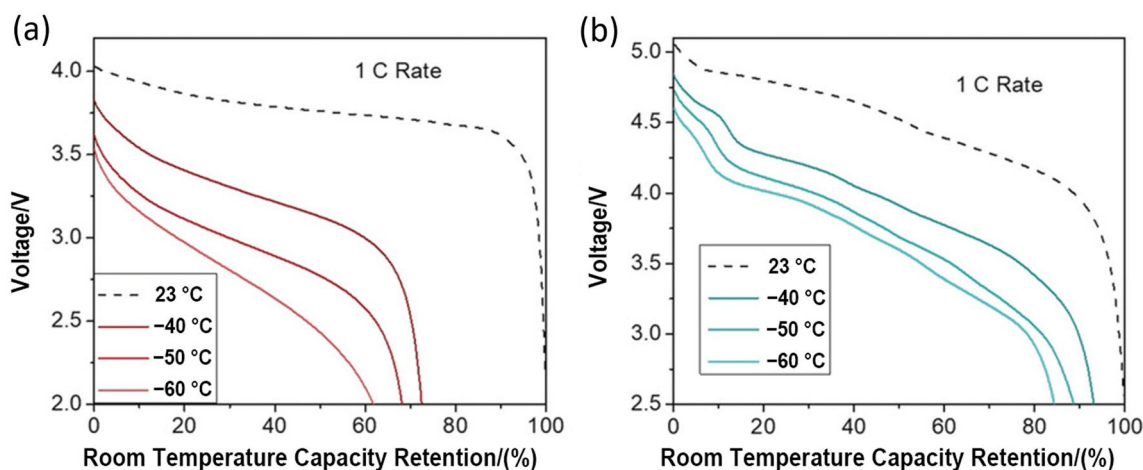
**Fig. 6** Discharge profiles of **a** graphite‖LiCoO$_2$, and **b** graphite‖graphite dual-ion battery (DIB) at different temperatures and 1 C rate using 2 M LiPF$_6$ in MP with 10% FEC. Reprinted with permission from Ref. [43]. Copyright © 2019, John Wiley and Sons

graphite‖LiCoO$_2$ full cells by having certain amount of FEC or VC additives as SEI enablers, thus making it possible to decouple the requirements for bulk ion transport and interphasial consideration. The stable interphase formed by FEC combined with high bulk electrolyte conductivity contributed by MP enabled greatly improved performance, delivering over 60% RT capacity at −60 °C and 1 C rate (Fig. 6a). Meanwhile, high oxidation stability of this electrolyte enabled stable graphite‖graphite cycling with the upper voltage cutoff at 5.2 V for the storage of PF$_6^-$ anion in graphite at the cathode side. Since the cathode chemistry is reversible anion intercalation/deintercalation into graphite, the energy-consuming desolvation process during discharge was eliminated due to the loosely solvated anions. As a result, this graphite‖graphite dual-ion battery (DIB) retained 93.1% and 84.4% of its RT capacity at −40 and −60 °C, respectively (Fig. 6b). Chen's group [44] further demonstrated stable charge and discharge performance of NMC111-graphite pouch cell in MP-based electrolyte at the subzero temperatures of −20 and −40 °C. Combining with FEC additive, MP-based electrolyte formed LiF-rich interphase layer on cathodes and anodes, which prevents the formation of thick CEI/SEI layers as well as metallic Li deposition on graphite anode. The LT performance of MA-based localized high concentration electrolyte (LHCE) with ultrahigh-voltage stability was investigated by Feng et al. [45] using short-chain fluorinated solvent 1,1,2,2-tetrafluoroethyl methyl ether (TFME) as diluent. The electrochemical window of LHCE containing LiBF$_4$ in FEC/MA/TFME solvents is up to 5.4 V, and its ionic conductivity is measured to be 0.803–3.330 mS cm$^{-1}$ in the temperature range from −50 to 25 °C. When the salt concentration is 4 M, the Li/LiNi$_{0.5}$Mn$_{1.5}$O$_4$ (LNMO) cell maintained 80.85% of its RT specific discharge capacity even at the LT of −50 °C. It should be noticed that this

is the first attempt to use LHCE for high-voltage Li/LNMO system at LTs.

To improve the fast-charge capability at LTs by reducing the desolvation energy, a weakly solvated solvent ethyl trifluoroacetate (ETFA) was used as a major component of LT electrolyte coupled with film-forming FEC as cosolvent. Although the low melting point and viscosity of ETFA can reduce Li$^+$ migration barriers at LTs, the weak affinity between ETFA-Li$^+$ can cause low Li$^+$ conductivity of the electrolyte. Therefore, FEC was introduced to enhance the solubility of salt and the stability of SEI [46]. This electrolyte demonstrated excellent compatibility with both LMA and graphite anode at wide-temperature range with fast charging rates. Moreover, the MA-based EC-free electrolyte developed by Zhang's group shows exceptional LT performance [47]. A novel EC-based electrolyte was designed by taking the advantages of muti-components: MA has ultralow viscosity and melting point resulting in better electrolyte performance at LTs; LiFSI is a good SEI formation salt in the absence of EC, while non-polar fluorinated ethers further can extend the liquid range of electrolytes. This electrolyte is featured with the ability to form stable and highly conducting SEIs on graphite, thus preventing Li plating during charging and securing long battery lifetime at subzero temperatures. As a result, the graphite/NCA pouch cell demonstrated extended cycle life at −15 °C with a 0.3 C charge rate and a high capacity retention of 76% of its RT capacity at −50 °C.

Some examples of LT electrolytes using linear carbonates and carboxylic esters as cosolvents are listed in Table 1. It should be noted that caution should be taken in comparing the performance since the results from different chemistry and cell designs are not comparable. This is also true for other tables in this paper.
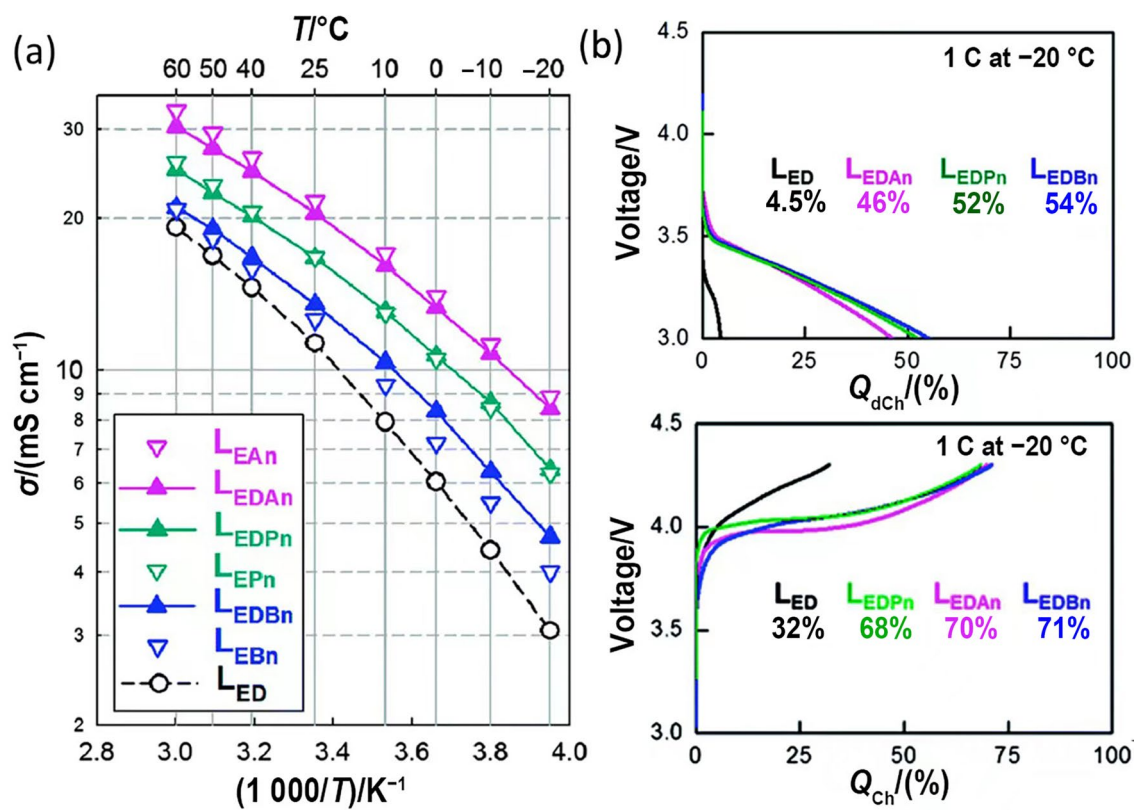
**Fig. 7 a** Ionic conductivity of 1 M LiPF$_6$ in various mixtures of solvents. The subscripts of "L" indicate the type of mixtures with 1:1 ratio of EC:nitrile or 1:1:1 ratio of EC:DMC:nitrile. For example: L$_{EAn}$ represents a mixture of EC and AN, L$_{EDAn}$ represents EC-DMC-AN mixture, L$_{EDPn}$ represents EC-DMC-propionitrile (PN) mixture, L$_{EAn}$ represents EC-PN mixture, L$_{EDBn}$ represents EC-DMC-butyronitrile (BN) mixture, L$_{EBn}$ represents EC-BN mixture, and L$_{ED}$ represents EC-DMC mixture. **b** Discharge and charge curves at −20 °C showing the retention of RT capacity. Capacities at the indicated C rates at ($Q_{LT}$) were normalized by the capacity at 0.2 C and RT ($Q_{RT}$/0.2 C). Reprinted with permission from Ref. [52]. Copyright © 2014, Royal Society of Chemistry

## 2.2 Other Solvents

### 2.2.1 Nitrile

Nitrile, especially acetonitrile (AN), has many excellent properties such as low viscosity, a low melting point and a high dielectric constant, making it a very good solvent for enhancing electrolyte ionic conductivity. Using the same salt LiPF$_6$, the AN-based electrolyte has an ionic conductivity more than twice the value of the EC-DMC-based electrolyte at RT [52]. Such high ionic conductivity is quite desirable for fast charging, as well as LT electrolytes. Unfortunately, AN has the incompatibility issue with graphite anodes because its reduction product fails to form a solid interphase. Therefore, AN must be used together with other solvent/additive that can form protective SEIs to obtain the reversible cycling in lithium-ion full cells. In addition, the potential toxicity of nitrile and nitrile decomposition products also needs to be considered.

Recently, Cho et al. [52] introduced nitriles with varying length of alkyl chains and low melting points into EC or EC-DMC-based electrolyte to lower the freezing point of solvent mixtures. The electrolyte ionic conductivity was greatly improved after introducing nitriles (Fig. 7a). The highly improved bulk ion transport properties effectively increased the discharge/charge capacity of graphite‖NCA full cells at LT (−20 °C) (Fig. 7b). However, pouch cells using electrolytes with shorter alkyl chain nitrile (i.e., AN) with a higher ionic conductivity delivered less discharge capacity at the same condition compared with propionitrile (PN), which has the best retention at −20 °C for RT capacity. This counter-intuitive difference must be attributed to the different interphases formed from the decomposition of these nitriles. Moreover, in all electrolyte systems studied by Cho, 2% FEC was used as SEI additive to relieve the graphite incompatibility issue of nitriles. Hilbig et al. [53] showed similar results, suggesting that AN is helpful for improving lithium-ion transport properties at LT (0 °C) but needs FEC as the additive to enable the reversible cycling for the graphite-anode-based full cells.
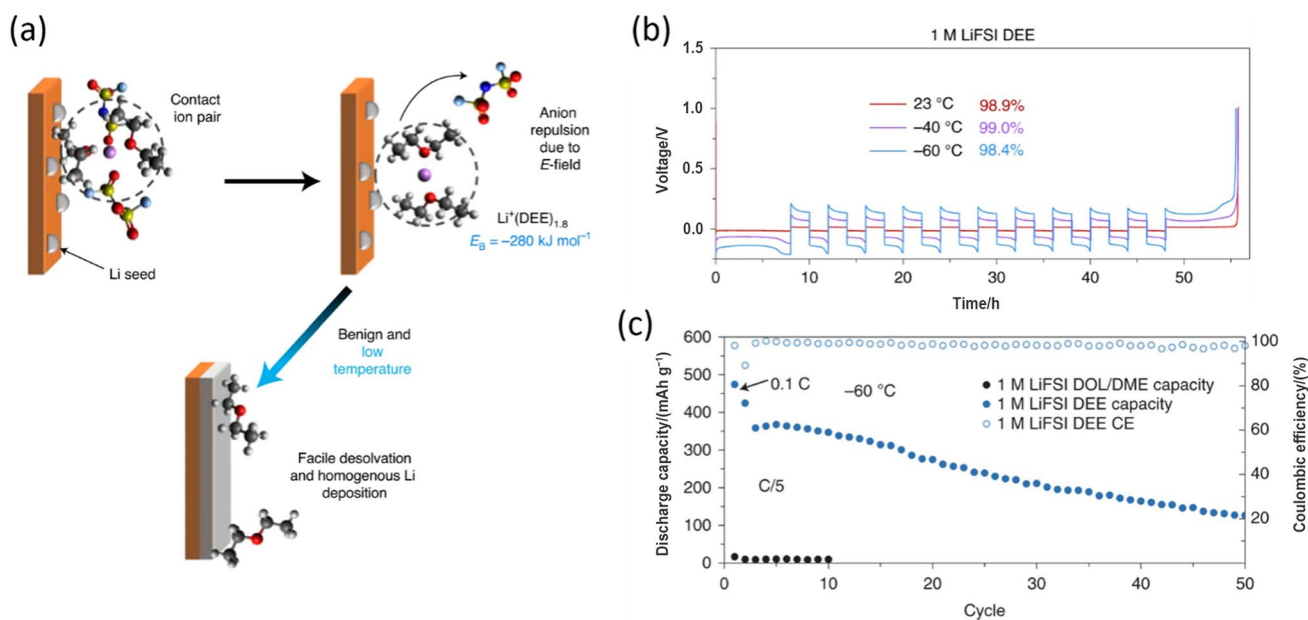
**Fig. 8** **a** Proposed desolvation mechanisms and corresponding Li$^+$/solvent binding energy obtained from quantum chemistry simulations in 1 M LiFSI DEE. **b** Plating/stripping profiles for CE determination in 1 M LiFSI DEE at 0.5 mA cm$^{-2}$ with SEI formation steps omitted. **c** Cycling performance of Li/SPAN using 1 M LiFSI in DEE electrolyte at $-60\,°C$ and 0.2 C. Reprinted with permission from Ref. [57]. Copyright © 2021, Nature publishing group

### 2.2.2 Ethers

Ethers have been considered as promising solvents for LT electrolytes due to the low viscosity and low melting points (Fig. 3). Their low dielectric constant may appear to be beneficial at LT for having lower desolvation energy, but the reality is that most of the ethers solvate Li$^+$ so tightly that the formed solvation cage would not release the coordinated Li$^+$ easily. This is because the ion–solvent interaction is determined by many factors beyond dielectric constants, and "donicity" and "denticity" are two parameters that make ethers an effective solvent for Li$^+$. The former describes the availability of the electron lone pair on the ether oxygen, while the latter relates to the possible chelation conformation that can be formed by ethers with more than one oxygen, as represented by the glymes. Despite low dielectric constant, glymes strongly bind to Li$^+$ resulting in the solvent co-intercalation into graphite electrodes. Armand et al. [54] proposed a family of "hindered glymes" with bulky groups that prevent solvent co-intercalation due to their larger size and lower binding energy to Li$^+$ making the Li$^+$ cation desolvation more favorable than co-intercalation. In addition, the poor oxidative stability largely limits the application of ethers in high-voltage rechargeable batteries. For these reasons, ethers are usually disfavored as an LT electrolyte solvent for Li$^+$. However, the disadvantage of a tightly bound ether solvation cage could be partially overcome by increasing the salt concentration, in which the

Li$^+$ approaches a solvated electrolyte state, as suggested by Watanabe et al. [55], and the desolvation energy becomes minimized by the closely solvation cages or contact-ion-pairs (CIPs). McDowell [56] reported that the Coulombic efficiency of Li metal anodes can be significantly improved at LTs ($-60\,°C$) by adding EC or FEC in the electrolyte of 0.8 M LiTFSI and 0.2 M LiNO$_3$ in DOL-DME solvents to tailor the solvation structure and SEI properties. Recently, Holoubek et al. [57] further advanced this idea by using 1 M LiFSI in DEE, for LT applications in Li metal batteries. Different from typical solvent-separated ion pair (SSIP) solvation structure, DEE electrolytes presented characteristic CIPs with 1.8 DEE oxygens and 2.0 FSI$^-$ oxygens per Li$^+$. Meanwhile, the Li$^+$(DEE)$_{1.8}$ complexes possessed a much lower binding energy of $-280$ kJ mol$^{-1}$ than that of Li$^+$(DME)$_{2.3}$ ($-414$ kJ mol$^{-1}$) formed in 1 M LiFSI in DOL-DME electrolytes shown in Fig. 8a. The low binding energy of Li$^+$(DEE)$_{1.8}$ provided a much favorable desolvation energy barrier to be overcome and resulted in excellent CE (98.4%) of Li/Cu cells at ultra-LTs ($-60\,°C$), as shown in Fig. 8b. Furthermore, LT cycling stability was also greatly improved by using the DEE electrolyte, demonstrated by the stable Li/sulfurized polyacrylonitrile (SPAN) cell cycling for about 50 cycles at $-60\,°C$ and a 0.2 C rate (Fig. 8c). In contrast, the Li/SPAN cell using 1 M LiFSI in DOL/DME failed immediately at $-60\,°C$. To realize the possible utilization of ether-based electrolytes for Ni-rich NMC cathodes, DME-based LHCE systems have been designed with
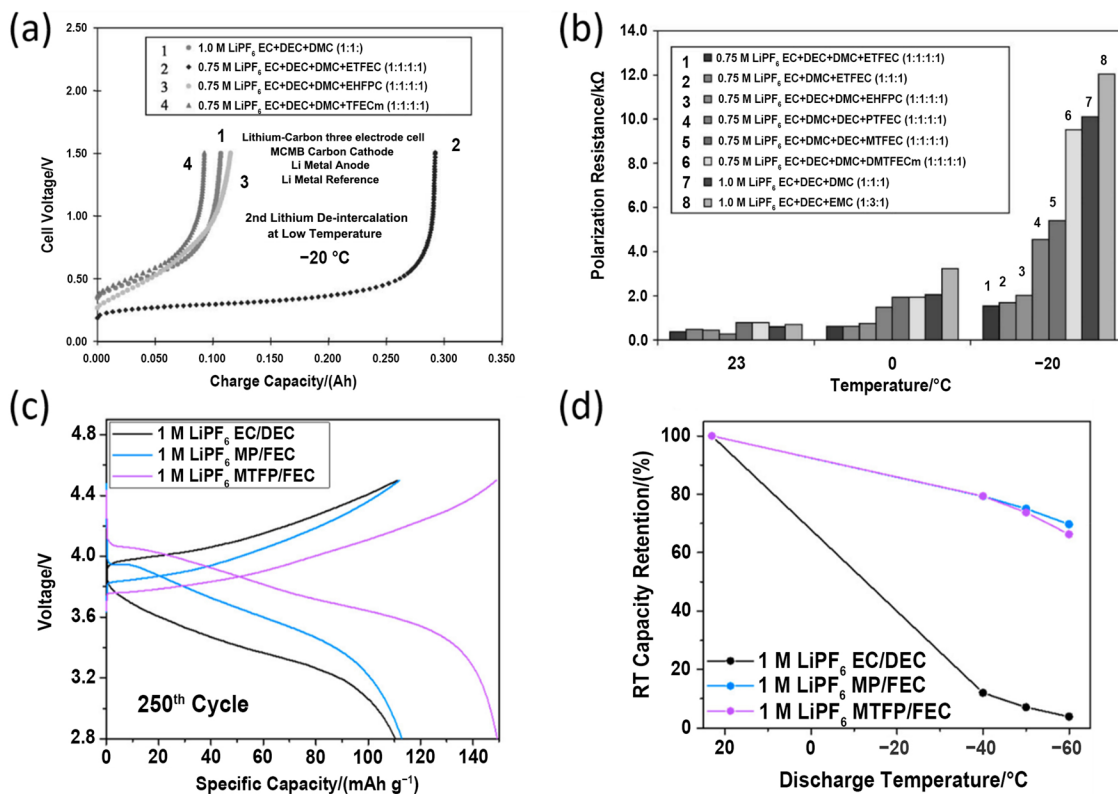
**Fig. 9 a** Lithium deintercalation of MCMB electrodes at −20 °C in contact with different electrolytes follows the lithium intercalation at −20 °C. Cells charged at 50 mA to 1.5 V. **b** Linear polarization resistance calculated from DC micropolarization plots of MCMB-carbon electrodes with different electrolytes at various temperatures. Reprinted with permission from Ref. [64]. Copyright © 2003, Else-vier. **c** Voltage profiles of Li‖NMC811 cells at RT at the 250th cycle. **d** Room-temperature capacity retention of Li‖NMC811 cells using different electrolytes at different temperatures. Reprinted with permission from Ref. [68]. Copyright © 2020, American Chemical Society

bis(2,2,2-trifluoroethyl) ether (BTFE) as the diluent, which allows for the modulation of the degree of ion-pairing while maintaining a relatively low bulk viscosity [58]. Both experimental and theoretical results demonstrated that there is a distinct ion-pairing transition when the local concentration exceeds 4 M (3:1 BTFE/DME ratio), which resulted in stable cycling of LMA and NMC811 cathodes even at LTs.

### 2.2.3 Fluorinated Solvents

In addition to the usage of low melting point and low viscosity solvents mentioned above, the application of fluorinated solvents which could significantly improve the interphase chemistry and oxidation stability has also been extensively investigated for LT electrolytes. Fluorination generally leads to a lower melting point [59], higher oxidation stability [60], better safety characteristics [61], and superior SEI formation capability [62]. Because of these advantages, various fluorinated solvents have been used for LT electrolytes. Here, the applications of fluorinated carbonates, fluorinated carboxylic esters, and fluorinated ethers are discussed.

Although fluorination can lead to higher viscosity (for example, at RT, the viscosity of EMC and fluoroethyl methyl carbonate are 0.68 and 1.4 cP, respectively [63]), the ionic conductivity is not always compromised since some fluorination may lead to higher dielectric constant. More importantly, better SEIs could be obtained by using fluorinated electrolytes. For example, Smart et al. [64] studied a series of fluorinated linear carbonates and found that these electrolytes were able to deliver much higher capacity than the non-fluorinated analogues at −20 °C (Fig. 9a). Among them, the electrolyte with ethyl-2,2,2-trifluoroethyl carbonate (ETFEC) exhibited the highest delivered capacity [64]. This is because fluorinated solvents can form less resistive SEI compared with their non-fluorinated counterparts. As shown in Fig. 9b, SEIs formed by the fluorinated linear carbonates have lower impedance than conventional EC-DEC-based electrolytes. Similar conclusion was reported in a separate study by Cho et al. [65]. Such low-impedance interphase is highly desirable for LT electrolytes, since more deliverable capacity of the whole cell can be obtained.

In addition to the formation of better SEIs, fluorination can also lower the highest occupied molecular orbital (HOMO) that often correlates with the increased oxidation stability of the electrolyte. It should be noted that some misconceptions simply correlating the HOMO with the oxidation stability and the lowest unoccupied molecular orbital (LUMO) with reduction stability of battery electrolytes were thoroughly discussed in the literature [66, 67]. Chen et al. [68] used a fluorinated carboxylic ester as cosolvent for an LT electrolyte and obtained both low viscosity and high oxidation stability. Cycling Li‖NMC811 cell between 2.0 and 4.5 V, the electrolyte using methyl 3,3,3-trifluoropropionate (MTFP)/FEC as the solvent retained 150 mAh g$^{-1}$ capacity after cycling at RT for over 250 cycles, while the cell using non-fluorinated counterpart only retained 110 mAh g$^{-1}$, as shown in Fig. 9c. Furthermore, although MTFP slightly increased the viscosity, after RT charging, the Li‖NMC811 cell using MTFP electrolytes delivered comparable capacity retention (~80%) as MP electrolytes did at −40 °C, which is much higher than that using EC-DEC as solvent (~10 %) (Fig. 9d).

Like carboxylic esters, ethers also have the disadvantage of low oxidation stability. In addressing this problem, fluorination improves the oxidation stability of ethers and shows better compatibility with cathodes while keeping the advantage of low viscosity of ethers. Recently, Wang's group used TTE as a cosolvent in an LT electrolyte (i.e., the salt is LiFSI and other cosolvents are FEMC and FEC) and obtained impressive LT electrochemical performance [62]. The Li‖LiNi$_{0.8}$Co$_{0.15}$Al$_{0.05}$O$_2$ cell can be cycled well using a cutoff voltage of 4.3 V for charging. The ionic conductivity is also superior as demonstrated by the fact that even at −85 °C, the cell can still deliver ~50 % of its room-temperature capacity.

In addition to the well-known carbonate, ester and ether solvents, several novel solvents have been also introduced in LT LIB systems as cosolvents or additives. A novel cosolvent of 2,2,2-trifluoroethyl N-caproate (TFENH) could help to lower the viscosity and improve the ionic conductivity of electrolytes, due to the priority distribution of TFENH in bulk electrolytes, which results in improved cycling stability and capacity retention of LiCoO$_2$/graphite cell at −35 °C compared to that with commercial carbonate-based electrolytes [69]. Lu et al. also explored electrochemical performance of a graphite anode at different subzero temperatures in an electrolyte with 25% TFENH as cosolvent, and demonstrated that at a relatively higher charge rate of 0.2 C, the graphite anode maintained 92% of RT capacity at −50 °C. Such enhanced performance is attributed to the formation of a thin and stable SEI on the surface of graphite to reduce charge transfer resistance [70].

### 2.2.4 Gel Polymer Electrolytes

In general, the lower ionic conductivity of gel polymer electrolytes might suggest that they are a poor candidate for LT battery operation [71]. However, good results have been obtained when Smart et al. [72] studied the electrochemical performance of gel polymer electrolytes which were impregnated with both all carbonate-based electrolytes and linear carboxyl ester containing solutions, in prototype 7 Ah cells manufactured by LG Chem. Interestingly, the gel polymer cells showed excellent performance at LTs. The gel polymer cell containing electrolyte of 1 M LiPF$_6$ in EC:DEC:DMC:EMC (1:1:1:3, volume ratio) delivered nearly full (> 99%) RT capacity when discharged at −40 °C using a C/10 rate (Fig. 10a). After increasing the discharge rate to C/5, this cell still delivered over 94% of RT capacity. Other gel polymer cell systems containing MB or EB as cosolvent also showed exceptionally good performance at ultra-LTs (from −60 to −80 °C). The cell using MB-based electrolytes delivered 80% of its RT capacity when discharged at −60 °C (Fig. 10b). This work suggested that the ionic conductivity of polymer electrolytes is largely affected by the liquid electrolyte components. Therefore, other promising LT liquid electrolytes could also be applied in gel polymer electrolytes to obtain desirable improved safety characteristics.

Polymer could also be utilized as cosolvent for preparing LT electrolytes. Recently, Kasprzyk et al. [73] prepared a new type of non-crystallizing solvent by mixing EC with poly(ethylene glycol) dimethyl ether (PEG250). Because of the special interactions between planar EC and PEG250 chain, this mixture exhibited a super low glass transition temperature in the range from −93 to −95 °C, and an ionic conductivity of 0.014 mS cm$^{-1}$ at −60 °C. Coupling with their compatibility in a Li‖LFP battery, this new electrolyte demonstrated great potential for extreme LT battery applications.

### 2.2.5 Liquified Gas Electrolytes (LGEs)

Apart from commonly used liquid and gel polymer electrolytes mentioned above, a recently proposed LGE concept takes advantage of the extremely low viscosity and melting points of fluorinated and semifluorinated gases that become liquids capable of dissolving lithium salts as liquified gas electrolytes, which opens a new frontier, using liquified solvents at LTs or moderate pressure from the gas state at RT. Although liquified gas solvents have a moderate dielectric constant (10–15), their super low viscosity and superior dielectric-fluidity factor make them highly promising for LT applications [74]. A liquified gas electrolyte with a formulation of 0.2 M LiTFSI in fluoromethane (FM)
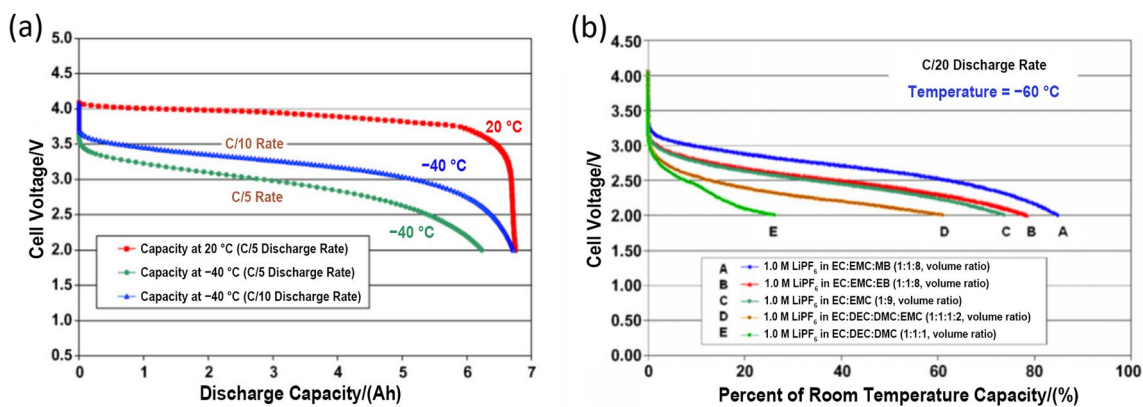
**Fig. 10 a** Discharge capacity (Ah) of a 7 Ah cell using a polymer gel electrolyte containing 1.0 M LiPF$_6$ in EC:DEC:DMC:EMC (1:1:1:3%, volume ratio) at $-40$ °C using C/5 (1.40 A) and C/10 (0.700 A) discharge rates to 2.0 V, compared to the performance obtained at 23 °C. (Cell charged to 4.1 V at RT prior to the discharge at LT.) **b** Discharge capacity (Ah) of a 7 Ah cell containing various LT polymer gel electrolytes at $-60$ °C using a C/20 (0.35 A) discharge rate to 2.0 V. (Cells charged to 4.1 V at RT prior to the discharge at LT using a C/5 charge rate.) Reprinted with permission from Ref. [72]. Copyright © 2007, Elsevier

with carbon dioxide ($CO_2$) as additive was tested by using a Li‖LiCoO$_2$ half-cell. At $-10$ °C and C/10, the FM electrolyte retained 98.3% of its RT capacity, while the EC-DEC electrolyte only delivered 86.2%, as shown in Fig. 11a. This excellent LT performance was due to not only the exceptionally good ionic conductivity of the liquified gas, but also the excellent interphase formed in the FM electrolyte. Based on XPS results, SEI composition generated in different electrolytes is plotted in Fig. 11b. In contrast to the polymer-like SEIs formed in conventional carbonate electrolytes with

high impedance, a ceramic-like SEI with high Li mobility through the grain boundaries was generated on Li foil using the FM electrolyte, enabling facile Li transportation through the interphase.

Initial formulations suffered from low salt solubility and conductivity causing limited rate performance and temperature range. Usage of the stronger (compared to semi-fluorinated short alkanes) Li$^+$ coordinating nitriles such as acetonitrile, linear and cyclic ether cosolvents improved salt dissociation and solubility resulting in a substantial increase
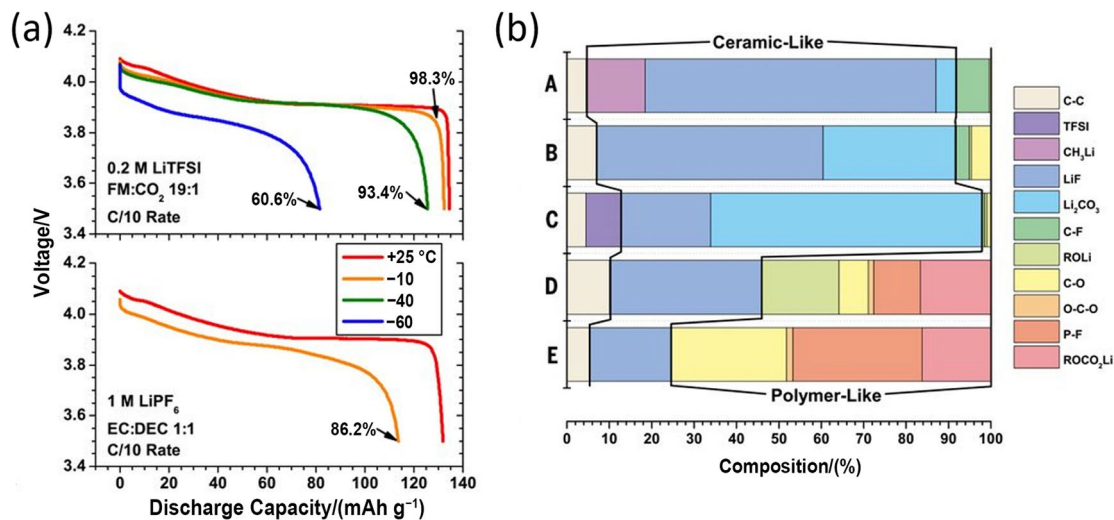


**Fig. 11 a** Comparison of voltage versus discharge capacity over various temperatures at the C/10 rate of a LiCoO$_2$ electrode with a Li metal anode using liquified gas electrolytes and conventional electrolytes. **b** Composition percentage of Li metal surface products calculated from XPS results: Li metal after being (A) submerged in FM for three days, (B) submerged in FM:CO$_2$ (19:1) for three days, (C) cycled 400 times in 0.2 M LiTFSI in FM:CO$_2$ (19:1), (D) submerged in 1 M LiPF$_6$ in EC:DEC (1:1) for 3 days, and (E) cycled 400 times in 1 M LiPF$_6$ in EC:DEC (1:1). No washing of the Li electrode was done before XPS analysis. Reprinted with permission from Ref. [74]. Copyright © 2017, American Association for the Advancement of Science (AAAS)

of the Li$^+$ charge carriers, especially at lower temperatures, without sacrificing their mobility [75–77]. Excellent conductivity (> 4 mS cm$^{-1}$) was reported from −78 to 75 °C with an unexpectedly high lithium transference number ($t_+$) of 0.72 [76]. High $t_+$ was attributed to the existence of free solvent separated Li$^+$ that moved in the low viscosity liquefied solvent while all anions were part of the larger and slower moving ionic aggregates. Importantly, during nail penetration test performed on cells with LGEs, the non-toxic solvent rapidly evaporated and immediately escaped after penetration. The cells cooled down and the electrolyte conductivity dropped as a result of the solvent evaporation which shut down the ion transport and thermal runaway reactions [77]. Meng's group [78] recently developed a novel LGE by adding the simplest (liquefied) ether to a non-flammable low-solvating hydrofluorocarbon mixture. The LGE based on 1,1,1,2-tetrafluoroethane and pentafluoroethane delivered high ionic conductivity > 3 mS cm$^{-1}$ within the temperature range from −78 to 80 °C, with non-flammable and fire-extinguishing features. In rationally designed LGEs, solvated FSI$^-$ and dimethyl ether (Me$_2$O) dominate the solvation structure, which is believed to reduce the free Me$_2$O solvent amount leading to the improvement of the oxidative stability and the salt decomposition to form a LiF-rich SEI on the anode. As a result of the beneficial solvation chemistry and a fluorine-rich environment, a lithium cycling at > 99% Coulombic efficiency for over 200 cycles at 3 mA cm$^{-2}$ and 3 mAh cm$^{-2}$ was demonstrated. Moreover, within the wide-temperature range, LMBs retained Coulombic efficiencies of 97.3%, 97.2%, 95.2% and 91.0% at 0, −20, −40 and −60 °C, respectively. The LGE with oxidation stability up to 4.4 V enabled Li/NMC622 cells exhibiting stable cycling properties from −60 to 55 °C.

### 2.2.6 Aqueous Electrolytes

In addition to the non-aqueous electrolytes, LIBs with aqueous electrolytes have received widespread attention for large-scale energy storage due to their high safety, low cost, environmental amity and higher ionic conductivity compared with commercial LIBs using carbonate electrolytes. However, a narrow electrochemical stability window of 1.23 V and poor LT performance including low power density and severe capacity degradation are also critical issues to be addressed. Several strategies such as designing water-in-salt electrolytes (WiSEs) and hydrate melt electrolytes, introducing cosolvents as well as regulating interphasial chemistry have been used for widening the working voltage and improving the wide-temperature performance of aqueous LIBs. Suo et al. [79] firstly developed WiSEs to broaden the voltage window of electrolytes to 3 V, where a high concentration (21 M) of LiTFSI salt was dissolved in water and an anion-derived SEI was formed to inhibit

the decomposition of water. Although the WiSE effectively brings the freezing point down, the salt will crystallize out when the concentration of salt exceeds a certain threshold. Therefore, the composition and concentration of aqueous electrolytes need to be properly balanced. To understand the limiting step at subzero temperatures, Yushin et al. comprehensively investigated the performance of LCO electrodes using water-based electrolyte solutions based on three different low-cost inorganic salts (LiNO$_3$, Li$_2$SO$_4$, LiCl) and proposed that charge transfer resistance is the largest impedance contributor at LTs [80]. Among various electrolytes, the water-based electrolyte using LiCl salt for the LCO cathode cell retained nearly 72% of its RT capacity at −40 °C, which is much higher than that of traditional organic electrolytes. In WiSE, the freezing point can be lowered by choosing appropriate salts, and the composition of SEIs can be also tuned accordingly. The hybrid non-aqueous/aqueous electrolyte system using cosolvent inherits the key physicochemical advantages of both solvents and demonstrated promising electrochemical performance. DMSO, as hydrogen bond acceptor, can mix with water with any ratio and the freezing temperature of DMSO/water mixture could be as low as about −140 °C, and therefore has been used as cosolvent/additive for aqueous LIBs. Tao's group [81] designed an ultralow freezing point electrolyte using DMSO as additive with 0.3 molar fraction, enabling a capacity retention as high as 60% of its RT capacity at −50 °C. Ethylene glycol (EG) is a well-known antifreeze additive with a high dielectric constant ($\varepsilon = 37$ at 25 °C), which can reduce the freezing point of aqueous electrolyte to be lower than −24 °C. By adding EG as additive, the LT rate performance of LiFePO$_4$ cathode at −20 °C has been successfully optimized due to the improved ionic mobility [82]. Acetonitrile (AN) itself possesses a low freezing point, high $\varepsilon$ and best oxidation stability over than 5 V, widely used as cosolvent/additive for non-aqueous LIBs for extending operation voltage. In acetonitrile/water in salt hybrid electrolytes, electrostatic cation–anion attractions weakened due to the spatial isolation caused by acetonitrile molecules, while the coordination between water molecules and Li$^+$ enhanced. As a result, the hybrid WiSE with an optimal concentration of 5 M demonstrates improved conductivity, decreased viscosity and a lowered freezing temperature compared to the 21 M WiSE [83]. To extend the working voltage limit of aqueous electrolytes, Xu's group [84] increased the salt concentration of LiTFSI to 15.3 M in AN-WiSE, where the presence of interfacial water at the negatively charged electrode surface has been minimized, resulting in uniform and thin interphase consisting of an organic outer layer based on nitrile and sulfamide species and an inner layer rich in LiF. More importantly, the stable electrochemical window has been expended to 4.5 V, enabling a LiMn$_2$O$_4$/

$Li_4Ti_5O_{12}$ full cell with excellent cycling stability and rate capability at both ambient and sub-ambient temperatures. Recently, a new concentrated aqueous/non-aqueous electrolyte has been designed by Ma et al. [85] using DOL. This electrolyte has high stability against reduction, low viscosity and a low freezing point. The water/DOL hybrid electrolyte displays a stable electrochemical window of 4.7 V, which is attributed to the reduced content of the free water molecules at the anode surface, leading to robust LiF-rich SEI formation that substantially suppresses hydrogen evolution. At LTs, the remaining liquid phase predominantly consists of the $Li^+$-DOL solvation complex, whose weak binding energy benefits the $Li^+$ desolvation process at the electrode, as evidenced by the low activation energy barrier and the high exchange current density for $Li^+$ de/intercalation to electrodes. In another work reported by Liu's group [86], sulfolane (SL) was selected as the cosolvent of antifreeze and the activity inhibitor of water, because of its low toxicity, high miscibility with water, high oxidation stability and strong interaction with water molecules. An expanded electrochemical stability window of 3.8 V has been achieved due to the formation of SL contained solvation sheath and strengthen O–H bond of water, inhibiting the decomposition of water. In this electrolyte, SL and water molecules can separate each other without forming a large-scale hydrogen bond network and $LiClO_4$ can also break the hydrogen bond network further acting as a fluxing agent, it can suppress aggregation and crystallization of electrolyte components, as well as reduce the glass-transition temperature of the electrolyte to −110 °C. As a result, the LMO/LTO full cell demonstrated a high operating voltage of 2.7 V and excellent electrochemical performance with an ultrahigh specific capacity retention ratio up to 98% from 0 to −20 °C. Although, WiSE presented promising LT performance, the super-high concentration of these toxic Li salts in WIS electrolytes raises concerns of high cost, high viscosity, poor wettability toward electrodes, and environmental hazards. Therefore, Wang's group [87] developed localized water-in-salt electrolytes (LWiSEs) with low-cost and high safety for aqueous lithium-ion batteries, in which they used inexpensive and eco-friendly $LiNO_3$ salt to replace the toxic and costly Li salts, and lowered the electrolyte salt concentration by introducing diluents that dissolve the water but not the inorganic salts. As discussed in the previous sections, tremendous efforts have been made for improving the LT performance of non-aqueous LIBs using various electrolyte additives while there is still plenty of room for exploring additives with low melting points and low viscosity.
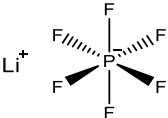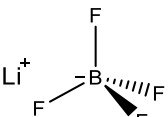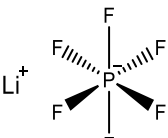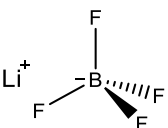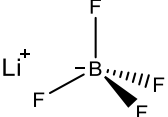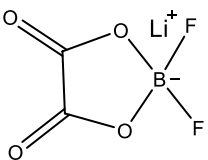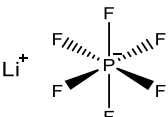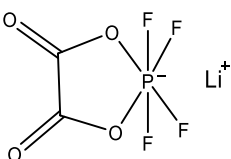
## 3 Salts

From the cation–anion dissociation perspective for salt selections, larger anions are more desirable than the smaller ones, because the negative charge is more delocalized, which in turn reduces the Coulombic attraction between counterions. For those complex anions, substitutions of functional groups with high electronegativity are also desired, because they can effectively pull away the formal charge from the central atom. For these two reasons, salts with large anions and high degree of fluorination, such as $PF_6^-$, $BF_4^-$, $TFSI^-$ and $FSI^-$, are easier to dissociate than those with small anions. However, excessively large anions can lead to low mobility which is adverse for ion transport, which can be seen in the examples of bis[(pentafluoroethyl)sulfonyl]imide (BETI) or other poly-TFSI anions. Therefore, the anion in the lithium salt should have the appropriate size being neither too big nor too small. Considering all these parameters, $LiPF_6$ represents an excellent balanced property compared to other salts, such as $LiBF_4$, $LiClO_4$, and $LiAsF_6$. However, bulk electrolyte conductivity is not the only attribute that needs to be considered in selecting salts. The chemical and electrochemical stability, compatibility with the cathode and anode, the impedance, the contribution to interphasial chemistry, as well as the cost and toxicity are also very important and need to be considered. Different salts used for LT electrolytes are summarized in Table 3.

As the most commonly used salt in organic electrolytes, $LiPF_6$ is the first choice for LT electrolytes. However, its sensitivity to moisture results in HF formation, which induces transition metal dissolution of NMCs, resulting in cell degradation. Therefore, alternative salts have been investigated for LIBs to enhance the cyclic performance. For example, 1 M $LiAsF_6$ in EC:EMC:MA:toluene (1:1:1:1, volume ratio) quaternary solvents displayed high ionic conductivity values as 1.830 and 1.100 mS $cm^{-1}$ at −40 and −50 °C, respectively [94]. Zhang et al. [95] found that although a $LiBF_4$-based electrolyte has an overall lower ionic conductivity than the electrolyte using $LiPF_6$, it delivered higher capacity at −30 °C than the $LiPF_6$-based electrolyte, as shown in Fig. 12a. Based on the EIS results, the impedance of the electrolytes using these two salts are plotted in Fig. 12b. It can be clearly seen that the interphase impedance, especially the charge transfer resistance of the $LiBF_4$-based electrolyte, is lower than that of the $LiPF_6$-based electrolyte, showing the origin of the capacity difference. Other study also suggested that $LiBF_4$-based electrolytes demonstrate great potential for LT operation, while hydrolysis susceptibility, relatively low ionic conductivity, and inefficient SEI formation capability are issues needed to be addressed.

Oxalate-based anions can form good SEIs themselves; hence, their presence can potentially enable the application

**Table 3**  Various salts used for LT electrolytes

| Electrolyte | Salt | Salt structure | Cell system | [Capacity/(mAh g$^{-1}$) or capacity retention]/(current density or C rate)/(temperature/°C) | References |
|---|---|---|---|---|---|
| 1 M LiPF$_6$ in PC:EC:EMC (1:1:3) with 1.0% (weight percentage) VC | LiPF$_6$ | | Graphite\|\|lithium nickel-based mixed oxide | E1: 72%/0.5 mA cm$^{-2}$/−30<br>E1: ~0/0.5 mA cm$^{-2}$/−50 | [95] |
| 1 M LiBF$_4$ in PC:EC:EMC (1:1:3) with 1.0% (weight percentage) VC | LiBF$_4$ | | Graphite\|\|lithium nickel-based mixed oxide | 86%/0.5 mA cm$^{-2}$/−30<br>~20%/0.5 mA cm$^{-2}$/−50 | [95] |
| 1 M LiPF$_6$ in EC:EMC:GBL (1:1:1) | LiPF$_6$ | | Graphite\|\|lithium nickel-based mixed oxide | 76%/NA/−20<br>62%/NA/−30 | [109] |
| 1 M LiBF$_4$ in EC:EMC:GBL (1:1:1) | LiBF$_4$ | | Graphite\|\|lithium nickel-based mixed oxide | 89%/NA/−20<br>74%/NA/−30 | [109] |
| 1 M LiBF$_4$ in PC:EC:EMC (1:1:3) with 2.0% (molar percentage) LiBOB | LiBF$_4$ | | Graphite\|\|LiNiO$_2$ | 63%/0.5 mA cm$^{-2}$/−40<br>83%/0.5 mA cm$^{-2}$/−30 | [99] |
| 1.0 M LiDFOB in PC:EC:EMC (3:3:4) | LiDFOB | | Graphite\|\|LiNi$_{0.80}$Co$_{0.15}$Al$_{0.05}$O$_2$ | 67.4%/0.45 C/−30<br>81.7%/0.45 C/−20 | [96] |
| 1.2 M LiPF$_6$ in EC:EMC (3:7) | LiPF$_6$ | | Graphite\|\|NMC111 | ~100/0.1 C/−10 | [98] |
| 1.2 M LiPF$_4$(C$_2$O$_4$) in PC:EMC (3:7) | LiPF$_4$(C$_2$O$_4$) | | Graphite\|\|NMC111 | ~100/0.1 C/−10 | [98] |

of solvents like PC and GBL, which have the advantage of low melting points, but suffer from the problem of poor SEI formation [96–100]. However, in those cases, the high impedance of oxalate-derived SEI causes another problem for LT electrolytes. Lucht et al. [101] designed a novel electrolyte, 1 M LiDFOB GBL:MB (1:1) [LiDFOB: lithium difluoro(oxalato)borate], with higher ionic conductivity at −10 °C but delivering relatively lower discharge capacity than the LiPF$_6$-based electrolyte (Fig. 12c), which can be attributed to the larger SEI resistance resulted from LiDFOB decomposition (Fig. 12d). Based on these considerations,

oxalate-based salts are not good candidates as major salts, but more often used as additives or cosalts. To combine the good ionic conductivity of LiBF$_4$ and decent SEI formation capability from LiBOB, a LiBF$_4$:LiBOB (9:1, molar ratio) dual-salt system was developed by Xu et al. [99, 102], in PC/EC/EMC ternary solvent the Li-LiFePO$_4$ (LFP) cell showed enhanced cyclic performance in a wide-temperature range from −50 to 90 °C. The LiDFOB-LiBF$_4$ dual-salt in EC/dimethyl sulfite (DMS)/EMC solvents also showed an acceptable ionic conductivity of 1 mS cm$^{-1}$ at −40 °C, especially enhanced capacity retention at LTs. Zhang et al. [103]
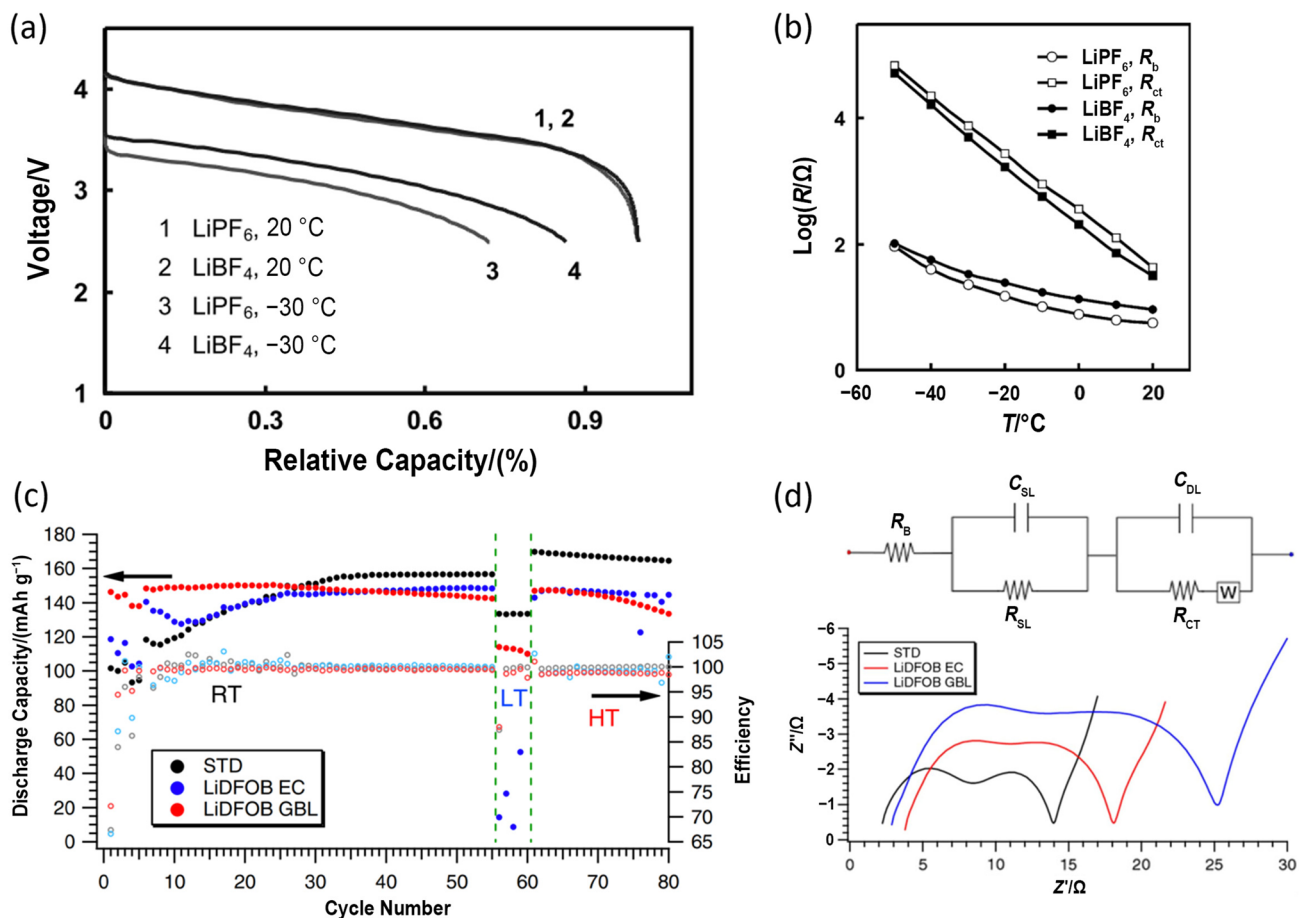
**Fig. 12 a** Effect of salts on the discharge voltage and capacity of Li-ion cells at 0.5 mA cm$^{-2}$. **b** Temperature dependence of $R_b$ and $R_{ct}$ of the Li-ion cells with different salts. Reprinted with permission from Ref. [95]. Copyright © 2002, Elsevier. **c** Cycling performance for various electrolyte formulations. The first 55 cycles were at RT (16 °C), the next five were at LT (−10 °C), and the last 20 were at high temperature (HT, 55 °C). **d** EIS after 25 cycles at 16 °C. STD denotes 1 M LiPF$_6$ in 1:1:1 EC:DMC:DEC; LiDFOB EC denotes LiDFOB/EC/DMC/DEC electrolyte formulation; and LiDFOB GBL denotes LiDFOB/GBL/MB formulation. Reprinted with permission from Ref. [101]. Copyright © 2015, IOP publishing group

comprehensively investigated the LT performance of dual-salt electrolyte systems with different LiBF$_4$/LiDFOB ratios. Compared to the pure LiBF$_4$ single salt system, the electrolyte with LiDFOB exhibited increased ionic conductivity due to its larger anionic radius and good dissociation with solvents. The dual-salt electrolyte with a LiBF$_4$:LiDFOB ratio of 8:2 enabled LiCoO$_2$ cathodes with a high capacity retention of 98.67% at −20 °C after 300 cycles.

LiTFSI and LiFSI salts have attracted a lot of attention recently, due to their high solubility in aprotic solvents enabled by the stabilization of the negative charge provided by the strong electron-withdrawing group (−CF$_3$ or −F) [6]. When the electrolytes containing high concentration of these salts are used in Li metal anode cells, they can form salt anion-derived SEI with a LiF-rich component which is beneficial for anode protection and electrochemical performance [104]. However, when it comes to LT application, the high viscosity of high

concentration electrolyte (HCE) is a problem. An effective measure to address this issue is to introduce diluents (i.e., hydrofluoroethers) to form the LHCE which has the advantages of both good SEI formation capability and low viscosity [62, 105–107]. Such strategy has been used to extend the operating temperature of lithium metal batteries as presented by Zhao and coworkers [108]. A novel LHCE system has been designed by using LiTFSI and LiDFOB as dual-salt, inexpensive and commonly used TMS (sulfolane) and EA as solvents and HFE (hydrofluoroether) as diluent. The synergistic effect of multiple components prevents the freezing of the electrolyte even at −80 °C, thus enabling an NMC532-Li cell having 75% RT capacity at −40 °C, and fast-charge/discharge cyclic stability at a 1 C rate.

# 4 Additives

Introducing additives is a very effective and cost-efficient approach to modifing certain properties of electrolytes. Since only a small amount of additive is used, the negative impact to the electrolyte bulk properties such as viscosity and dielectric constant is minimized. Therefore, additives are especially favored by the LIB industry, because the advantages of widely used carbonate-based electrolyte systems can be utilized and their disadvantages can be effectively reduced by additives.

The choice of additives depends on the desired functionalities, such as stabilizing the interphase, improving the electrolyte safety, and decreasing the interphase impedance. For LT electrolyte application, decreasing the interphase impedance is particularly important since it can improve the overall kinetics of the cell and offset the negative effects on transport property caused by the LT. Therefore, this review focuses more on those additives that have direct effects on decreasing the interphase impedance. Additives are categorized as molecular-type and ionic-type, and their LT performance is summarized in Table 4 and Table 5, respectively.

## 4.1 Molecular Additives
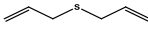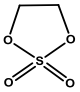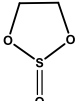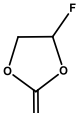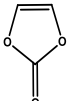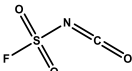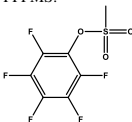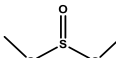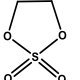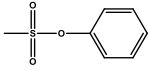
Sulfur-containing compounds, such as 1,3,2-dioxathiolane-2,2-dioxide (DTD) and 1,3-propanesultone (1,3-PS), have been extensively studied as electrolyte additives to form stable SEI layers on graphite and suppress graphite exfoliation in PC-based electrolytes. Moreover, it has been reported that some sulfur-containing additives result in SEI layers that are less resistive [33]. This excellent property makes them promising candidates for LT applications. Recently, Yang's group [110] compared the LT performance of three different common sulfur-containing additives, DTD, 1,3-PS, and ethylene sulfite (ES) (Fig. 13). The electrolyte using DTD additive has the highest cycling capacity retention at −15 °C due to its lowest impedance, which distinctly improved the LT battery performance. On the other hand, although both 1,3-PS and ES can provide SEI protection for graphite electrode, their high impedance negatively affected the electrochemical cycling performance. The electrolyte using 1,3-PS delivered even lower capacity at LT compared to the electrolyte withou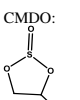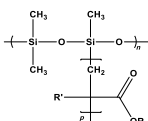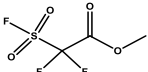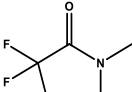t additive. The high ionic conductivity of DTD-derived SEIs observed in this work is in good agreement with the results previously reported in the literature by other groups, in which it was attributed to the reduction products such as $Li_2SO_3$ and $ROSO_2Li$ [111]. However, there are discrepancies about the ionic conductivity of 1,3-PS-derived SEIs reported [112]. Lucht's group observed high ionic conductivity of 1,3-PS-derived SEIs and attributed it to the reduction product of lithium alkylsulfonate ($RSO_3Li$), while

others reported low ionic conductivity of 1,3-PS-derived SEI [112]. In addition to 1,3-PS and DTD, DMS and methylene methanedisulfonate (MMDS) have also been studied, showing capability for low-impedance SEI formation [113–115]. Furthermore, in addition to the sulfur-containing additives mentioned above, elemental sulfur and allyl disulfide were also reported to have the capability to reduce SEI impedance as well, which can effectively improve LT battery performance [116, 117].

Organophosphates have attracted a lot of attention as electrolyte additive for reducing the flammability and enhancing the oxidation stability of electrolytes [118]. As a typical example, tris(trimethylsilyl)phosphite (TMSP) demonstrated stable film-forming capability at both cathodes and anodes [119, 120]. Xu et al. [121] compared electrochemical performance of LIBs with different additives such as FEC, PS, VC and TMSP. Graphite-NMC full cell exhibited superior performance at −40 °C with 0.5% TMSP additive, which is contributed to the formation of robust and ultrathin CEI on cathodes and consuming HF produced in $LiPF_6$-based electrolytes during cycling. Later, Cui's group developed binary functional additives containing high-voltage electrolytes for wide-temperature application [122]. The synergistic effect of TMSP and 1,3-propanediolcyclic sulfate (PCS) additives in ester-based electrolytes significantly enhanced the cycling performance of the high-voltage LNMO/MCMB full cell in the temperature range from −60 to 50 °C by generating species like P-O, $ROSO_2Li$ and $Li_2SO_4$ on MCMB anode, and suppressing the side reaction between ester solvent and MCMB.

As mentioned in the solvent section, fluorinated compounds have been widely used as cosolvents owing to their excellent SEI film-forming abilities. Considering the problem of increased viscosity if a large percentage of fluorinated compounds is used, researchers have also studied the application of using small amount of them as electrolyte additives to take advantage of the better SEI structures, while minimizing their negative impact on viscosity. Normally, LiF is the main decomposition product from fluorinated compound additive, which is favorable to form mechanically stronger, more flexible and stabler surface film to protect electrodes. Some researchers also believed that the incorporation of LiF in the SEI helps ionic transportation. FEC is a widely used and extensively studied additive in LIB and LMA systems, as it can participate in SEI formation due to its higher reduction potential compared to non-fluorinated carbonates, enhancing its capability in forming a LiF-rich SEI to protect graphite and LMA, which in turn improves the cycling stability and capacity retention at RT [123, 124]. In addition to the merits of FEC at RT, using FEC as an additive to improve LT LIB performance has also been reported. By using conventional carbonate electrolyte with FEC as the additive, it was reported that a capacity

**Table 4** LT electrolytes using molecule additives; wt% means the weight percentage

| Electrolyte | Additive | Additive molecule structure | Cell system | [Capacity/(mAh g$^{-1}$) or capacity retention]/(current density or C rate)/ (temperature/°C) | References |
|---|---|---|---|---|---|
| 1 M LiPF$_6$ in EC:EMC:DEC (3:2:5) | 0.5 wt% sulfur additive in graphite electrode | NA | Li‖graphite | ~47 mAh g$^{-1}$/0.05 C/−30 | [116] |
| 1 M LiPF$_6$ in EC:EMC:DEC (3:2:5) | 2 wt% allyl sulfide | | Li‖graphite | ~60 mAh g$^{-1}$/0.05 C/−30 | [117] |
| 1 M LiPF$_6$ in EC:EMC (3:7) | 1% DTD | | Li‖graphite | Cycling: 111 mAh g$^{-1}$/50/0.2 C/−15 | [110] |
| 1 M LiPF$_6$ in EC:EMC (3:7) | 1% ES | | Li‖graphite | Cycling: 50 mAh g$^{-1}$/50/0.2 C/−15 | [110] |
| 1 M LiPF$_6$ in EC:DMC:EMC (1:1:1) | 2% FEC | | Li‖graphite | 320 mAh g$^{-1}$/0.067 C/−20 | [125] |
| 1.2 M LiPF$_6$ in EC:EMC:MB (2:2:6) | 2% VC | | MCMB‖LiNi$_x$Co$_{1-x}$O$_2$ | 90.06%/25 mA/−20 76.43%/25 mA/−40 | [132] |
| 1 M LiPF$_6$ in EC:DMC (1:1) | 2 wt% fluorosulfonyl isocyanate (FI) | | Li‖graphite | ~350 mAh g$^{-1}$/0.1 C/0 ~80 mAh g$^{-1}$/0.1 C/−20 | [128] |
| 1 M LiPF$_6$ in EC:EMC (1:2) | 1.0 wt% 2,3,4,5,6-pentafluorophenyl methanesulfonate (PFPMS) | PFPMS: | Graphite‖NMC532 | 66.3%/0.5 C/−20 | [129] |
| 1 M LiPF$_6$ in EC:EMC (1:2) | 0.5 wt% dimethyl sulfite (DMS) | | Graphite‖NMC532 | 82.13%/0.2 C/−20 74.28%/0.5 C/−20 Cycling: 98.84%/50/0.2C/−10 | [130] |
| 1 M LiPF$_6$ in EC:EMC (1:2) | 0.5 wt% 1,3,2-dioxathiolane 2,2-dioxide (DTD) | | Graphite‖NMC532 | 72.59%/0.2 C/−20 68.64%/0.5 C/−20 Cycling: 81.14%/50/0.2 C/−10 | [130] |
| 1 M LiPF$_6$ in EC:EMC (1:2) | 1 wt% phenyl methanesulfonate (PhMS) | | Graphite‖NMC532 | 89.1%/0.5 C/0 82.0%/0.5 C/−10 67.4%/0.5 C/−20 Cycling: 73.8%/100/0.2 C/−10 | [131] |
| 1 M LiPF$_6$ in PC:DMC | 2 vol% 4-chloromethyl-1,3,2-dioxathiolane-2-oxide (CMDO) + 5 vol% FEC | CMDO: | Li‖MCMB | 26.4 mAh g$^{-1}$/0.1 C/−10 | [33] |
| 1 M LiPF$_6$ in PC:DMC | 2 vol% CMDO + 3 vol% EC + 5 vol% FEC | | Li‖MCMB | 90.5 mAh g$^{-1}$/0.1 C/−10 | [33] |
| 1 M LiPF$_6$ in EC:PC:DEC:VC:FEC (20:5:55:20:2:5) | 1 wt% poly[dimethylsiloxane-co-(siloxane-g-acrylate)] (PDMS-A) | | Graphite‖LiCoO$_2$ | 94 mAh g$^{-1}$/0.1 C/−20 34 mAh g$^{-1}$/0.5 C/−20 | [133] |
| 1 M LiPF$_6$ in EC:EMC (3:7) | 1 wt% methyl 2,2-difluoro-2-fluorosulfonylacetate (MDFA) | | Graphite‖LiCoO$_2$ | ~1 620 mAh/0.5 C/−10 | [134] |
| 1 M LiPF$_6$ in EC:DEC:EMC (2:1:4) | N,N dimethyltrifluoroacetamide (DTA) | | Li‖graphite | 114.6 mAh g$^{-1}$/0.1 C/−20 Cycling: 94.8%/100/0.1 C/−20 | [135] |

**Table 5** LT electrolytes using ionic additives

| Electrolyte | Additive | Additive molecule structure | Cell system | [Capacity/(mAh g$^{-1}$) or capacity retention]/(current density or C rate)/ (temperature/°C) | References |
|---|---|---|---|---|---|
| 1.2 M LiPF$_6$ in EC:EMC:MB (2:2:6) | Lithium oxalate (saturated) | | MCMB‖LiNi$_x$Co$_{1-x}$O$_2$ | 85.70%/25 mA/−20<br>74.32%/25 mA/−40 | [132] |
| 1.2 M LiPF$_6$ in EC:EMC:MB (2:2:6) | 0.10 M LiBOB | | MCMB‖LiNi$_x$Co$_{1-x}$O$_2$ | 88.23%/25 mA/−20<br>76.53%/25 mA/−40 | [132] |
| 1 M LiPF$_6$ in EC:PC:EMC (2:1:7) | 0.04 M CsPF$_6$ | NA | Graphite‖NCA | 126 mAh g$^{-1}$ (75%)/0.2 C/−30<br>103 mAh g$^{-1}$ (61%)/0.2 C/−40 | [140] |
| 1 M LiPF$_6$ in EC:PC:EMC (4:1:7) | 1% LiPO$_2$F$_2$ (inorganic species rich SEI, low impedance) | | Graphite‖NMC532 | 71.9%/0.5 C/−20<br>57.93%/0.5 C/−30<br>Cycling: 91.3%/100/0.5C/−20 | [142] |
| 1 M LiPF$_6$ in EC:EMC (1:2) | 1% lithium difluorobis(oxalato) phosphate (LiDFBOP) | | Graphite‖NMC532 | 49%/0.2 C/−30<br>Cycling: 93%/50/0.5 C/−20 | [143] |
| 1 M LiPF$_6$ in EC:EMC (3:7) | 0.2 M LiFSI | | Graphite‖LiCoO$_2$ | 106 mAh g$^{-1}$/0.1 C/−20<br>103 mAh g$^{-1}$/0.2 C/−20<br>97 mAh g$^{-1}$/0.5 C/−20<br>89 mAh g$^{-1}$/1 C/−20<br>69 mAh g$^{-1}$/2 C/−20<br>17 mAh g$^{-1}$/5 C/−20 | [139] |
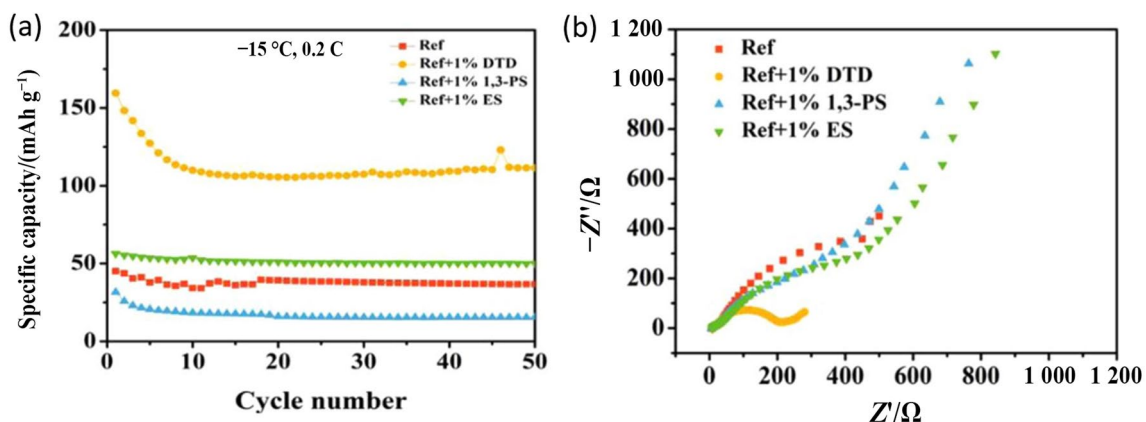


**Fig. 13** **a** Cycling performance of graphite/Li/Li T-shaped Swagelok three electrodes battery using different kinds of electrolytes at −15 °C; **b** EIS results after 50 cycles at 0.2 C and −15 °C. Ref: 1 M LiPF$_6$ in EC:EMC (3:7, volume ratio). Reprinted with permission from Ref. [110]. Copyright © 2018, IOP publishing group

of ∼ 320 mAh g$^{-1}$ was delivered when a Li/graphite cell was discharged at −20 °C (a 1/15C rate). In contrast, only ∼ 175 mAh g$^{-1}$ was obtained at the same condition for a cell using the electrolyte without FEC (Fig. 14a) [125]. This difference

was attributed to the decreased charge transfer and the SEI impedance after forming LiF-rich SEIs with FEC. Unfortunately, the benefit of using FEC decreased rapidly during cycling and became insignificant after 25 cycles at −20
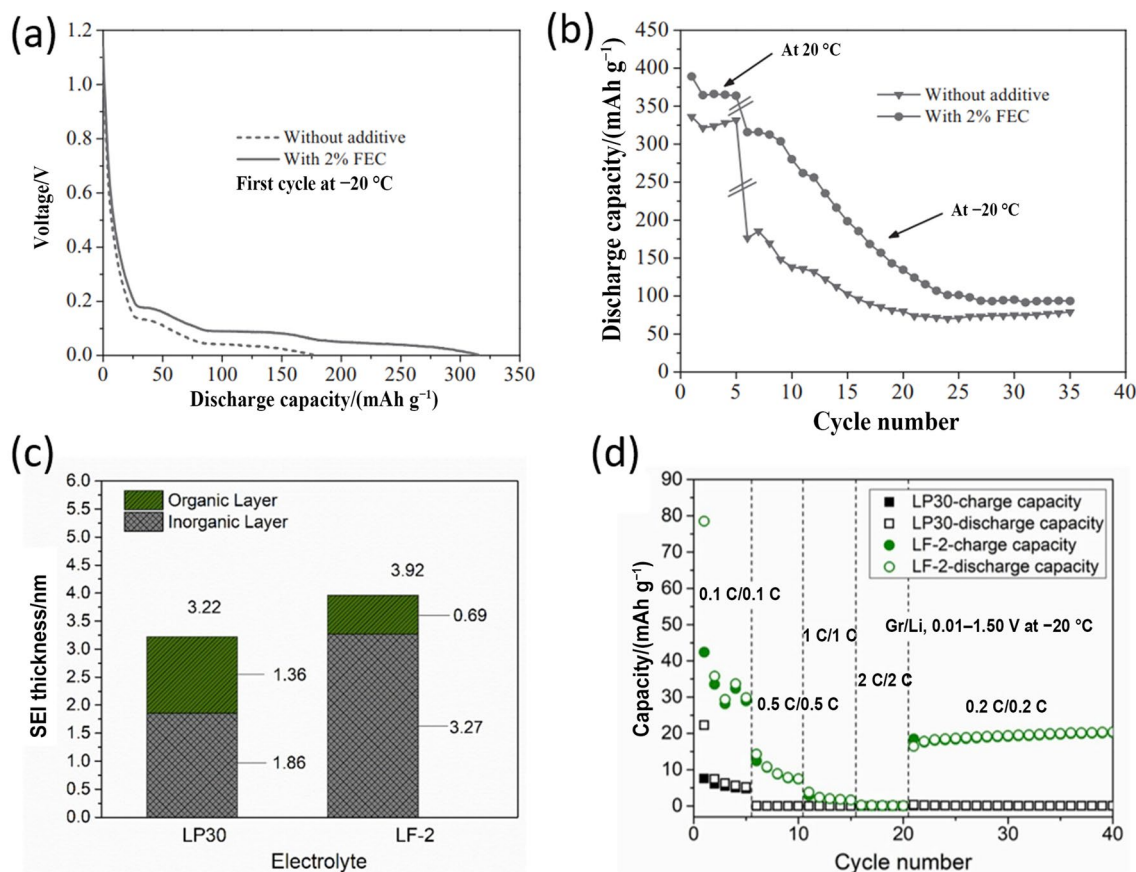
**Fig. 14 a** The comparison of first discharge capacity for cells using electrolytes with and without 2 vol% FEC additive; **b** the cycling performance of these cells at 20 and −20 °C. Reprinted with permission from Ref. [125]. Copyright © 2012, IOP publishing group. **c** Thickness of organic and inorganic layers in SEI formed in LP30 and LF-2 electrolytes; **d** rate capability of graphite/Li coin cells using LP30 and LF-2 electrolytes at −20 °C [LP30: 1 M LiPF$_6$ in EC:DMC (1:1, in volume ratio); LF-2: 2 wt% FI+LP30]. Reprinted with permission from Ref. [128]. Copyright ©, 2015 Elsevier

°C, as shown in Fig. 14b, due to the rapid SEI impedance buildup. Traditional film-forming additives show irreplaceable advantages in terms of stable interphasial chemistry on both cathodes and anodes. However, the powerful film-forming characteristics sometimes result in high interphasial resistance, especially at LTs, which induces large voltage polarization and cell performance degradation. Therefore, novel film-forming additives enabling the formation of interphase layers with controllable thickness have been developed. Erythritol bis(carbonate) (EBC) is a promising additive for enhancing LT performance of LIBs, which has two EC-like structures in a single molecule with low LUMO energy levels [9]. By forming a stable and thick SEI layer on graphite anode, the conventional carbonate-based electrolyte with 2 wt% (wt% means the weight percentage) of EBC enables the Ah-scale NMC532-artificial graphite (AG) pouch cell to have enhanced cyclic stability at 0 and −20 °C. Multi-model characterization results suggested that the structural stability of the electrodes maintained well in the

electrolyte with EBC additive by forming a stable interphase on the electrode surface, which further inhibits the Li dendrite formation on the AG surface as well as the Ni/Li site mixing in NMC cathodes. More recently, Zhang et al. [126] also designed novel fluorine-rich electrolytes by introducing 4,4′-sulfonyldiphenol (FS) and perfluoro *n*-butylsulfonyl fluoride (PBF) as coadditive to improve the LT performance of conventional carbonate-based electrolytes. The synergy of FS and PBF enables commercial EC/DMC-based electrolytes to show high Li transference numbers and Li$^+$ diffusion coefficients at harsh environment. In addition, FS and PBF additives changed the SEI composition at −60 °C and the proportion of inorganic components (LiF, Li$_x$N, and Li$_x$S) increased significantly, which is beneficial for stabilizing the Li metal anode performance. As a result, the Li-LFP cell demonstrated excellent fast-charge performance and long-term cycle capability. At −40 °C, the Li-LFP cell showed 90% capacity retention after 100 cycles at the cathode-limited areal capacity (5 mAh cm$^{-2}$). These results suggested

that PF and FS additives have a great potential in the development of commercial LMBs at harsh conditions. The fluorination of polar solvent could enhance the electronegativity and reduce the polarity, which is another essential strategy to improve the LT performance of electrolytes by reducing the intrinsic solvating power of solvents. To comprehensively investigate the effect of the fluorination degree of polar solvent on solvation structure such as the solvation number and solvation power, Li's group compared properties and electrochemical performance of FEC and difluoro EC (DFEC) with different fluorination degrees [127]. Experimental and calculation results demonstrated that the Li$^+$-dipole interaction strength gradually decreases from 1.90 to 1.66 eV and then to 1.44 eV with an increase of the fluorination degree from EC to FEC and DFEC, respectively. More interestingly, the DFEC-based electrolyte displays six times faster ion desolvation rates than that of the EC-based electrolyte at −20 °C. As a result, NMC811-Li cells with the DFEC-based electrolyte displayed better fast-charge capability and long-term cyclability in the temperature range from −30 to 25 °C compared to that with the EC-based electrolyte. It can be seen that the ion–dipole strategy provides a new approach toward the rational design of electrolyte engineering for LT lithium batteries with fast charging kinetics.

Organic additives with multiple functional groups are used as LT electrolyte additives as well. It was reported that isocyanate-based additives can be electrochemically polymerized and form polyamide-like SEIs. Shi et al. [128] used fluorosulfonyl isocyanate (FI) to improve the LT performance. In this work, the SEI components were quantified by XPS using LiF as an indicator, and the SEI was considered as having an "inorganic layer" adjacent to the graphite anode and an "organic layer" adjacent to the electrolyte. The thicknesses of the inorganic and organic layers were estimated based on the XPS spectra acquired after different sputtering times. They reported that compared with the SEI formed in conventional carbonate electrolytes without FI additive, the SEI formed in the electrolyte with FI additive was thicker, having thicker inorganic layers but thinner organic layers (Fig. 14c). LP30 [1 M LiPF$_6$ in EC:DMC (1:1, volume ratio)] was used as a reference electrolyte. The LP30 with 2 wt% FI is coded as LF-2. The thickness reduction of the organic species layer was attributed to the suppression of carbonate solvent decomposition, while the increased thickness of the inorganic layer was attributed to the FI-derived SEI components. The SEI with a thinner organic layer is beneficial for reducing diffusion limitation. Although the inorganic layer was thicker by using FI, it is mainly composed of LiF, ROSO$_2$Li, Li$_2$S, Li$_2$SO$_3$ and a low concentration of Li$_2$CO$_3$, Li$_2$O and Li$_x$PF$_y$O$_z$, resulting in overall lower interface resistance. Therefore, the cells containing FI additives delivered ∼ 80 mAh g$^{-1}$ discharge capacity at −20

°C, greatly improved from the ~20 mAh g$^{-1}$ low capacity for the cell using an electrolyte without FI additive (Fig. 14d). One problem of using FI as additive is the low initial Coulombic efficiency, caused by the consumption of Li through SEI formation during the first cycle. This work clearly demonstrated the importance of identifying and quantifying the different organic and inorganic ingredients in the SEI, their chemical source, as well as their functionalities on electrochemical performance of batteries at different temperatures. The positive impact of increased inorganic components in SEIs, especially the amount of LiF derived from FI additive, agrees well with the widely accepted concept about LiF being the critical component of "good SEIs". However, the so called "inorganic layer" used there may cause some confusion, since the "good SEIs" is believed to have both organic and inorganic (with critical component LiF) components to get the flexibility and proper mechanical properties of SEIs, rather than the separated pure organic and inorganic layers. Therefore, an "inorganic-rich layer" or "LiF-rich layer" might be a better expression.

On the other hand, there are competing arguments regarding the effects of inorganic components of SEIs in the literature claiming that improved battery performance was obtained at LTs by decreasing inorganic species including LiF in SEIs. Yang et al. [129] reported 2,3,4,5,6-pentafluorophenyl methanesulfonate (PFPMS) as an additive to improve a graphite∥NCM523 cell performance over a wide-temperature range. The PFPMS was able to participate in both SEI and CEI formation, which stabilizes NCM523 and graphite based on the theoretical calculation and experimental results. By utilizing PFPMS as an additive, lower cell polarization and higher capacity retention were obtained at LTs (Fig. 15a). Specifically, cells containing PFPMS delivered 72.3% and 66.3% of the RT capacity when discharged at −20 °C, with 0.2 C and 0.5 C rates, respectively, better than 67.8% and 55.0% for the cells without additives and 70.5% and 62.1% for the cells with 1% VC additive under the same conditions. This improved performance was attributed to the as-formed lower resistance interphase in PFPMS electrolytes compared to VC-additive and no-additive systems, resulting in better ionic conductivity at LTs in full cells. According to the XPS results (Fig. 15b), this low impedance SEI was composed of S-containing decomposition products (i.e., ROSO$_2$Li), and less LiF and Li$_2$CO$_3$, yielding faster ionic transportation.

A separate work from Li's group claimed similar observation. They compared the performance using DMS and DTD as additives in 1 M LiPF$_6$ in EC:EMC (1:2, weight ratio) [130]. The electrochemical performance at −20 °C and a C/2 rate was measured by using graphite∥NCM523 cells. The cells using DMS electrolytes showed the best results (Fig. 15d), which delivered 74.28% of RT capacity, followed
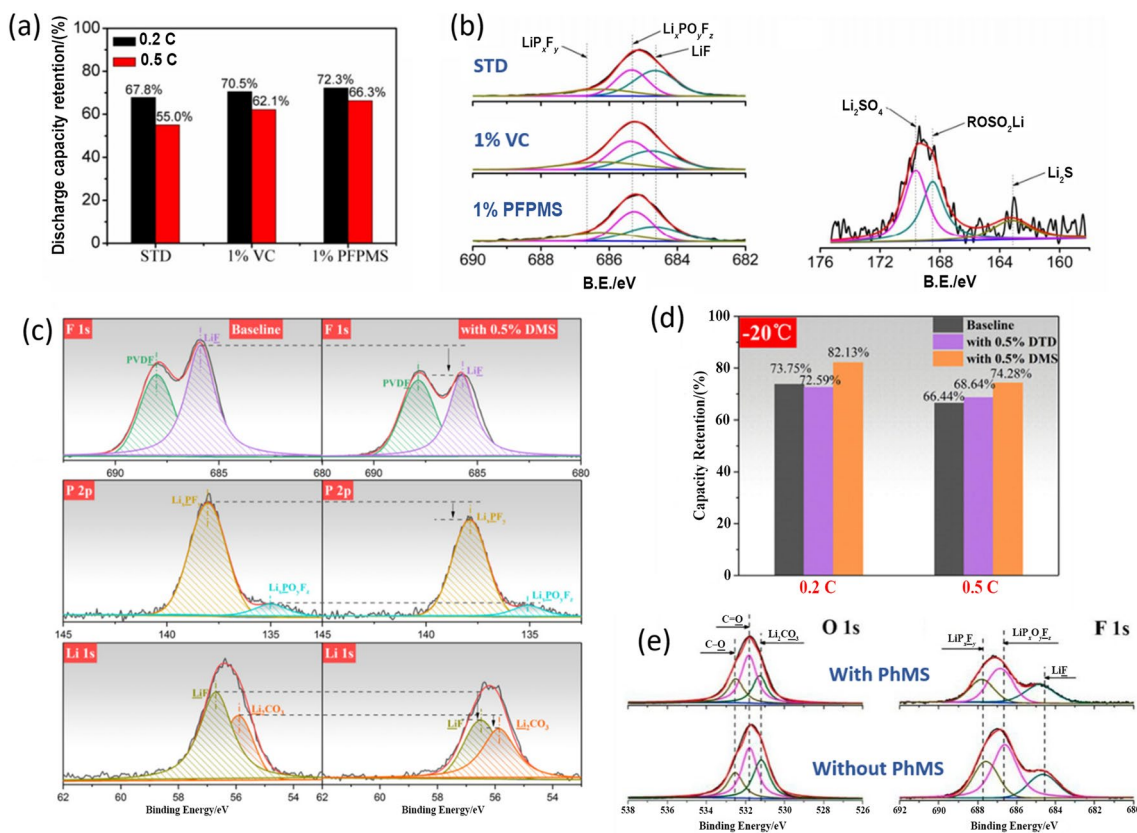
**Fig. 15 a** Capacity retention of graphite‖LiNi$_{0.5}$Co$_{0.2}$Mn$_{0.3}$O$_2$ full cells at −20 °C using electrolytes of STD [1 M LiPF$_6$ in a 1:2 (weight ratio) mixture of EC and EMC], STD with 1% VC, and STD with 1% PFPMS; **b** XPS spectra of F 1s measured from the cycled graphite anode using STD with 1% VC, and STD with 1% PFPMS electrolytes, and S 2p XPS spectra of cycled graphite anode with 1% PFPMS additive. Reprinted with permission from Ref. [129]. Copyright © 2018, American Chemical Society. **c** XPS profiles of F 1s, P 2p, Li 1s spectra on the graphite anodes from the full cells after 50 cycles at 0.2 C and −10 °C using baseline [1 M LiPF$_6$ in 1:2 (weight ratio) EC:EMC] and 0.5% DMS additive containing electrolytes. **d** Capacity retention of graphite‖LiNi$_{0.5}$Co$_{0.2}$Mn$_{0.3}$O$_2$ pouch cells compared to the capacity at RT at 0.2 C and 0.5 C rates and −20 °C using electrolytes without additives and with 0.5% DTD and DMS additives. Reprinted with permission from Ref. [130]. Copyright © 2019, American Chemical Society. **e** XPS spectra for O 1s and F 1s measured from the graphite anode after 100 cycles at −10 °C using electrolytes with and without 1wt% PhMS. Reprinted with permission from Ref. [131]. Copyright © 2019, Elsevier

by the DTD-based cell (68.64%) and the electrolyte without additive (66.44%). According to EIS results, the DMS-based electrolyte system had the lowest $R_{sei}$ and $R_{ct}$ at both RT and LT, indicating more ionic conductive SEIs formed by DMS. The DTD system also had lower resistance compared to baseline at RT, while the charge transfer resistance of the DTD system at LT increased significantly and was even higher than the baseline electrolyte, implying sluggish charge transfer of DTD formed SEIs at LTs. To study the different ionic transportation behavior of DMS and DTD systems, SEI analysis and theoretical calculations were carried out. Based on the XPS results (Fig. 15c), lower amounts of LiF and Li$_2$CO$_3$ were generated by decomposition of carbonate electrolytes and LiPF$_6$ in DMS-presence, indicating more protective nature of as-formed SEI from DMS. In addition, DMS reduction products (CH$_3$OSO) has lower binding energy with Li$^+$ compared that of DTD (OCH$_2$CH$_2$SO$_3$),

suggesting a faster ionic migration through such SEI. Moreover, CH$_3$OSO experienced less structural change after combining with Li$^+$ compared to DTD, implying a stabler structure in this SEI. This stable and low resistance SEI greatly improved the LT performance. Recently, the improved LT electrochemical performance by using phenyl methanesulfonate (PhMs) additive [131] was ascribed to the decreased interphase impedance as well. According to the XPS results of graphite after 100 cycles shown in Fig. 15e, less inorganic species (LiF, Li$_2$CO$_3$) were observed on graphite surface while using PhMs additive, thereby decreasing the resistance. Although most of the results of these studies [129–131] are very valuable, what they claimed that fewer inorganic species would be beneficial for lowing interphase impedance based on XPS results might be debatable. In contradiction to the negative effects of inorganic component in SEI claimed in these studies [129–131], the positive

impact of LiF inside SEI for anode protection has also been widely reported by experimental results from many other groups. Therefore, the role of LiF in SEIs and its impact on the ionic transportation remains a controversial topic, with more thorough studies needed, which should take into account the size, morphology, crystallinity, and the amounts of LiF generated using different electrolyte systems. Furthermore, the conclusion merely based on the surface sensitive XPS results [129–131] may need to be re-examined by other characterization techniques.

## 4.2 Ionic Additives

Some boron-based salts described in Sect. 3, such as LiBOB, LiDFOB and similar derivatives, were also used as electrolyte additives due to their good SEI film-forming properties [136, 137]. For example, to combine the advantage of the excellent LT performance of $LiBF_4$ and the low melting point of PC, a system of electrolytes using 1.0 M $LiBF_4$ in 1:1:3 PC:EC:EMC was studied [99]. However, the cells using such electrolyte encounter solvent intercalation into graphite anodes because no stable SEI can be formed at an insufficient content of EC. Hence, LiBOB was introduced into this electrolyte system, which forms an SEI with

semicarbonate-like products (Fig. 16a) [99]. It was demonstrated that 1%–5% (molar percentage) LiBOB was sufficient to enable graphite anode cycling reversibly in 1.0 M $LiBF_4$ in 1:1:3 PC:EC:EMC and 1.0 M $LiBF_4$ in 1:1 PC:EC, respectively, while maintaining the excellent cycling performance of $LiBF_4$-PC-based electrolytes at LTs. The cell using the electrolyte of 1.0 M (0.98 M $LiBF_4$ + 0.02 M LiBOB) in 1:1:3 PC:EC:EMC was able to deliver 83% and 63% of RT discharge capacity at −30 and −40 °C, respectively (Fig. 16b).

One critical problem of Li-ion cells operating at LTs is the metallic Li plating, which occurs when cells are charged at LTs, at excessive rates, and/or at high voltage. In those situations, the Ohmic drops that occur in both bulk electrolytes and electrodes as well as interphases constitute a diffusion-controlled layer, so that an excessive driving force is needed at the electrode-side to move $Li^+$. As a result, the potential of the electrode ventures into the negative territory vs. $Li^+$, causing the reduction of $Li^+$ at the electrode/interphase/electrolyte junction. Since $Li^0$ is intrinsically unstable against electrolytes, further electrolyte decomposition happens. Li plating and the above concomitant processes can cause internal short and irreversible capacity loss. The SEI layer has been recognized as an important factor that
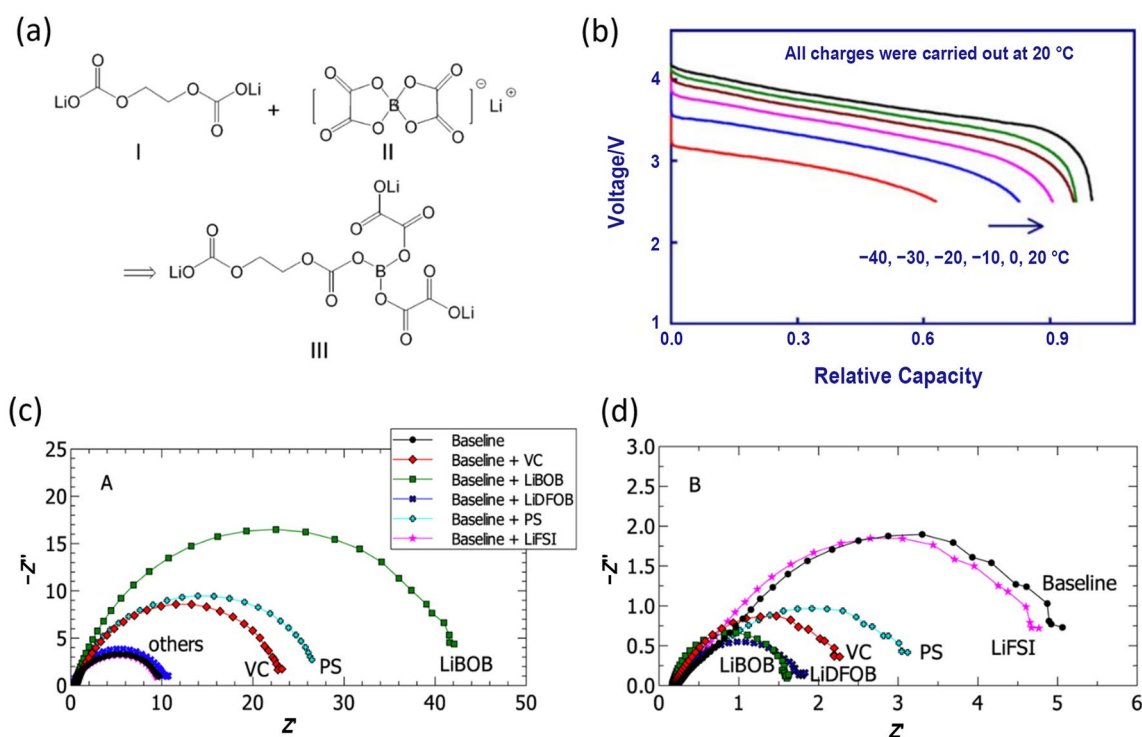


**Fig. 16 a** Reaction scheme of LiBOB with semicarbonates in SEI. **b** Discharge capacity of the graphite‖$LiNiO_2$ cell with the electrolyte of 1.0 M (0.98 M $LiBF_4$ + 0.02 M LiBOB) in 1:1:3 PC:EC:EMC at LTs. Reprinted with permission from Ref. [99]. Copyright © 2006, Else-

vier. **c** EIS measured at −30 °C for the graphite anodes. **d** EIS measured at −30 °C for the $LiNiCoAlO_2$ cathodes using electrolytes with different additives. Reprinted with permission from Ref. [138]. Copyright © 2020, IOP publishing group

influences lithium plating positively or negatively. Recently, Jones et al. [138] conducted a systematic study on electrochemical behaviors, especially the effects of additives on Li plating suppression. It was reported that the addition of ionic additive LiFSI can suppress the Li plating compared to the baseline cell. In contrast, adding VC or LiBOB to the baseline electrolyte resulted in worsened Li plating. This is because additives affected interphase impedance differently at the anodes and cathodes. According to the EIS data (Fig. 16c, d), both LiBOB and VC increased the SEI impedance at anodes as compared with baseline electrolytes but decreased the CEI impedance at cathodes. This unbalanced kinetics on anodes and cathodes at LTs resulted in higher polarization on the anode side while accelerating delithiation of cathodes and increased the possibility for lithium plating. The positive impact by LiFSI on suppressing the Li plating and retaining higher capacity retention at LTs was later confirmed in a recent paper by Pham et al. [139]. For the graphite‖LiCoO$_2$ cell using 1 M LiPF$_6$/EC:EMC baseline electrolytes with 0.2 M LiFSI additive, the SEI impedance was significantly decreased and Li plating was suppressed compared with the baseline electrolyte. In addition, when cycled between 3.0 and 4.3 V at −20 °C, the cell using LiFSI additive delivered ~30% higher capacity than the baseline electrolyte at all rates of 0.1 C, 0.2 C, 0.5 C, 1 C, and 2 C.

Apart from using salts that are already well known as additives, various lesser-known additives were also studied and showed promising results. For example, Xu's group reported using 0.04 M CsPF$_6$ as additive in 1 M LiPF$_6$ EC:PC:EMC (2:1:7, weight ratio) electrolyte [140] through the preferential solvation by EC of Cs$^+$ and the subsequent higher reduction potential of the complex cation. The PC decomposition and graphite exfoliation were effectively suppressed by adjusting the EC/PC ratio in electrolytes to achieve a reductive decomposition of Cs$^+$-(EC)$_m$ ($1 \leqslant m \leqslant 2$) complex preceding that of Li$^+$-(PC)$_n$ ($3 \leqslant n \leqslant 5$) (Fig. 17a).

Such Cs$^+$ containing interphase is stable, ultrathin, and compact, leading to significant improvement in battery performance. This excellent SEI with smaller impedance demonstrated great electrochemical performance at LTs (Fig. 17b). The graphite‖LiNi$_{0.8}$Co$_{0.15}$Al$_{0.05}$O$_2$ (NCA) pouch cell using 1.0 M LiPF$_6$ in EC:PC:EMC (1:1:8, weight ratio) with 0.05 M CsPF$_6$ delivered 68% capacity at −40 °C and C/5 rate, much higher than that of conventional electrolytes (20%) [141].

Fluoro-phosphate-based ionic compounds also showed great potential as LT electrolyte additives. To improve the ionic transportation in SEIs, lithium difluorophosphate (LiPO$_2$F$_2$) was used as additive for 1 M LiPF$_6$ in EC:EMC:PC (4:7:1, weight ratio) baseline electrolytes [142]. According to the morphology and composition characterization results, a thin, dense and smooth SEI layer containing more inorganic components such as LiF and Li$_2$CO$_3$ was formed on graphite anodes, showing the capability to protect the graphite anode through 100 cycles at 0 °C. This SEI with rich inorganic species has much lower ionic resistance compared to that of baseline electrolyte at 0 °C (Fig. 18a). Therefore, both the discharge capacity and cycling stability at LT saw great improvement (Fig. 18b). At −20 °C, the retention of RT capacity of graphite‖NMC532 cells using LiPO$_2$F$_2$ additive was 71.9%, much better than the 49.4% for the baseline electrolyte. Meanwhile, as displayed in Fig. 18c, after 100 cycles at −20 °C, the cells with LiPO$_2$F$_2$ obtained a high capacity retention of 91%, delivering 91.7 mAh g$^{-1}$. In contrast, the cell without LiPO$_2$F$_2$ experienced severe capacity drop, with only 9.6 mAh g$^{-1}$ capacity left and corresponding to a capacity retention of ~16% only.

Another phosphate salt, lithium difluorobis(oxalato) phosphate (LiDFBOP), was also studied as additive to improve SEI ionic conductivity [143]. According to the electron affinity calculation and experimental results, LiDFBOP is electrochemically reduced prior to carbonate solvents
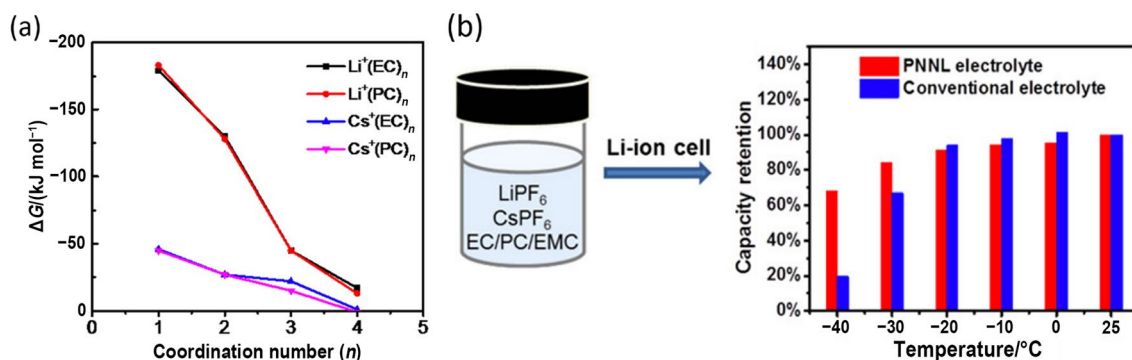


**Fig. 17** **a** Variation of solvation energy with coordination number for Li$^+$-(sol)$_{n=1-4}$ and Cs$^+$-(sol)$_{n=1-4}$ (where sol = EC, PC). Reprinted with permission from Ref. [140]. Copyright © 2015, American Chemical Society. **b** Capacity retention of graphite‖NCA cells using

PNNL electrolyte [1.0 M LiPF$_6$ in EC:PC:EMC (1:1:8, weight ratio) with 0.05 M CsPF$_6$], and conventional electrolyte [1.0 M LiPF$_6$ in EC:EMC (3:7, volume ratio)]. Reprinted with permission from Ref. [141]. Copyright © 2017, American Chemical Society
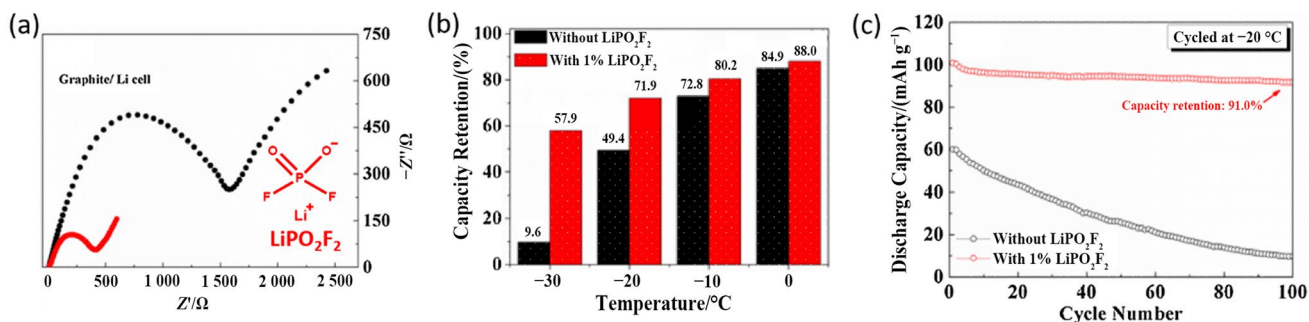
**Fig. 18 a** EIS of the half cells at 0 °C: the graphite/Li cell at 0.01 V. The half cells were cycled 3 times at RT before EIS measurement. **b** Capacity retention of graphite‖LiNi$_{0.5}$Co$_{0.2}$Mn$_{0.3}$O$_2$ cells with a rate of 0.5 C discharged to 2.75 V at various LTs. **c** Cyclic performance and Coulombic efficiency of graphite‖LiNi$_{0.5}$Co$_{0.2}$Mn$_{0.3}$O$_2$ cells with a rate of 0.5 C cycled at a potential range of 2.75–4.20 V at 0 °C. Reprinted with permission from Ref. [142]. Copyright © 2016, Elsevier

during discharge, whose reduction process scheme is shown in Fig. 19a. After one-electron reduction, one of the C–O bonds is broken, the resulted radicals are then self-polymerized, and the combination of this polymer anion and lithium cation constructed the SEI on graphite. This is beneficial to ionic transportation in SEIs, resulting in the decreased interface resistance (the sum of $R_{sei}$ and $R_{ct}$) of graphite anodes at 0 °C [from 1 935 to 820 Ω after adding 0.5% LiDFBOP in the baseline electrolyte (1 M LiPF$_6$ in PC:EMC, 1:1 in weight ratio)] (Fig. 19b). Similar polymerized CEIs were formed on NCM523 cathode surface with decreased $R_{cei}$ and $R_{ct}$. Therefore, with the increased ionic conductivity on both sides, the charge/discharge performance at LTs was significantly improved by introducing LiDFBOP additive.

The discharge capacity retention at −30 °C for the baseline electrolyte was quite low at only 14%, in strong contrast with the capacity retention of 49% at −30 °C from the cell with 1% LiDFBOP additive. In addition, the cycling stability at LT was also improved. The capacity retention after 200 cycles was increased from 57% to 94% at 0 °C and C/5 rate after adding LiDFBOP (Fig. 19c).

## 4.3 Ionic Liquid Additives

Apart from commonly used electrolytes, ionic liquids were often used as an independent type of electrolytes for LIBs due to some of their desired properties, such as low flammability, high stability, and tunable polarity. Utilizing ionic
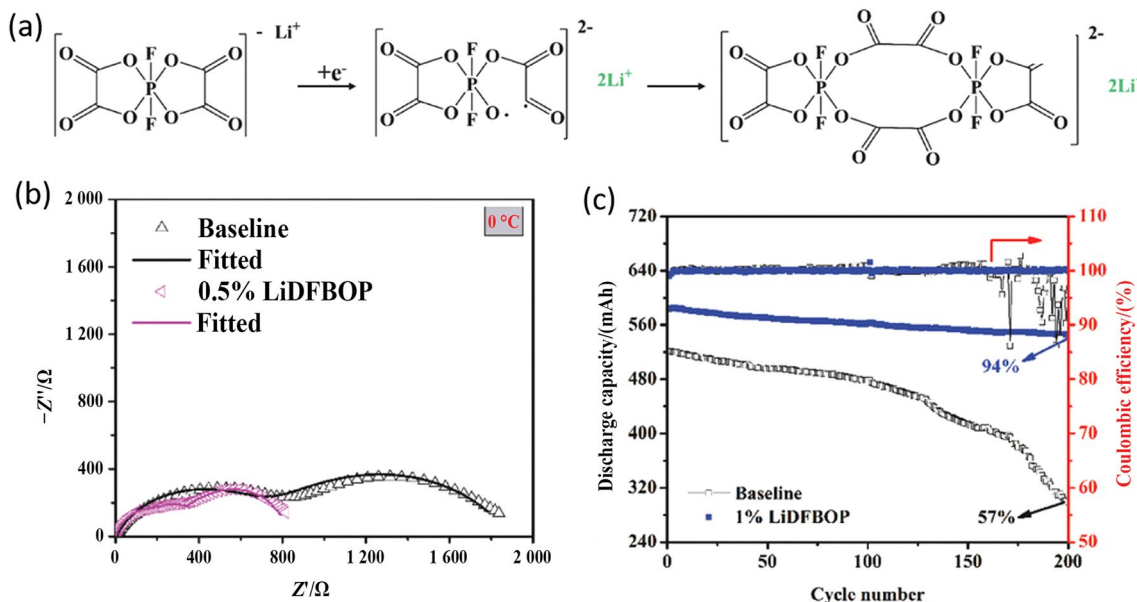


**Fig. 19 a** Mechanism for the formation of anode interface film from LiDFBOP. **b** EIS of graphite electrodes after 3 cycles at 0 °C obtained charge transfer ($R_{ct}$, red line) resistance by fitting. **c** Cyclic stability and Coulombic efficiency of graphite‖LiNi$_{0.5}$Co$_{0.2}$Mn$_{0.3}$O$_2$ cell in baseline and 1% LiDFBOP-containing electrolytes under 0.5 C at a potential range of 3.00–4.35 V at 0 °C. Reprinted with permission from Ref. [143]. Copyright © 2018, John Wiley and Sons

liquids as electrolyte additives was also practiced. However, it should be noted that, once ionic liquid is introduced into a liquid electrolyte, it is no longer an ionic liquid anymore, but an ionic additive dissolved by non-aqueous solvents. Wang et al. [144] reported using 1-ethyl-3-methylimidazole tetrafluoroborate (EMI-BF$_4$) as additive in an electrolyte of 1 M LiPF$_6$ in EC:EMC (1:2, weight ratio) for a graphite‖NCM523 cell at LTs. BF$_4$ anions can form low resistance CEIs and SEIs on NCM cathode and graphite anode, respectively, and EMI cations can help to obtain high ionic conductivity and low viscosity, hence EMI-BF$_4$ was hoped to maintain these advantages. According to the electrochemical measurements, an electrolyte with the EMI-BF$_4$ additive showed higher reduction potential (0.95 V of EMI, 1.7 V of BF$_4$), and lower oxidation potential (~3.5 V) compared to carbonate solvents, implying that this additive can participate in the formation of the SEI and the CEI. The additive-derived surface films prevented the continuous reaction between the electrolyte and electrodes, keeping the structural integrity of NCM cathode and graphite anode. Besides the protection nature, the SEI and CEI surface films containing more LiF and less Li$_2$CO$_3$ resulted in higher ionic conductivity at both room and LTs based on EIS results. Therefore, by using EMI-BF$_4$ as an additive, a graphite‖NCM523 cell can deliver 45.8% of RT capacity when discharged at −30 °C, much higher compared to the baseline electrolyte without additive (16.3%), as shown in Fig. 20a. Moreover, the long cycling performance at LT was also improved, as the cell containing EMI-BF$_4$ additive kept 89.4% capacity retention, higher than 81% for the baseline electrolyte after cycling at −10 °C after 150 cycles (Fig. 20b).

A couple of years ago, an electrolyte system blending ionic liquid (IL)-decorated poly (methyl methacrylate) (PMMA) nanoparticles with 1 M LiTFSI dissolved in a mixture of PC and MA was reported [145]. By adding PMMA-IL-TFSI, this electrolyte exhibits an ionic conductivity of $9.15 \times 10^{-4}$ S cm$^{-1}$ even at −40 °C, which is several orders of magnitude higher than the baseline electrolyte without additives. The improved ionic conductivity at LT was attributed to the liquid component in the electrolyte and the unique grafting structure of IL groups on PMMA nanoparticles. It was demonstrated that the PMMA-IL-TFSI additive can improve the reversible capacity and rate capability of Li$_4$Ti$_5$O$_{12}$ (LTO)/Li half cells at LT. In addition, the Li deposition morphology change and EIS results indicated that the enhancement in battery performance is mainly attributed to the increase of ion conduction via the formation of a stable and effective SEI film on the electrode. Compared with the capacities of around 94 mAh g$^{-1}$ (0 °C), 40 mAh g$^{-1}$ (−20 °C), and 5 mAh g$^{-1}$ (−40 °C) for the cells in baseline electrolytes without additive, the cells using PMMA-IL-TFSI nanoparticle containing electrolyte delivered much higher reversible discharge capacities of around 107 mAh g$^{-1}$ (0 °C), 84 mAh g$^{-1}$ (−20 °C), and 48 mAh g$^{-1}$ (−40 °C). Comparing to the capacity obtained at 20 °C, the discharge capacity retention was improved from 84.6%, 36%, and 4.5% to 93.8%, 73.6%, and 42.1% at 0 °C, −20 °C, and −40 °C respectively after 90 cycles (Fig. 21).

## 5 Conclusions and Outlook

Tremendous challenges remain for LIBs aiming to operate at LTs, which include poor capacity and energy retention ratios compared to RT operation; decreased rate capability; deteriorated cyclability; and Li metal plating on graphite anodes during fast charging. These negative impacts caused by LT
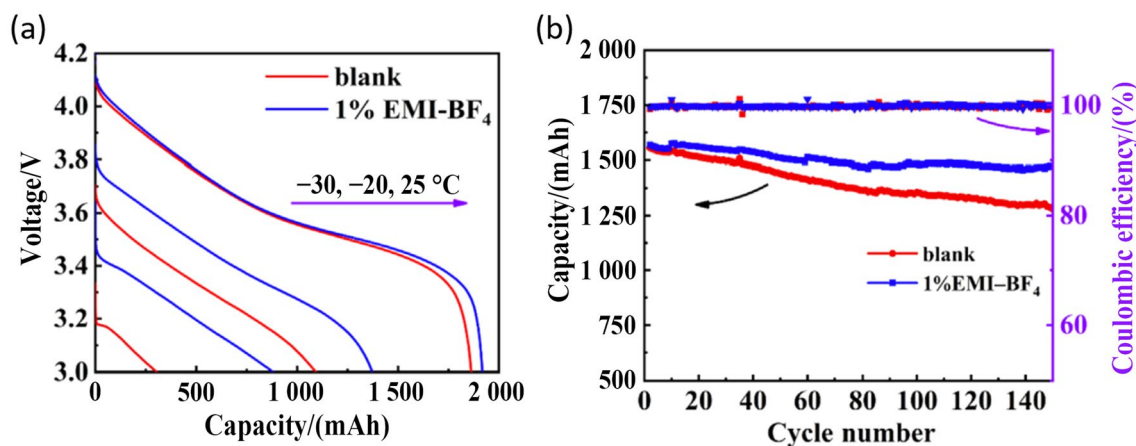
**Fig. 20 a** Discharge curves of the graphite‖NCM523 full cells at different temperatures at 0.5 C. **b** The cycle stability and Coulombic efficiency of the graphite‖NCM523 full cells at a voltage range of 2.75–4.20 V at −10 °C. Reprinted with permission from Ref. [144]. Copyright © 2016, Elsevier
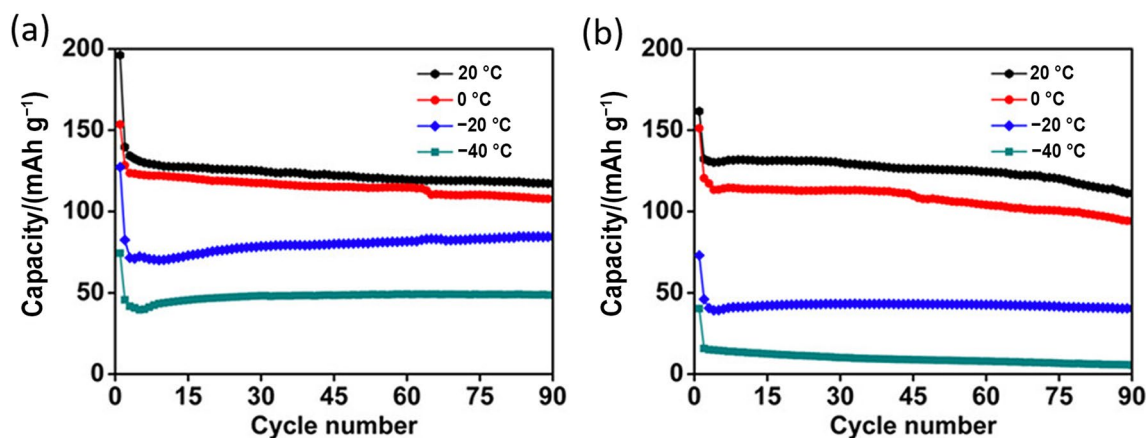
**Fig. 21** Cycling performance of LTO/Li cells in the 1 M LiTFSI in PC-MA electrolyte **a** with and **b** without PMMA-IL-TFSI at 0.5 C at various LTs. Reprinted with permission from Ref. [145]. Copyright © 2018, American Chemical Society

can be mainly categorized into two aspects: (i) decreased ionic conductivity in bulk electrolytes due to increased solvent viscosity; (ii) increased charge transfer resistance owing to sluggish ionic transport across SEIs and more difficult desolvation processes, especially at the graphite/electrolyte interface. In particular, cells at discharged states have higher $R_{ct}$ compared to charged state cells, so charging a cell at LTs is more difficult compared to discharging. Therefore, approaches aiming to improve battery performance at LTs through electrolyte development have been focused on these directions with various levels of success. As comprehensively summarized in this review, remarkable progress has been made in enhancing the LT performance of LIBs and LMBs including fast-charge capability at subzero condition, long-term cyclic stability and higher capacity retention, There are still crucial issues significantly affecting the performance of LIBs at LTs needing to be addressed: (1) how to rationally tailor electrolyte compositions to balance the requirements of low viscosity, high ionic conductivity and stable SEIs/CEIs; (2) it is essential to understand the mechanism of slow interfacial kinetics including Li$^+$ desolvation, Li$^+$ diffusion crossing SEIs/CEIs and charge transfer; (3) it is also essential to investigate different SEI compositions formed on graphite anodes at various temperatures; (4) in addition to the electrolyte engineering, compatibility between electrolytes and electrodes, such as wettability, interphasial chemistry should also be considered.

## 5.1 Electrolyte Engineering

Introducing low viscosity and low melting point solvent/cosolvent to counter the decreased ionic conductivity in bulk electrolyte at LTs is an extensively used strategy. Linear carbonates, carboxylic esters, and nitrile compounds serve as some good examples. Combining advantages of different

solvents in a multi-solvent electrolyte is a simple and effective approach to improving the LT performance of LIBs. For example, linear carbonates can effectively lower the viscosity and enhance the ionic conductivity of the electrolyte, while esters have low freezing points. Therefore, better LT performance can be realized in binary/ternary electrolytes containing carbonates and esters. The development of novel electrolyte solvents (i.e., isoxazole [146, 147]) is highly desirable as well. These solvents have been used to reduce or to entirely eliminate the use of EC, which has high viscosity and melting points. Despite the successful examples of this strategy, many reports [148, 149] have pointed out that the SEI plays an equally important role as by the ionic conductivity of bulk electrolyte on battery performance at LTs, which prevents the complete removal of EC. In other words, the SEI chemistry is another critical criterion for solvent selection, of the same importance with the low viscosity and melting points. In this aspect various fluorinated solvents have been explored, largely based on their capability to change the SEI formation chemistry and provide a fluorine source for the critical component of LiF. Apart from using fluorinated solvents, alternating salts and/or introducing additives are more effective ways in forming better SEIs with lower impedance. LHCE could be one of the promising approaches for improving the LT performance of LIBs, based on their successful application in stabilizing SEIs on lithium metal anodes and improving the performance of LMBs in wide-temperature ranges [62, 150]. Increasing the salt concentration will result in reduced salt-solvent coordination as well as the number of free solvent molecules. Therefore, decomposition products from anion-reduction rather than solvent-reduction are dominant in the SEI. Such SEI is remarkably distinct from those formed in conventional electrolytes and exhibit better anode protection. However, the high viscosity of concentrated electrolytes (about ten times greater than

that of conventional electrolytes) limits their application at LTs. The introduction of an inert solvent as diluent to form so called LHCE has successfully overcome the drawbacks of the HCE while maintaining their advantages of forming anion-derived SEIs. Recently, "ultralow-concentration" electrolyte was proposed by Hu and coworkers [151] to reduce both the cost and viscosity of the concentrated electrolytes. Interestingly, Na-ion systems in such electrolytes demonstrated excellent LT performance benefiting from the low viscosity and well-formed organic-dominant SEI (here again, the controversial conclusion about the impact of organic-dominated vs. inorganic-dominated SEIs is made). Yu's group [152] utilized the synergistic effect of LiDFP, LiBOB, LiFSI and LiTFSI salts to design low concentration electrolytes with carbonate-based solvents. Typically, reducing the concentration of Li salts decreases the conductivity of the electrolyte. However, due to the better wettability of LiFSI and LiTFSI toward PE separator, the conductivity decrement of the electrolyte is relatively mild. In addition, the LiF-rich, flexible SEI film formed on Li metal surface by the decomposition of LiDFP and LiBOB further prevents Li dendrite formation and parasitic reaction. More recently, Lee's group [153] also demonstrated formation of robust and conductive SEI (and CEI) layers on Li metal anodes (and LFP cathodes) in ether-based low concentration bi-salt electrolytes, in which 0.3 M LiFSI and 0.2 M LiTFSI were used as salts and 1,4-dioxane was used as weakly solvating solvent. Li/Cu cell showed a high Coulombic efficiency of 99.2%, which is attributed to the LiF-rich SEI layer formed on Li metal anodes. To increase the oxidation stability of low concentration electrolytes, Guam et al. [154] regulated the solvation structure by introducing TTE as the diluent cosolvent in carbonate-based electrolytes. The introduction of TTE not only enhanced the nonflammability of the electrolytes, but also increased the oxidation stability of the electrolytes due to reduced free solvent molecules. Moreover, LiF-rich CEI layers on cathode surface enhanced the cyclic performance of graphite/NCM523 full cells. Therefore, low/ultralow-concentration electrolytes might be able to open a new approach for the LT electrolytes, in addition to the liquefied gas electrolytes [74]. It should be noted that the composition and solvation structure of low concentrated electrolytes should be carefully tuned for maintaining the oxidation and reduction stability as well as ionic conductivity of the electrolyte, rather than just simply reduce the concentration of Li salts. A concept of high-entropy electrolyte has also been introduced by Chen's group recently for extending the operation temperature of LIBs to $-130$ °C [155]. Compared to conventional electrolytes, molecularly disordered solvent mixture in decimal solvent-based high-entropy electrolyte can reduce the crystallinity of electrolytes and resulting in a high ionic conductivity of 0.62 mS cm$^{-1}$ at $-60$ °C, enabling remarkable performance (~ 80 % capacity retention at $-40$

°C) of the LIB cell using it. High-entropy electrolyte would be another effective approach for LT electrolyte development. For screening electrolyte components efficiently, high throughput screening machine-learning methods, as well as the electrolyte genome have also been introduced.

As an interesting example of electrolyte engineering for LMAs stably cycled at LTs, an anionic coordination manipulation strategy was proposed to reduce the disadvantages of HCEs described in previous sections. Peng's group [156] designed a multilayer solvation structure electrolyte (MSSE) by manipulating the anionic species of FSI$^-$ and NO$_3^-$ with different coordinating abilities. This multi-layer solvation sheath derived from FSI$^-$ and NO$_3^-$ anions, using DME as solvent and TTE as diluent not only enables high $t_+$ up to 0.9 and fast desolvation process but also improves cyclic stability of LMA at subzero temperatures. Electrolyte engineering is especially useful in optimizing electrolyte components to maximize the synergistic effects of multiple components. Such optimization usually requires large number of experiments and a suitable screening method, playing a critical role for designing novel high performance electrolytes. To simplify the optimization process of electrolyte formula, Li's group [157] utilized a uniform design method which was developed by Fang et al. [158, 159] based on the principle of "uniformly scattered points". In this method, the required number of experiments will be greatly reduced since every level for each independent component will be tested only once. For the electrolyte developed in their study, isobutyl acetate (iBA), PC and DME solvents involved as independent components and 11 experimental points were selected for each component for concentration of salt from zero to 1 mol L$^{-1}$. After achieving the electrochemical curves of these points, a functional relationship of cell parameters (e.g., specific capacity) with electrolyte formulas can be established, thus optimal electrolyte formula can be determined according to the maximum point of the multivariate function. Coupling with bi-salt (0.78 M LiBF$_4$ + 0.22 M LiFSI), the electrolyte achieved a high ionic conductivity of 1.15 mS cm$^{-1}$ at $-60$ °C, thereby the lithium/graphite fluoride cells delivered more than 52% of the RT capacity at $-60$ °C. Another new strategy has been proposed by Cao's group [160] more recently defined as coordination number rule, which can modulate the electrochemical window of electrolyte by creating an anion-induced ion–solvent-coordinated structure through adjusting the coordination number of solvent and cosolvents. Based on this rule, the electrolyte containing both high and low coordination number solvents demonstrated improved reduction stability at the graphite anode, while the electrolyte with pure high coordination number solvent undergoing severe side reaction due to the strong polar solvent can fully dissociate lithium salt to form less anion contained solvation structure. Non-metallic charge carrier-based batteries have also shown

excellent performance in some recent reports, especially the use of proton as an attractive charge carrier has received much attention, due to its smallest ionic size and lightest weight, superior to almost all other cations, thus aqueous proton battery presents fast kinetics at LTs [161].

## 5.2 Understanding the Nature of SEI Layer

Although a lot of progress has been made on tailoring better SEI for LT operation through electrolyte engineering, the precise knowledge about SEI formation mechanism, $Li^+$-conduction mechanism in SEI, the composition, structure, morphology of SEI, as well as their correlation with battery performance remain little understood. Two general consensus among large number of researchers might be worthwhile to be pointed out: (1) LiF is a critical component for "good SEI" [162], although how these LiF exist in SEI is unclear; and (2) the SEI components derived from the decomposition of anions are generally better than those derived from solvent decomposition.

Although it has been widely accepted that forming "good SEI" is the most effective and important way to improve the LT battery performance, and many encouraging results have been reported, these efforts are still mainly empirical approaches. This is due to the lack of clear picture about how a "good SEI" is formed, what are the key functioning components of it and what are the functionalities of these key components. Answering these critical questions requires the development of new characterization tools together with modeling and theoretical calculations. So far, most of the SEI characterization studies have been carried out by using surface sensitive XPS, with limited information obtained about the elemental contents of the SEI. We are glad to see more and more advanced spectroscopic and imaging characterization tools, such as nuclear magnetic resonance (NMR), X-ray diffraction (XRD) and pair distribution function (PDF), neutron diffraction and PDF, and cryo-TEM, have been developed and applied for battery research, many of which are designed for electrolyte and SEI studies. We would like to introduce several examples of using these characterization techniques. Although the SEI samples studied in the following examples were collected on graphite or lithium metal anode at RT, their results provide important information for understanding the SEI formation mechanism and are quite valuable for LT electrolyte development. The first example is a recent work published by Shadike et al. [163] using XRD and X-ray PDF to study SEIs. They collected SEI samples from LMA in Li/Cu cells in HCE and low concentration electrolyte (LCE) using 5 M and 1 M LiFSI, respectively. Synchrotron-based XRD and PDF analysis were used to identify and quantify two elusive components LiH and LiF. High abundance of LiH was confirmed by XRD. Differing from conventional bulk LiF, they discovered a new type

of LiF differing from bulk LiF, and named it as SEI $(LiF)_{sei}$, which has unique structural features including larger lattice parameter and smaller grain size (< 3 nm), and is favored for $Li^+$ transport. This discovery clarified the puzzle on how an ionic insulator like (bulk) LiF can be a critical component for good SEI. The relative contents of LiH, LiF and dead $Li^0$ in SEI are quantified, showing higher $(LiF)_{sei}$ and lower dead $Li^0$ contents in SEIs recovered from the HCE compared with their LCE counterparts. PDF technique differentiated key amorphous components originated from the decomposition of solvents (no good components) or anion (good components), mostly SEI $LiF_{sei}$. The knowledge obtained in this work provides comprehensive insight in understanding the "good SEI" formation mechanism and is valuable for the development of LT electrolytes. Another examples are using cryogenic TEM (cryo-EM) to study SEIs, as represented by the pioneer works from the research groups led by Meng [164] and Cui [165]. In the former [164], cryo-EM was reported to outperform other techniques used for characterizing the sensitive chemical composition and spatial distribution of the SEI, as well as the morphology at nanoscale. For the first time, cryo-TEM elucidates the nanostructure of the electrochemically deposited Li (EDLi) and its surface SEI film. Furthermore, distinctive surface layers were constructed by adding functional cesium ion $(Cs^+)$ and zinc $(Zn^{2+})$ additives, and their relationships with the Coulombic efficiency (CE) were analyzed. Their findings demonstrate the power of cryo-TEM for beam-sensitive battery materials and provide new perspectives on (1) the structure of the EDLi and SEI, (2) the effects of metal ions as electrolyte additives on the EDLi morphology, and (3) the relationship between the SEI and the CE. In the latter [165], the SEI was revealed to contain small crystalline domains (diameter ~ 3 nm) dispersed randomly throughout an amorphous matrix that coats the Li metal. These crystalline grains are the inorganic components of the SEI, identified to be Li oxide and Li carbonate by matching their lattice spacings. The amorphous matrix is likely the organic polymer formed by carbonate electrolyte decomposition. The SEI formed in this standard electrolyte resembles the mosaic structure predicted by Peled et al. [166], who described the SEI as a heterogeneous distribution of inorganic and organic components. They also observed a completely different SEI structure when it was formed in a carbonate-based electrolyte with 10% FEC. Instead of a random distribution of organic and inorganic components, the SEI formed in the presence of FEC is more ordered and appears to have a multilayer structure, consistent with the multilayer system proposed by Aurbach et al. [167]. The inner layer appears to be an amorphous polymer matrix, whereas the outer layer is determined to be large grains (~ 15 nm) of Li oxide with clear lattice fringes. Strangely, the signature of Li fluoride (LiF) lattice was not detected, even though LiF is considered to

be a primary reason for performance enhancement [162]. To identify the SEI component on graphite anodes, Wang et al. [30] harvested whole SEIs from large size graphite anodes and investigated the composition using NMR. Their results show that lithium ethylene mono-carbonate (LEMC), instead of lithium ethylene di-carbonate (LEDC), becomes the major organic components in the SEI on graphite anodes in $LiPF_6$-EC/DMC electrolytes, after prolonged cycling. The results of the above examples demonstrated that new tools will be able to help us to gain more fundamental understanding of SEIs and provide us valuable insights on the SEI chemistry that have been impossible to study using the traditional characterization techniques. The knowledge gained on SEIs using these advanced techniques will guide us to design better electrolytes and interphases for batteries with LT operation capabilities.

## 5.3 Electrode Engineering

Electrode materials are less critical for the LT operation of LIBs compared to electrolytes. Nevertheless, several issues of electrodes need to be addressed for fast charging capability and safety operation of LIBs at LT. Graphite is the most successful anode material for LIBs, while the large overpotential induced by poor $Li^+$ diffusion kinetics, the low Coulombic efficiency induced by SEI formation and the Li plating at LTs should be considered. Typically, surface coating with amorphous silicon nanolayer or doping with nanometal particles can improve initial Coulombic efficiency and $Li^+$ diffusion kinetics [168, 169]. In addition, mild oxidation of graphite and particle size reduction are considered as effective approaches for reducing overpotential effectively at LTs. Commercial cathodes such as NMCs, LFP and $LiCoO_2$ demonstrated different LT performance according to their own properties. Large overpotential at LT operation requires high-voltage stability, especially when Ni-rich NMCs are used. Typically, solid-solution reaction-based cathodes have better LT performance compared to LFP, which has phase-transformation during electrochemical cycling. Moreover, spinel structured cathodes with 3D $Li^+$ channels have better ionic conductivity than NMCs with 2D channels and LFP with 1D channels. Although LFP has advantages of safety and long cycle life, its relatively poor electronic conductivity should be considered and improved for LT operation.

Organic cathode materials typically demonstrate fast-charge kinetics compared with inorganic TM-based cathodes especially at LT operation. For the organic electrodes, charge storage sites are mainly located on the surface of organic solids or large interstitial space, thus being beneficial to the reaction kinetics at LTs. In addition, flexible structure and molecular diversity and multi electron transfer capability of organic cathodes make them a promising choice for LT LIBs. However, poor electronic conductivity of organic electrode typically requires addition of large amount of conductive agents or binders to increase the utilization rate of active material, resulting in a low arial loading, large amount of electrolyte required, as well as high negative/positive ratio. However, more systematic analysis on reaction mechanism including bulk redox chemistry and electrode/electrolyte stability of organic electrodes is needed before the practical application of organic cathode can be realized.

## 5.4 Preventing Lithium Plating on Graphite Surface at LTs

Lithium plating on graphite anodes is one of the major issues which induces cell degradation and severe safety risks. Typically, lithium plating occurs thermodynamically due to the polarization of electrode at harsh conditiosn such as a high state of charge (SOC), high charging rate and LT. Once Li plated on the surface of graphite rather than intercalated into graphite, thick SEIs and more dead lithium form via parasitic reaction, which consumes limited electrolyte and lithium sources. Anode engineering including reducing particle size, coating the graphite with metal oxides, increasing lithium diffusion, reducing electrode tortuosity and designing nanostructured carbon materials significantly prevents lithium plating. Several electrolyte engineering methods have been reported, such as increasing the ionic conductivity of electrolytes by introducing solvents with low viscosity, stabilizing SEIs by tuning electrolyte solvation structure or introducing electrolyte additives as well as optimizing $Li^+$ transfer numbers. It is possible to avoid Li plating by selecting anodes with higher potential than graphite such as metal oxides or alloy anodes [170]. In addition to the material or electrolyte design, the improvement of charging protocols is also beneficial for suppressing the lithium plating on graphite surface. Pre-heating during initial charging and low-rate charging during activation processes are considered as effective approaches for suppressing lithium plating at LTs. Mechanism study of lithium plating behavior under operating conditions is essential for further optimizing LT and fast charging performance of LIBs. During past decades, several diagnostic approaches such as electron microscopy, spectroscopic techniques and acoustic methods have been developed for detecting both morphology and chemistry of lithium plating. However, most of these measurements were conducted at the coin cell level only and not easy to apply for real-time detection at the pouch cell level. Therefore, more efforts should be made to develop in operando characterization techniques for quantifying/qualifying lithium plating under real operating conditions.

## Declarations

**Competing interest**  The authors declare no competing interest.

**Ethical statement**  I hereby declare that this manuscript is the result of independent creation of the authors listed in it under the reviewers' comments. Except for the quoted contents, this manuscript does not contain any research achievements that have been published or written by other individuals or groups. I am the corresponding author representing all other authors of this manuscript. The legal responsibility of this statement shall be borne by me.

## References

1. Larcher, D., Tarascon, J.M.: Towards greener and more sustainable batteries for electrical energy storage. Nat. Chem. **7**, 19–29 (2015). https://doi.org/10.1038/nchem.2085

2. Tarascon, J.M., Armand, M.: Issues and challenges facing rechargeable lithium batteries. Nature **414**, 359–367 (2001). https://doi.org/10.1038/35104644

3. Zhang, S.S., Xu, K., Jow, T.R.: Low temperature performance of graphite electrode in Li-ion cells. Electrochim. Acta **48**, 241–246 (2002). https://doi.org/10.1016/S0013-4686(02)00620-5

4. Nagasubramanian, G.: Electrical characteristics of 18 650 Li-ion cells at low temperatures. J. Appl. Electrochem. **31**, 99–104 (2001). https://doi.org/10.1023/A:1004113825283

5. Zhu, G.L., Wen, K.C., Lv, W.Q., et al.: Materials insights into low-temperature performances of lithium-ion batteries. J. Power Sources **300**, 29–40 (2015). https://doi.org/10.1016/j.jpowsour.2015.09.056

6. Xu, K.: Nonaqueous liquid electrolytes for lithium-based rechargeable batteries. ChemInform **35**, 5 (2004). https://doi.org/10.1002/chin.200450271

7. Fong, K.D., Self, J., Diederichsen, K.M., et al.: Ion transport and the true transference number in nonaqueous polyelectrolyte solutions for lithium ion batteries. ACS Cent. Sci. **5**, 1250–1260 (2019). https://doi.org/10.1021/acscentsci.9b00406

8. Piao, N., Gao, X.N., Yang, H.C., et al.: Challenges and development of lithium-ion batteries for low temperature environments. eTransportation **11**, 100145 (2022). https://doi.org/10.1016/j.etran.2021.100145

9. Qian, Y.X., Chu, Y.L., Zheng, Z.T., et al.: A new cyclic carbonate enables high power/low temperature lithium-ion batteries. Energy Storage Mater. **45**, 14–23 (2022). https://doi.org/10.1016/j.ensm.2021.11.029

10. Xu, K., von Cresce, A., Lee, U.: Differentiating contributions to "ion transfer" barrier from interphasial resistance and Li$^+$ desolvation at electrolyte/graphite interface. Langmuir **26**, 11538–11543 (2010). https://doi.org/10.1021/la009994

11. Jow, T.R., Delp, S.A., Allen, J.L., et al.: Factors limiting Li$^+$ charge transfer kinetics in Li-ion batteries. J. Electrochem. Soc. **165**, A361–A367 (2018). https://doi.org/10.1149/2.1221802jes

12. Zhang, S.S.: Challenges and strategies for fast charge of Li-ion batteries. ChemElectroChem **7**, 3569–3577 (2020). https://doi.org/10.1002/celc.202000650

13. Li, Q.Y., Lu, D.P., Zheng, J.M., et al.: Li$^+$-desolvation dictating lithium-ion battery's low-temperature performances. ACS Appl. Mater. Interfaces **9**, 42761–42768 (2017). https://doi.org/10.1021/acsami.7b13887

14. Zhang, S.S., Xu, K., Jow, T.R.: The low temperature performance of Li-ion batteries. J. Power Sources **115**, 137–140 (2003). https://doi.org/10.1016/S0378-7753(02)00618-3

15. Fan, J., Tan, S.: Studies on charging lithium-ion cells at low temperatures. J. Electrochem. Soc. **153**, A1081 (2006). https://doi.org/10.1149/1.2190029

16. Wang, C.Y., Zhang, G.S., Ge, S.H., et al.: Lithium-ion battery structure that self-heats at low temperatures. Nature **529**, 515–518 (2016). https://doi.org/10.1038/nature16502

17. Lin, W., Zhu, M.Y., Fan, Y., et al.: Low temperature lithium-ion batteries electrolytes: rational design, advancements, and future perspectives. J. Alloys Compd. **905**, 164163 (2022). https://doi.org/10.1016/j.jallcom.2022.164163

18. Ding, M.S.: Liquid-solid phase diagrams of ternary and quaternary organic carbonates. J. Electrochem. Soc. **151**, A731 (2004). https://doi.org/10.1149/1.1690782

19. Dong, X.L., Wang, Y.G., Xia, Y.Y.: Promoting rechargeable batteries operated at low temperature. Acc. Chem. Res. **54**, 3883–3894 (2021). https://doi.org/10.1021/acs.accounts.1c00420

20. Smart, M.C., Ratnakumar, B.V., Surampudi, S.: Electrolytes for low-temperature lithium batteries based on ternary mixtures of aliphatic carbonates. J. Electrochem. Soc. **146**, 486–492 (1999). https://doi.org/10.1149/1.1391633

21. Ding, M.S.: Liquid-solid phase equilibria and thermodynamic modeling for binary organic carbonates. J. Chem. Eng. Data **49**, 276–282 (2004). https://doi.org/10.1021/je034134e

22. Smart, M.C., Ratnakumar, B.V., Ewell, R.C., et al.: The use of lithium-ion batteries for JPL's Mars missions. Electrochim. Acta **268**, 27–40 (2018). https://doi.org/10.1016/j.electacta.2018.02.020

23. Ein-Eli, Y., McDevitt, S.F., Laura, R.: The superiority of asymmetric alkyl methyl carbonates. J. Electrochem. Soc. **145**, L1–L3 (1998). https://doi.org/10.1149/1.1838196

24. Ein-Eli, Y., Thomas, S.R., Koch, V., et al.: Ethylmethylcarbonate, a promising solvent for Li-ion rechargeable batteries. J. Electrochem. Soc. **143**, L273–L277 (1996). https://doi.org/10.1149/1.1837293

25. Plichta, E.J., Hendrickson, M., Thompson, R., et al.: Development of low temperature Li-ion electrolytes for NASA and DoD applications. J. Power Sources **94**, 160–162 (2001). https://doi.org/10.1016/S0378-7753(00)00578-4

26. Xiao, L.F., Cao, Y.L., Ai, X.P., et al.: Optimization of EC-based multi-solvent electrolytes for low temperature applications of lithium-ion batteries. Electrochim. Acta **49**, 4857–4863 (2004). https://doi.org/10.1016/j.electacta.2004.05.038

27. Smart, M.C., Ratnakumar, B.V., Whitcanack, L.D., et al.: Improved low-temperature performance of lithium-ion cells with quaternary carbonate-based electrolytes. J. Power Sources **119**(120/121), 349–358 (2003). https://doi.org/10.1016/S0378-7753(03)00154-X

28. Ein-Eli, Y., McDevitt, S.F., Aurbach, D., et al.: Methyl propyl carbonate: a promising single solvent for Li-ion battery electrolytes. J. Electrochem. Soc. **144**, L180–L184 (1997). https://doi.org/10.1149/1.1837792

29. Nan, B., Chen, L., Rodrigo, N.D., et al.: Enhancing Li$^+$ transport in NMC811‖graphite lithium-ion batteries at low temperatures by using low-polarity-solvent electrolytes. Angewandte Chemie Int. **61**, e202205967 (2022). https://doi.org/10.1002/anie.202205967

30. Wang, L.N., Menakath, A., Han, F.D., et al.: Identifying the components of the solid-electrolyte interphase in Li-ion batteries. Nat. Chem. **11**, 789–796 (2019). https://doi.org/10.1038/s41557-019-0304-z

31. Xing, L.D., Zheng, X.W., Schroeder, M., et al.: Deciphering the ethylene carbonate-propylene carbonate mystery in Li-ion batteries. Acc. Chem. Res. **51**, 282–289 (2018). https://doi.org/10.1021/acs.accounts.7b00474

32. Gao, Y., Rojas, T., Wang, K., et al.: Low-temperature and high-rate-charging lithium metal batteries enabled by an electrochemically active monolayer-regulated interface. Nat. Energy **5**, 534–542 (2020). https://doi.org/10.1038/s41560-020-0640-7

33. Wotango, A., Su, W.N., Haregewoin, A.M., et al.: Designed synergetic effect of electrolyte additives to improve interfacial chemistry of MCMB electrode in propylene carbonate-based electrolyte for enhanced low and room temperature performance. ACS Appl. Mater. Interfaces **10**, 25252–25262 (2018). https://doi.org/10.1021/acsami.8b02185

34. Yamada, Y., Koyama, Y., Abe, T., et al.: Correlation between charge-discharge behavior of graphite and solvation structure of the lithium ion in propylene carbonate-containing electrolytes. J. Phys. Chem. C **113**, 8948–8953 (2009). https://doi.org/10.1021/jp9022458

35. Liu, X.W., Shen, X.H., Li, H., et al.: Ethylene carbonate-free propylene carbonate-based electrolytes with excellent electrochemical compatibility for Li-ion batteries through engineering electrolyte solvation structure. Adv. Energy Mater. **11**, 2003905 (2021). https://doi.org/10.1002/aenm.202003905

36. Qin, M.S., Liu, M.C., Zeng, Z.Q., et al.: Rejuvenating propylene carbonate-based electrolyte through nonsolvating interactions for wide-temperature Li-ions batteries. Adv. Energy Mater. **12**, 2201801 (2022). https://doi.org/10.1002/aenm.202201801

37. Ein-Eli, Y., Thomas, S.R., Chadha, R., et al.: Li-ion battery electrolyte formulated for low-temperature applications. J. Electrochem. Soc. **144**, 823–829 (1997). https://doi.org/10.1149/1.1837495

38. Ein-Eli, Y., Aurbach, D.: The correlation between the cycling efficiency, surface chemistry and morphology of Li electrodes in electrolyte solutions based on methyl formate. J. Power Sources **54**, 281–288 (1995). https://doi.org/10.1016/0378-7753(94)02085-H

39. Smart, M.C., Ratnakumar, B.V., Surampudi, S., et al.: Irreversible capacities of graphite in low-temperature electrolytes for lithium-ion batteries. J. Electrochem. Soc. **146**, 3963–3969 (1999). https://doi.org/10.1149/1.1392577

40. Smart, M.C., Ratnakumar, B.V., Surampudi, S.: Use of organic esters as cosolvents in electrolytes for lithium-ion batteries with improved low temperature performance. J. Electrochem. Soc. **149**, A361 (2002). https://doi.org/10.1149/1.1453407

41. Smart, M.C., Ratnakumar, B.V., Chin, K.B., et al.: Lithium-ion electrolytes containing ester cosolvents for improved low temperature performance. J. Electrochem. Soc. **157**, A1361 (2010). https://doi.org/10.1149/1.3501236

42. Petibon, R., Harlow, J., Le, D.B., et al.: The use of ethyl acetate and methyl propanoate in combination with vinylene carbonate as ethylene carbonate-free solvent blends for electrolytes in Li-ion batteries. Electrochim. Acta **154**, 227–234 (2015). https://doi.org/10.1016/j.electacta.2014.12.084

43. Holoubek, J., Yin, Y.J., Li, M.Q., et al.: Exploiting mechanistic solvation kinetics for dual-graphite batteries with high power output at extremely low temperature. Angewandte Chemie Int. Ed. **58**, 18892–18897 (2019). https://doi.org/10.1002/anie.201912167

44. Cho, Y.G., Li, M.Q., Holoubek, J., et al.: Enabling the low-temperature cycling of NMC‖graphite pouch cells with an ester-based electrolyte. ACS Energy Lett. **6**, 2016–2023 (2021). https://doi.org/10.1021/acsenergylett.1c00484

45. Feng, T.T., Yang, G.Z., Zhang, S., et al.: Low-temperature and high-voltage lithium-ion battery enabled by localized high-concentration carboxylate electrolytes. Chem. Eng. J. **433**, 134138 (2022). https://doi.org/10.1016/j.cej.2021.134138

46. Yang, Y., Fang, Z., Yin, Y., et al.: Synergy of weakly-solvated electrolyte and optimized interphase enables graphite anode charge at low temperature. Angewandte Chemie Int. Ed. **61**, e202208345 (2022). https://doi.org/10.1002/anie.202208345

47. Yao, Y.X., Yao, N., Zhou, X.R., et al.: Ethylene-carbonate-free electrolytes for rechargeable Li-ion pouch cells at sub-freezing temperatures. Adv. Mater. **34**, 2206448 (2022). https://doi.org/10.1002/adma.202206448

48. Zhang, S.S., Xu, K., Allen, J.L., et al.: Effect of propylene carbonate on the low temperature performance of Li-ion cells. J. Power Sources **110**, 216–221 (2002). https://doi.org/10.1016/S0378-7753(02)00272-0

49. Oldiges, K., Michalowsky, J., Grünebaum, M., et al.: Tetrahydrothiophene 1-oxide as highly effective co-solvent for propylene carbonate-based electrolytes. J. Power Sources **437**, 226881 (2019). https://doi.org/10.1016/j.jpowsour.2019.226881

50. Zonouz, A.F., Mosallanejad, B.: Use of ethyl acetate for improving low-temperature performance of lithium-ion battery. Monatshefte Für Chemie Chem. Mon. **150**, 1041–1047 (2019). https://doi.org/10.1007/s00706-019-2360-x

51. Sazhin, S.V., Khimchenko, M.Y., Tritenichenko, Y.N., et al.: Performance of Li-ion cells with new electrolytes conceived for low-temperature applications. J. Power Sources **87**, 112–117 (2000). https://doi.org/10.1016/S0378-7753(99)00434-6

52. Cho, Y.G., Kim, Y.S., Sung, D.G., et al.: Nitrile-assistant eutectic electrolytes for cryogenic operation of lithium ion batteries at fast charges and discharges. Energy Environ. Sci. **7**, 1737–1743 (2014). https://doi.org/10.1039/C3EE43029D

53. Hilbig, P., Ibing, L., Streipert, B., et al.: Acetonitrile-based electrolytes for lithium-ion battery application. Curr. Top. Electrochem. **20**, 1 (2018). https://doi.org/10.31300/CTEC.20.2018.1-13

54. Shanmukaraj, D., Grugeon, S., Laruelle, S., et al.: Hindered glymes for graphite-compatible electrolytes. Chemsuschem **8**, 2691–2695 (2015). https://doi.org/10.1002/cssc.201500502

55. Ueno, K., Murai, J., Ikeda, K., et al.: Li$^+$ solvation and ionic transport in lithium solvate ionic liquids diluted by molecular solvents. J. Phys. Chem. C **120**, 15792–15802 (2016). https://doi.org/10.1021/acs.jpcc.5b11642

56. Thenuwara, A.C., Shetty, P.P., Kondekar, N., et al.: Efficient low-temperature cycling of lithium metal anodes by tailoring the solid-electrolyte interphase. ACS Energy Lett. **5**, 2411–2420 (2020). https://doi.org/10.1021/acsenergylett.0c01209

57. Holoubek, J., Liu, H.D., Wu, Z.H., et al.: Tailoring electrolyte solvation for Li metal batteries cycled at ultra-low temperature. Nat. Energy (2021). https://doi.org/10.1038/s41560-021-00783-z

58. Holoubek, J., Kim, K., Yin, Y.J., et al.: Electrolyte design implications of ion-pairing in low-temperature Li metal batteries. Energy Environ. Sci. **15**, 1647–1658 (2022). https://doi.org/10.1039/D1EE03422G

59. Jow, T.R., Xu, K., Borodin, O., et al. (eds.): Electrolytes for Lithium and Lithium-Ion Batteries. Springer, Heidelberg (2004). https://doi.org/10.1007/978-1-4939-0302-3

60. Xu, K.: Electrolytes and interphases in Li-ion batteries and beyond. Chem. Rev. **114**, 11503–11618 (2014). https://doi.org/10.1021/cr500003w

61. Fan, X.L., Chen, L., Borodin, O., et al.: Non-flammable electrolyte enables Li-metal batteries with aggressive cathode chemistries. Nat. Nanotechnol. **13**, 715–722 (2018). https://doi.org/10.1038/s41565-018-0183-2

62. Fan, X.L., Ji, X., Chen, L., et al.: All-temperature batteries enabled by fluorinated electrolytes with non-polar solvents. Nat. Energy **4**, 882–890 (2019). https://doi.org/10.1038/s41560-019-0474-3

63. Takehara, M., Tsukimori, N., Nanbu, N., et al.: Physical and electrolytic properties of fluoroethyl methyl carbonate. Electrochem. **71**, 1201–1204 (2003). https://doi.org/10.5796/electrochemistry.71.1201

64. Smart, M.C., Ratnakumar, B.V., Ryan-Mowrey, V.S., et al.: Improved performance of lithium-ion cells with the use of fluorinated carbonate-based electrolytes. J. Power Sources **119**(120/121), 359–367 (2003). https://doi.org/10.1016/S0378-7753(03)00266-0

65. Im, J., Lee, J., Ryou, M.H., et al.: Fluorinated carbonate-based electrolyte for high-voltage Li(Ni$_{0.5}$Mn$_{0.3}$Co$_{0.2}$)O$_2$/graphite lithium-ion battery. J. Electrochem. Soc. **164**, A6381–A6385 (2017). https://doi.org/10.1149/2.0591701jes

66. Peljo, P., Girault, H.H.: Electrochemical potential window of battery electrolytes: the HOMO-LUMO misconception. Energy Environ. Sci. **11**, 2306–2309 (2018). https://doi.org/10.1039/C8EE01286E

67. Borodin, O.: Challenges with prediction of battery electrolyte electrochemical stability window and guiding the electrode-electrolyte stabilization. Curr. Opin. Electrochem. **13**, 86–93 (2019). https://doi.org/10.1016/j.coelec.2018.10.015

68. Holoubek, J., Yu, M.Y., Yu, S.C., et al.: An all-fluorinated ester electrolyte for stable high-voltage Li metal batteries capable of ultra-low-temperature operation. ACS Energy Lett. **5**, 1438–1447 (2020). https://doi.org/10.1021/acsenergylett.0c00643

69. Guo, R., Han, W.: The effects of electrolytes, electrolyte/electrode interphase, and binders on lithium-ion batteries at low temperature. Mater. Today Sustain. **19**, 100187 (2022). https://doi.org/10.1016/j.mtsust.2022.100187

70. Lu, W., Xiong, S.Z., Xie, K., et al.: Identification of solid electrolyte interphase formed on graphite electrode cycled in trifluoroethyl aliphatic carboxylate-based electrolytes for low-temperature lithium-ion batteries. Ionics **22**, 2095–2102 (2016). https://doi.org/10.1007/s11581-016-1743-9

71. Matsuda, Y., Fukushima, T., Katoh, Y., et al.: Characteristics of gel alkylene oxide polymer electrolytes containing γ-butyrolactone. J. Power Sources **119**(120/121), 473–477 (2003). https://doi.org/10.1016/S0378-7753(03)00265-9

72. Smart, M.C., Ratnakumar, B.V., Behar, A., et al.: Gel polymer electrolyte lithium-ion cells with improved low temperature performance. J. Power Sources **165**, 535–543 (2007). https://doi.org/10.1016/j.jpowsour.2006.10.038

73. Kasprzyk, M., Zalewska, A., Niedzicki, L., et al.: Non-crystallizing solvent mixtures and lithium electrolytes for low temperatures. Solid State Ion. **308**, 22–26 (2017). https://doi.org/10.1016/j.ssi.2017.05.014

74. Rustomji, C.S., Yang, Y., Kim, T., et al.: Liquefied gas electrolytes for electrochemical energy storage devices. Meet. Abstr. **5**, 1089 (2016). https://doi.org/10.1149/ma2016-03/2/1089

75. Yang, Y., Davies, D.M., Yin, Y.J., et al.: High-efficiency lithium-metal anode enabled by liquefied gas electrolytes. Joule **3**, 1986–2000 (2019). https://doi.org/10.1016/j.joule.2019.06.008

76. Yang, Y., Yin, Y.J., Davies, D.M., et al.: Liquefied gas electrolytes for wide-temperature lithium metal batteries. Energy Environ. Sci. **13**, 2209–2219 (2020). https://doi.org/10.1039/d0ee01446j

77. Davies, D.M., Yang, Y., Sablina, E.S., et al.: A safer, wide-temperature liquefied gas electrolyte based on difluoromethane. J. Power Sources **493**, 229668 (2021). https://doi.org/10.1016/j.jpowsour.2021.229668

78. Yin, Y.J., Yang, Y., Cheng, D.Y., et al.: Fire-extinguishing, recyclable liquefied gas electrolytes for temperature-resilient lithium-metal batteries. Nat. Energy **7**, 548–559 (2022). https://doi.org/10.1038/s41560-022-01051-4

79. Suo, L.M., Borodin, O., Gao, T., et al.: "Water-in-salt" electrolyte enables high-voltage aqueous lithium-ion chemistries. Science **350**, 938–943 (2015). https://doi.org/10.1126/science.aab1595

80. Ramanujapuram, A., Yushin, G.: Understanding the exceptional performance of lithium-ion battery cathodes in aqueous electrolytes at subzero temperatures. Adv. Energy Mater. **8**, 1802624 (2018). https://doi.org/10.1002/aenm.201802624

81. Nian, Q.S., Wang, J.Y., Liu, S., et al.: Aqueous batteries operated at − 50 °C. Angew. Chem. Int. Ed. **58**, 16994–16999 (2019). https://doi.org/10.1002/anie.201908913

82. Tron, A., Jeong, S., Park, Y.D., et al.: Aqueous lithium-ion battery of nano-LiFePO$_4$ with antifreezing agent of ethyleneglycol for low-temperature operation. ACS Sustain. Chem. Eng. **7**, 14531–14538 (2019). https://doi.org/10.1021/acssuschemeng.9b02042

83. Dou, Q.Y., Lei, S.L., Wang, D.W., et al.: Safe and high-rate supercapacitors based on an "acetonitrile/water in salt" hybrid electrolyte. Energy Environ. Sci. **11**, 3212–3219 (2018). https://doi.org/10.1039/C8EE01040D

84. Chen, J.W., Vatamanu, J., Xing, L.D., et al.: Improving electrochemical stability and low-temperature performance with water/acetonitrile hybrid electrolytes. Adv. Energy Mater. **10**, 1902654 (2020). https://doi.org/10.1002/aenm.201902654

85. Ma, Z.K., Chen, J.W., Vatamanu, J., et al.: Expanding the low-temperature and high-voltage limits of aqueous lithium-ion battery. Energy Storage Mater. **45**, 903–910 (2022). https://doi.org/10.1016/j.ensm.2021.12.045

86. Liu, J.H., Yang, C., Chi, X.W., et al.: Water/sulfolane hybrid electrolyte achieves ultralow-temperature operation for high-voltage aqueous lithium-ion batteries. Adv. Funct. Mater. **32**, 2106811 (2022). https://doi.org/10.1002/adfm.202106811

87. Jaumaux, P., Yang, X., Zhang, B., et al.: Localized water-in-salt electrolyte for aqueous lithium-ion batteries. Angew. Chem. Int. Ed. **60**, 19965–19973 (2021). https://doi.org/10.1002/anie.202107389

88. Smith, K.A., Smart, M.C., Surya Prakash, G.K., et al.: Electrolytes containing fluorinated ester co-solvents for low-temperature Li-ion cells. ECS Trans. **11**, 91–98 (2008). https://doi.org/10.1149/1.2938911

89. Xu, J., Wang, X., Yuan, N.Y., et al.: Extending the low temperature operational limit of Li-ion battery to − 80 °C. Energy Storage Mater. **23**, 383–389 (2019). https://doi.org/10.1016/j.ensm.2019.04.033

90. Fang, S.H., Wang, G.J., Qu, L., et al.: A novel mixture of diethylene glycol diethylether and non-flammable methyl-nonafluorobutyl ether as a safe electrolyte for lithium ion batteries. J. Mater. Chem. A **3**, 21159–21166 (2015). https://doi.org/10.1039/C5TA05242D

91. Shi, P., Fang, S.H., Luo, D., et al.: A safe electrolyte based on propylene carbonate and non-flammable hydrofluoroether for high-performance lithium ion batteries. J. Electrochem. Soc. **164**, A1991–A1999 (2017). https://doi.org/10.1149/2.1181709jes

92. Liu, Y., Fang, S.H., Shi, P., et al.: Ternary mixtures of nitrile-functionalized glyme, non-flammable hydrofluoroether and fluoroethylene carbonate as safe electrolytes for lithium-ion batteries. J. Power Sources **331**, 445–451 (2016). https://doi.org/10.1016/j.jpowsour.2016.09.087

93. Shi, P., Fang, S.H., Huang, J., et al.: A novel mixture of lithium bis(oxalato)borate, gamma-butyrolactone and non-flammable hydrofluoroether as a safe electrolyte for advanced lithium ion batteries. J. Mater. Chem. A **5**, 19982–19990 (2017). https://doi.org/10.1039/C7TA05743A

94. Shiao, H.C., Chua, D., Lin, H.P., et al.: Low temperature electrolytes for Li-ion PVDF cells. J. Power Sources **87**, 167–173 (2000). https://doi.org/10.1016/S0378-7753(99)00470-X

95. Zhang, S.S., Xu, K., Jow, T.R.: A new approach toward improved low temperature performance of Li-ion battery. Electrochem. Commun. **4**, 928–932 (2002). https://doi.org/10.1016/S1388-2481(02)00490-3

96. Zhang, S.S.: An unique lithium salt for the improved electrolyte of Li-ion battery. Electrochem. Commun. **8**, 1423–1428 (2006). https://doi.org/10.1016/j.elecom.2006.06.016

97. Zhang, S.S.: Electrochemical study of the formation of a solid electrolyte interface on graphite in a $LiBC_2O_4F_2$-based electrolyte. J. Power Sources **163**, 713–718 (2007). https://doi.org/10.1016/j.jpowsour.2006.09.040

98. Zhou, L., Lucht, B.L.: Performance of lithium tetrafluorooxalatophosphate (LiFOP) electrolyte with propylene carbonate (PC). J. Power Sources **205**, 439–448 (2012). https://doi.org/10.1016/j.jpowsour.2012.01.067

99. Zhang, S.S., Xu, K., Jow, T.R.: Enhanced performance of Li-ion cell with $LiBF_4$-PC based electrolyte by addition of small amount of LiBOB. J. Power Sources **156**, 629–633 (2006). https://doi.org/10.1016/j.jpowsour.2005.04.023

100. Takami, N., Ohsaki, T., Hasebe, H., et al.: Laminated thin Li-ion batteries using a liquid electrolyte. J. Electrochem. Soc. **149**, A9 (2002). https://doi.org/10.1149/1.1420704

101. Lazar, M.L., Lucht, B.L.: Carbonate free electrolyte for lithium ion batteries containing γ-butyrolactone and methyl butyrate. J. Electrochem. Soc. **162**, A928–A934 (2015). https://doi.org/10.1149/2.0601506jes

102. Xu, K., Zhang, S.S., Lee, U., et al.: LiBOB: is it an alternative salt for lithium ion chemistry? J. Power Sources **146**, 79–85 (2005). https://doi.org/10.1016/j.jpowsour.2005.03.153

103. Zhang, L.J., Sun, Y.X., Zhou, Y., et al.: Investigation of the synergetic effects of $LiBF_4$ and LiODFB as wide-temperature electrolyte salts in lithium-ion batteries. Ionics **24**, 2995–3004 (2018). https://doi.org/10.1007/s11581-018-2470-1

104. Qian, J.F., Henderson, W.A., Xu, W., et al.: High rate and stable cycling of lithium metal anode. Nat. Commun. **6**, 6362 (2015). https://doi.org/10.1038/ncomms7362

105. Chen, S.R., Zheng, J.M., Yu, L., et al.: High-efficiency lithium metal batteries with fire-retardant electrolytes. Joule **2**, 1548–1558 (2018). https://doi.org/10.1016/j.joule.2018.05.002

106. Zheng, Y., Soto, F.A., Ponce, V., et al.: Localized high concentration electrolyte behavior near a lithium-metal anode surface. J. Mater. Chem. A **7**, 25047–25055 (2019). https://doi.org/10.1039/C9TA08935G

107. Ren, X.D., Chen, S.R., Lee, H., et al.: Localized high-concentration sulfone electrolytes for high-efficiency lithium-metal batteries. Chem **4**, 1877–1892 (2018). https://doi.org/10.1016/j.chempr.2018.05.002

108. Lin, S.S., Hua, H.M., Lai, P.B., et al.: A multifunctional dual-salt localized high-concentration electrolyte for fast dynamic high-voltage lithium battery in wide temperature range. Adv. Energy Mater. **11**, 2101775 (2021). https://doi.org/10.1002/aenm.202101775

109. Jow, T.R., Ding, M.S., Xu, K., et al.: Nonaqueous electrolytes for wide-temperature-range operation of Li-ion cells. J. Power Sources **119**(120/121), 343–348 (2003). https://doi.org/10.1016/S0378-7753(03)00153-8

110. Wu, Z.L., Li, S.G., Zheng, Y.Z., et al.: The roles of sulfur-containing additives and their working mechanism on the temperature-dependent performances of Li-ion batteries. J. Electrochem. Soc. **165**, A2792–A2800 (2018). https://doi.org/10.1149/2.0331811jes

111. Li, X.C., Yin, Z.L., Li, X.H., et al.: Ethylene sulfate as film formation additive to improve the compatibility of graphite electrode for lithium-ion battery. Ionics **20**, 795–801 (2014). https://doi.org/10.1007/s11581-013-1036-5

112. Zhang, B., Metzger, M., Solchenbach, S., et al.: Role of 1, 3-propane sultone and vinylene carbonate in solid electrolyte interface formation and gas generation. J. Phys. Chem. C **119**, 11337–11348 (2015). https://doi.org/10.1021/acs.jpcc.5b00072

113. Zuo, X.X., Fan, C.J., Xiao, X., et al.: High-voltage performance of $LiCoO_2$/graphite batteries with methylene methanedisulfonate as electrolyte additive. J. Power Sources **219**, 94–99 (2012). https://doi.org/10.1016/j.jpowsour.2012.07.026

114. Xia, J., Sinha, N.N., Chen, L.P., et al.: A comparative study of a family of sulfate electrolyte additives. J. Electrochem. Soc. **161**, A264–A274 (2013). https://doi.org/10.1149/2.015403jes

115. Xia, J., Harlow, J.E., Petibon, R., et al.: Comparative study on methylene methyl disulfonate (MMDS) and 1,3-propane sultone (PS) as electrolyte additives for Li-ion batteries. J. Electrochem. Soc. **161**, A547–A553 (2014). https://doi.org/10.1149/2.049404jes

116. Jurng, S., Kim, H.S., Lee, J.G., et al.: Low-temperature characteristics and film-forming mechanism of elemental sulfur additive on graphite negative electrode. J. Electrochem. Soc. **163**, A223–A228 (2015). https://doi.org/10.1149/2.0421602jes

117. Jurng, S., Park, S., Yoon, T., et al.: Low-temperature performance improvement of graphite electrode by allyl sulfide additive and its film-forming mechanism. J. Electrochem. Soc. **163**, A1798–A1804 (2016). https://doi.org/10.1149/2.0051609jes

118. Hubble, D., Brown, D.E., Zhao, Y.Z., et al.: Liquid electrolyte development for low-temperature lithium-ion batteries. Energy Environ. Sci. **15**, 550–578 (2022). https://doi.org/10.1039/D1EE01789F

119. Mai, S.W., Xu, M.Q., Liao, X.L., et al.: Tris(trimethylsilyl)phosphite as electrolyte additive for high voltage layered lithium nickel cobalt manganese oxide cathode of lithium ion battery. Electrochim. Acta **147**, 565–571 (2014). https://doi.org/10.1016/j.electacta.2014.09.157

120. Yim, T., Han, Y.K.: Tris(trimethylsilyl) phosphite as an efficient electrolyte additive to improve the surface stability of graphite anodes. ACS Appl. Mater. Interfaces **9**, 32851–32858 (2017). https://doi.org/10.1021/acsami.7b11309

121. Liu, B., Li, Q.Y., Engelhard, M.H., et al.: Constructing robust electrode/electrolyte interphases to enable wide temperature applications of lithium-ion batteries. ACS Appl. Mater. Interfaces **11**, 21496–21505 (2019). https://doi.org/10.1021/acsami.9b03821

122. Xu, G.J., Huang, S.Q., Cui, Z.L., et al.: Functional additives assisted ester-carbonate electrolyte enables wide temperature operation of a high-voltage (5 V-class) Li-ion battery. J. Power Sources **416**, 29–36 (2019). https://doi.org/10.1016/j.jpowsour.2019.01.085

123. Michan, A.L., Parimalam, B.S., Leskes, M., et al.: Fluoroethylene carbonate and vinylene carbonate reduction: understanding lithium-ion battery electrolyte additives and solid electrolyte interphase formation. Chem. Mater. **28**, 8149–8159 (2016). https://doi.org/10.1021/acs.chemmater.6b02282

124. Zhang, X.Q., Cheng, X.B., Chen, X., et al.: Fluoroethylene carbonate additives to render uniform Li deposits in lithium metal batteries. Adv. Funct. Mater. **27**, 1605989 (2017). https://doi.org/10.1002/adfm.201605989

125. Liu, B.X., Li, B., Guan, S.Y.: Effect of fluoroethylene carbonate additive on low temperature performance of Li-ion batteries. Electrochem. Solid-State Lett. **15**, A77 (2012). https://doi.org/10.1149/2.027206esl

126. Zhang, D., Zhu, D.W., Guo, W.Y., et al.: The fluorine-rich electrolyte as an interface modifier to stabilize lithium metal battery at ultra-low temperature. Adv. Funct. Mater. **32**, 2112764 (2022). https://doi.org/10.1002/adfm.202112764

127. Wang, Z.X., Sun, Z.H., Shi, Y., et al.: Ion-dipole chemistry drives rapid evolution of Li ions solvation sheath in low-temperature Li batteries. Adv. Energy Mater. **11**, 2100935 (2021). https://doi.org/10.1002/aenm.202100935

128. Shi, J.L., Ehteshami, N., Ma, J.L., et al.: Improving the graphite/electrolyte interface in lithium-ion battery for fast charging and low temperature operation: fluorosulfonyl isocyanate as electrolyte additive. J. Power Sources **429**, 67–74 (2019). https://doi.org/10.1016/j.jpowsour.2019.04.113

129. Yang, T.X., Fan, W.Z., Wang, C.Y., et al.: 2,3,4,5,6-Pentafluorophenyl methanesulfonate as a versatile electrolyte additive matches $LiNi_{0.5}Co_{0.2}Mn_{0.3}O_2$/graphite batteries working in a

wide-temperature range. ACS Appl. Mater. Interfaces **10**, 31735–31744 (2018). https://doi.org/10.1021/acsami.8b04743

130. Guo, R.D., Che, Y.X., Lan, G.Y., et al.: Tailoring low-temperature performance of a lithium-ion battery via rational designing interphase on an anode. ACS Appl. Mater. Interfaces **11**, 38285–38293 (2019). https://doi.org/10.1021/acsami.9b12020

131. Lin, Y.C., Yue, X.P., Zhang, H., et al.: Using phenyl methanesulfonate as an electrolyte additive to improve performance of $LiNi_{0.5}Co_{0.2}Mn_{0.3}O_2$/graphite cells at low temperature. Electrochimica Acta **300**, 202–207 (2019). https://doi.org/10.1016/j.electacta.2019.01.120

132. Smart, M.C., Lucht, B.L., Dalavi, S., et al.: The effect of additives upon the performance of MCMB/$LiNi_xCo_{1-x}O_2$ Li-ion cells containing methyl butyrate-based wide operating temperature range electrolytes. J. Electrochem. Soc. **159**, A739–A751 (2012). https://doi.org/10.1149/2.058206jes

133. Kim, K.M., Ly, N.V., Won, J.H., et al.: Improvement of lithium-ion battery performance at low temperature by adopting polydimethylsiloxane-based electrolyte additives. Electrochim. Acta **136**, 182–188 (2014). https://doi.org/10.1016/j.electacta.2014.05.054

134. Xiang, F.Y., Wang, P.P., Cheng, H.: Methyl 2,2-difluoro-2-(fluorosulfonyl) acetate as a novel electrolyte additive for high-voltage $LiCoO_2$/graphite pouch Li-ion cells. Energy Technol. **8**, 1901277 (2020). https://doi.org/10.1002/ente.201901277

135. Zuo, W.Q.: Effect of N-N dimethyltrifluoroacetamide additive on low temperature performance of graphite anode. Int. J. Electrochem. Sci. **5**, 382–393 (2020). https://doi.org/10.20964/2020.01.08

136. Smart, M.C., Hwang, C., Krause, F.C., et al.: Wide operating temperature range electrolytes for high voltage and high specific energy Li-ion cells. ECS Trans. **50**, 355–364 (2013). https://doi.org/10.1149/05026.0355ecst

137. Cappetto, A., Cao, W.J., Luo, J.F., et al.: Performance of wide temperature range electrolytes for Li-Ion capacitor pouch cells. J. Power Sources **359**, 205–214 (2017). https://doi.org/10.1016/j.jpowsour.2017.05.071

138. Jones, J.P., Smart, M.C., Krause, F.C., et al.: The effect of electrolyte additives upon lithium plating during low temperature charging of graphite-LiNiCoAlO$_2$ lithium-ion three electrode cells. J. Electrochem. Soc. **167**, 020536 (2020). https://doi.org/10.1149/1945-7111/ab6bc2

139. Pham, H.Q., Chung, G.J., Han, J., et al.: Interface stabilization via lithium bis(fluorosulfonyl)imide additive as a key for promoted performance of graphite‖$LiCoO_2$ pouch cell under − 20 °C. J. Chem. Phys. **152**, 094709 (2020). https://doi.org/10.1063/1.5144280

140. Xiang, H.F., Mei, D.H., Yan, P.F., et al.: The role of cesium cation in controlling interphasial chemistry on graphite anode in propylene carbonate-rich electrolytes. ACS Appl. Mater. Interfaces **7**, 20687–20695 (2015). https://doi.org/10.1021/acsami.5b05552

141. Li, Q.Y., Jiao, S.H., Luo, L.L., et al.: Wide-temperature electrolytes for lithium-ion batteries. ACS Appl. Mater. Interfaces **9**, 18826–18835 (2017). https://doi.org/10.1021/acsami.7b04099

142. Yang, B.W., Zhang, H., Yu, L., et al.: Lithium difluorophosphate as an additive to improve the low temperature performance of $LiNi_{0.5}Co_{0.2}Mn_{0.3}O_2$/graphite cells. Electrochimica Acta **221**, 107–114 (2016). https://doi.org/10.1016/j.electacta.2016.10.037

143. Liao, B., Li, H.Y., Xu, M.Q., et al.: Designing low impedance interface films simultaneously on anode and cathode for high energy batteries. Adv. Energy Mater. **8**, 1800802 (2018). https://doi.org/10.1002/aenm.201800802

144. Wang, W.L., Yang, T.X., Li, S., et al.: 1-Ethyl-3-methylimidazolium tetrafluoroborate (EMI-BF$_4$) as an ionic liquid-type electrolyte additive to enhance the low-temperature performance of $LiNi_{0.5}Co_{0.2}Mn_{0.3}O_2$/graphite batteries. Electrochimica Acta **317**, 146–154 (2019). https://doi.org/10.1016/j.electacta.2019.05.027

145. Li, Y., Wong, K.W., Dou, Q.Q., et al.: Improvement of lithium-ion battery performance at low temperature by adopting ionic liquid-decorated PMMA nanoparticles as electrolyte component. ACS Appl. Energy Mater. **1**, 2664–2670 (2018). https://doi.org/10.1021/acsaem.8b00355

146. Rodrigo, N.D., Tan, S., Shadike, Z., et al.: Improved low temperature performance of graphite/Li cells using isoxazole as a novel cosolvent in electrolytes. J. Electrochem. Soc. **168**, 070527 (2021). https://doi.org/10.1149/1945-7111/ac11a6

147. Tan, S., Rodrigo, U.N.D., Shadike, Z., et al.: Novel low-temperature electrolyte using isoxazole as the main solvent for lithium-ion batteries. ACS Appl. Mater. Interfaces **13**, 24995–25001 (2021). https://doi.org/10.1021/acsami.1c05894

148. Wang, J.H., Zheng, Q.F., Fang, M.M., et al.: Concentrated electrolytes widen the operating temperature range of lithium-ion batteries. Adv. Sci. **8**, 2101646 (2021). https://doi.org/10.1002/advs.20210 1646

149. Zhang, X.H., Zou, L.F., Xu, Y.B., et al.: Advanced electrolytes for fast-charging high-voltage lithium-ion batteries in wide-temperature range. Adv. Energy Mater. **10**, 2000368 (2020). https://doi.org/10.1002/aenm.202000368

150. Yamada, Y., Wang, J.H., Ko, S., et al.: Advances and issues in developing salt-concentrated battery electrolytes. Nat. Energy **4**, 269–280 (2019). https://doi.org/10.1038/s41560-019-0336-z

151. Li, Y.Q., Yang, Y., Lu, Y.X., et al.: Ultralow-concentration electrolyte for Na-ion batteries. ACS Energy Lett. **5**, 1156–1158 (2020). https://doi.org/10.1021/acsenergylett.0c00337

152. Zheng, H., Xiang, H.F., Jiang, F.Y., et al.: Lithium difluorophosphate-based dual-salt low concentration electrolytes for lithium metal batteries. Adv. Energy Mater. **10**, 2001440 (2020). https://doi.org/10.1002/aenm.202001440

153. Pham, T.D., Bin Faheem, A., Nguyen, H.D., et al.: Enhanced performances of lithium metal batteries by synergistic effect of low concentration bisalt electrolyte. J. Mater. Chem. A **10**, 12035–12046 (2022). https://doi.org/10.1039/D2TA02743G

154. Guan, D.C., Hu, G.R., Peng, Z.D., et al.: A nonflammable low-concentration electrolyte for lithium-ion batteries. J. Mater. Chem. A **10**, 12575–12587 (2022). https://doi.org/10.1039/d2ta01760a

155. Zhang, W., Xia, H.R., Zhu, Z.Q., et al.: Decimal solvent-based high-entropy electrolyte enabling the extended survival temperature of lithium-ion batteries to − 130 °C. CCS Chem. **3**, 1245–1255 (2021). https://doi.org/10.31635/ccschem.020.202000341

156. Sun, N.N., Li, R.H., Zhao, Y., et al.: Anionic coordination manipulation of multilayer solvation structure electrolyte for high-rate and low-temperature lithium metal battery. Adv. Energy Mater. **12**, 2200621 (2022). https://doi.org/10.1002/aenm.202200621

157. Xue, W.R., Qin, T., Li, Q., et al.: Exploiting the synergistic effects of multiple components with a uniform design method for developing low-temperature electrolytes. Energy Storage Mater. **50**, 598–605 (2022). https://doi.org/10.1016/j.ensm.2022.06.003

158. Zhang, L., Liang, Y.Z., Jiang, J.H., et al.: Uniform design applied to nonlinear multivariate calibration by ANN. Anal. Chimica Acta **370**, 65–77 (1998). https://doi.org/10.1016/S0003-2670(98)00256-6

159. Ma, C.X., Fang, K.T.: A new approach to construction of nearly uniform designs. Int. J. Mater. Prod. Technol. **20**, 115 (2004). https://doi.org/10.1504/ijmpt.2004.003916

160. Liu, X.W., Shen, X.H., Luo, L.B., et al.: Designing advanced electrolytes for lithium secondary batteries based on the coordination number rule. ACS Energy Lett. **6**, 4282–4290 (2021). https://doi.org/10.1021/acsenergylett.1c02194

161. Wang, H., Chen, Z., Ji, Z., et al.: Temperature adaptability issue of aqueous rechargeable batteries. Mater. Today Energy **19**, 100577 (2021). https://doi.org/10.1016/j.mtener.2020.100577

162. Wang, C.S., Meng, Y.S., Xu, K.: Perspective: fluorinating interphases. J. Electrochem. Soc. **166**, A5184–A5186 (2018). https://doi.org/10.1149/2.0281903jes

163. Shadike, Z., Lee, H., Borodin, O., et al.: Identification of LiH and nanocrystalline LiF in the solid-electrolyte interphase of lithium

metal anodes. Nat. Nanotechnol. **16**, 549–554 (2021). https://doi.org/10.1038/s41565-020-00845-5

164. Wang, X.F., Zhang, M.H., Alvarado, J., et al.: New insights on the structure of electrochemically deposited lithium metal and its solid electrolyte interphases via cryogenic TEM. Nano Lett. **17**, 7606–7612 (2017). https://doi.org/10.1021/acs.nanolett.7b03606

165. Li, Y.Z., Li, Y.B., Pei, A., et al.: Atomic structure of sensitive battery materials and interfaces revealed by cryo-electron microscopy. Science **358**, 506–510 (2017). https://doi.org/10.1126/science.aam6014

166. Peled, E., Golodnitsky, D., Ardel, G.: Advanced model for solid electrolyte interphase electrodes in liquid and polymer electrolytes. J. Electrochem. Soc. **144**, L208–L210 (1997). https://doi.org/10.1149/1.1837858

167. Aurbach, D., Ein-Ely, Y., Zaban, A.: The surface chemistry of lithium electrodes in alkyl carbonate solutions. J. Electrochem. Soc. **141**, L1–L3 (1994). https://doi.org/10.1149/1.2054718

168. Kim, N., Chae, S., Ma, J., et al.: Fast-charging high-energy lithium-ion batteries via implantation of amorphous silicon nanolayer in edge-plane activated graphite anodes. Nat. Commun. **8**, 1–10 (2017). https://doi.org/10.1038/s41467-017-00973-y

169. Yan, Y., Ben, L.B., Zhan, Y.J., et al.: Nano-Sn embedded in expanded graphite as anode for lithium ion batteries with improved LT electrochemical performance. Electrochim. Acta **187**, 186–192 (2016). https://doi.org/10.1016/j.electacta.2015.11.015

170. Lin, X.K., Khosravinia, K., Hu, X.S., et al.: Lithium plating mechanism, detection, and mitigation in lithium-ion batteries. Prog. Energy Combust. Sci. **87**, 100953 (2021). https://doi.org/10.1016/j.pecs.2021.100953
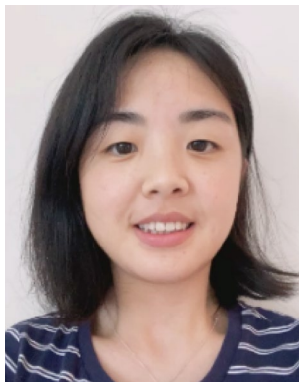


**Dr. Sha Tan** received her B.S. degree in Chemistry in 2016 from Chongqing University. She is currently pursuing for her Ph.D. degree in Chemistry at Stony Brook University, conducting research in the energy storage group under the supervision of Dr. Enyuan Hu and Dr. Xiao-Qing Yang in Brookhaven National Laboratory (BNL), USA. Her research interests focus on the electrolyte and solid electrolyte interphase engineering for wide-temperature lithium ion/lithium metal batteries, as well as mechanism studies using synchrotron-based characterization techniques.



**Dr. Zulipiya Shadike** is currently an Associate Professor in the School of Mechanical Engineering at Shanghai Jiao Tong University. She received her Ph.D. degree in Physical Chemistry from Fudan University in 2017 and then worked as a Research Associate at the Brookhaven National Laboratory (BNL). She was promoted to a staff scientist in 2020. Her research interests focus on developing high energy electrode materials as well as investigating the bulk/interphasial chemistry of lithium/sodium batteries. She was a recipient of the "Young Investigator Award" in 2019 from the Battery500 consortium supported by the U.S. Department of Energy.



**Mr. Xinyin Cai** received his B. S. and M. S. degrees in Materials Science and Engineering in 2018 and 2021 from Wuhan University of Technology. He is currently a Ph.D. student in the School of Mechanical Engineering at Shanghai Jiao Tong University. His research interests focus on investigation of anionic redox chemistry and local structure evolution mechanism of high energy cathode materials for sodium/lithium-ion batteries.



**Dr. Ruoqian Lin** is currently a technologist in Electrochemical Research, Technology & Engineering Group of JPL. Her research is focused on developing new energy storage materials and architectures for next-generation rechargeable batteries, including Li-ion batteries and multi-valent ion/metal batteries. Dr. Lin has a strong research background in understanding fundamental material sciences in Li-ion and beyond Li-ion batteries by utilizing state-of-the-art characterization techniques, such as transmission electron microscopy and synchrotron techniques. Dr. Ruoqian Lin obtained her Ph.D. in Material Sciences and Engineering from Stony Brook University, USA in 2018. Before joining JPL, she was a postdoctoral researcher at Brookhaven National Laboratory, USA.



**Atsu Kludze** received his B.S. in Chemical Engineering from Cornell University in 2021. During his time at Cornell University, he investigated nanoscale nucleation processes at the lithium–electrolyte interface as an undergraduate researcher within the Archer Research Group, while at Cornell, he did an internship at Brookhaven National Lab (BNL), USA under the guidance of Dr. Xiao-Qing Yang. Atsu is currently a Chemical Engineering PhD student at Yale University as an NSF Graduate Research Fellow and GEM Associate Fellow, advised by Professor Shu Hu.

**Dr. Borodin** is a scientist at a Battery Science Branch at US Army Research Laboratory that he joined in 2010. He graduated from University of Utah in 2000 and continued as a research faculty there for ten years. His current research focuses on a molecular scale modeling of battery electrolytes, solutions, polymers, electrochemical interfaces, reactivity and electrochemical stability of electrolytes at electrodes. Together with the experimental counterparts, he explores the mechanism of ionic transport, its connection to transference number and conductivity, key factors behind electrochemical reactivity of electrolytes at electrodes and a role the electrochemical double layer (EDL) structure plays in improving or degrading electrolyte stability, degradation and ion transport. He was part of the team that received University of Maryland Invention of the Year Award (2016) and Army Research Laboratory Award for Science (2017). He co-authored more than 220 publications in peer-reviewed journals, 6 book chapters and gave more than 100 conference presentations.

**Dr. Brett Lucht** is a Professor at the University of Rhode Island. His research is focused on novel electrolytes and electrolyte electrode interfaces for lithium-ion battery applications which include extending the calendar life, improving low-temperature properties, improving the performance of novel high capacity anodes such as lithium metal or silicon, and improving the performance of high-voltage cathode materials. He has regularly conduced both basic science and applied research and has collaborated extensively with industrial partners. Lucht has mentored more than 100 students including over 40 graduate students, 30 undergraduate students, 20 postdoctoral fellows, along with several visiting students.

**Dr. Chunsheng Wang** is a Robert Franklin and Frances Riggs Wright Distinguished Chair Professor in the Chemical & Biomolecular Engineering at the University of Maryland. He is an associate editor of *ACS Applied Energy Materials* and UMD Director of The UMD-ARL Center for Research in Extreme Battery. His research focuses on reachable batteries and fuel cells. He has published more than 330 papers. His work has been cited for more than 49 000 times with an *H*-index of 113. He has been listed as a Highly Cited Researcher since 2018 by Clarivate, and received the 2021 Battery Division Research Award from The Electrochemical Society.

**Dr. Enyuan Hu** is an chemist in the Chemistry Division of Brookhaven National Laboratory (BNL), USA. He obtained his Ph.D. degree from the Department of Mechanical Engineering at Stony Brook University. His research focuses on advanced battery material development and characterization.

**Dr. Kang Xu** Ph.D. (Chemistry, Arizona State University, 1996); M.S. (Polymer Chemistry, Institute of Chemical Physics, Academy of Sciences, 1988); B.S. (Chemistry, Southwest University, 1985). ECS Fellow, ARL Fellow, Former Team Leader of Electrolyte and Interface Science Team at US Army Research Laboratory. (ARL). Now the Chief Scientist at SolidEnergy Systems (SES), 35 Cabot Rd., Woburn, MA 01801, USA. Cofounder of Center of Research on Extreme Batteries (CREB), Advisory Board of *ACS Applied Materials*, Associate Editors for *Energy & Environmental Materials* and *Electrochemistry*, Guest-editor of *ECS Interface*. He has experience in electrolyte materials for 30 years, and has published more than 250 papers, 1 book, 5 chapters, and more than 20 patents. He has an *H* index of 105 with more than 40 000 citations. He has received more than 20 awards which include 2017 Department of Defense Scientist-of-the-Quarter, 2017 International Battery Association Technology Award, 2018 Electrochemical Society Battery Research Award and numerous ARL and DoD awards.

**Dr. Xiao-Qing Yang** is the group leader of the electrochemical energy storage group in the Chemistry Division of Brookhaven National Laboratory (BNL). He is the Principal Investigator (PI) for several Battery Material Research (BMR) programs including the Batter500 consortium at BNL funded by the Office of Vehicle Technologies, EE&RE, U.S. Department of Energy (USDOE). He received his B.S. degree in Material Science from Shannxi Mechanic Engineering Institute in Xi'an, China in 1976 and Ph.D. degree in Physics, from University of Florida, Gainesville, Florida, USA, in 1986. He received the "2012 Vehicle Technologies Program R&D Award" from the Vehicle Technologies Office of EE&RE, USDOE in May 2012. In January 2015, he received the IBA201 Research award from the International Battery Association (IBA).